COHERENCE 2013

Fusione Fredda/LENR: Da Fleishmann a Focardi

Roma, 15 ottobre, 2013

Piezonuclear fission reactions triggered by fracture and earthquakes: From the chemical evolution of our planet to the so-called cold fusion

Alberto Carpinteri

Department of Structural, Geotechnical and Building Engineering
Politecnico di Torino, Italy

ACKNOWLEDGEMENTS

G. Lacidogna, A. Manuello, O. Borla for their extensive collaboration

R. Sandrone for his contribution in geological issues

A. Chiodoni and S. Guastella for their contribution in micro-chemical analysis

L. Negri for his contribution in Planetary Science

D. Veneziano, A. Goi for their contribution in electrolysis experiments

NEUTRON EMISSION FROM FRACTURE AND EARTHQUAKES

NEUTRON EMISSION FROM EARTHQUAKES

- Sobolev, G.A., Shestopalov, I.P., Kharin, E.P. "**Implications of Solar Flares for the Seismic Activity of the Earth**". Izvestiya, *Phys. Solid Earth* **34**: 603-607 (1998).
- Volodichev, N.N., Kuzhevskij, B.M., Nechaev, O. Yu., Panasyuk M., and Podorolsky M.I., "**Lunar periodicity of the neutron radiation burst and seismic activity on the Earth**", *Proc. of the 26th International Cosmic Ray Conference*, Salt Lake City, 17-25 August, 1999.
- Kuzhevskij, M., Nechaev, O. Yu. and Sigaeva, E. A., "Distribution of neutrons near the Earth's surface", *Natural Hazards and Earth System Sciences*, **3**: 255-262 (2003).
- Kuzhevskij, M., Nechaev, O. Yu., Sigaeva, E. A. and Zakharov, V. A., "Neutron flux variations near the Earth's crust. A possible tectonic activity detection", *Natural Hazards and Earth System Sciences*, **3**: 637-645 (2003).
- Sigaeva, E., Nechaev, O., Panasyuk, M., Bruns, A., Vladimirsky, B. and Kuzmin Yu., "**Thermal neutrons' observations before the Sumatra earthquake**", *Geophysical Research Abstracts*, **8**: 00435 (2006).

(Continued)

As reported in the literature, an average thermal neutron flux up to 10^0 cm^{-2} s^{-1} **(10^3 times the background level)** was detected in correspondence to earthquakes with a magnitude of the 4th degree in Richter Scale (Volodichev N.N., et al. (1999)).

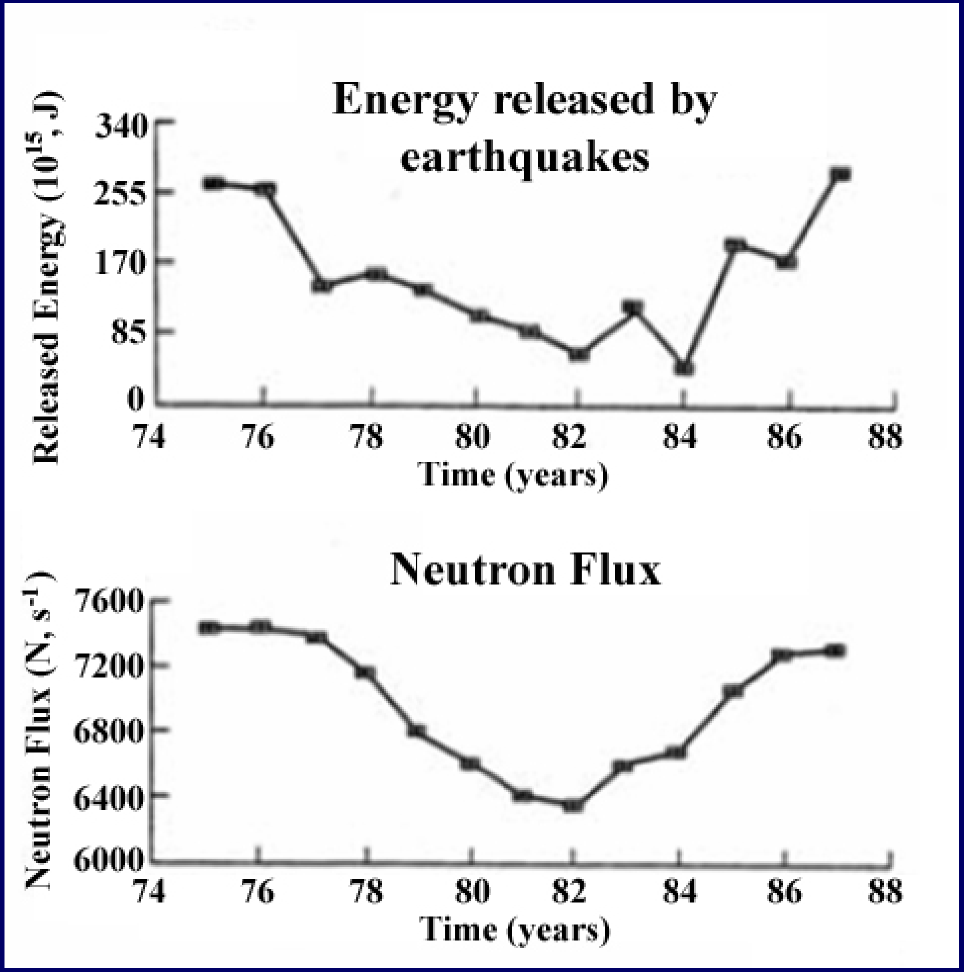

Global seismic activity and neutron flux measurements in the period 1975-1987. **Laboratory of Geophysical Precursors**, Oblast' Murmansk, Apatity, **Kola Peninsula**, Russia (Sobolev et al. 1998).

NEUTRON EMISSION FROM ROCK SPECIMENS

During a preliminary experimental analysis four rock specimens were used:

- two made of **Carrara marble**, specimens P1 and P2;
- two made of **Luserna granite**, specimens P3 and P4;
- all of them measuring **6x6x10 cm^3**.

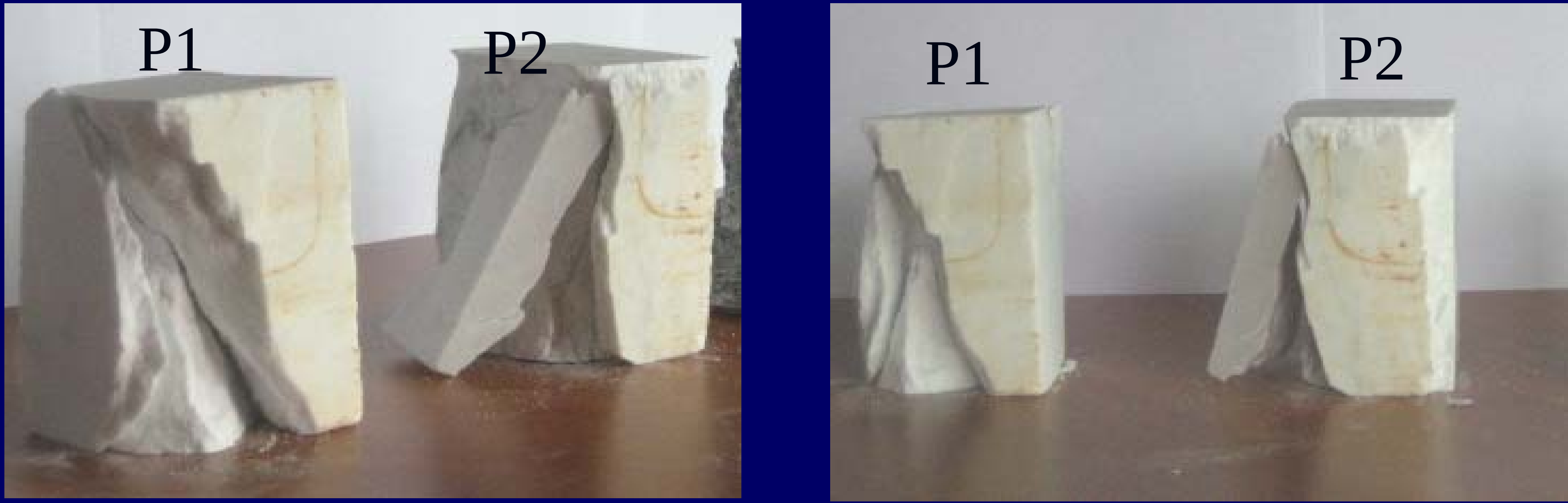

Specimens P1 and P2 in Carrara marble following compression failure.

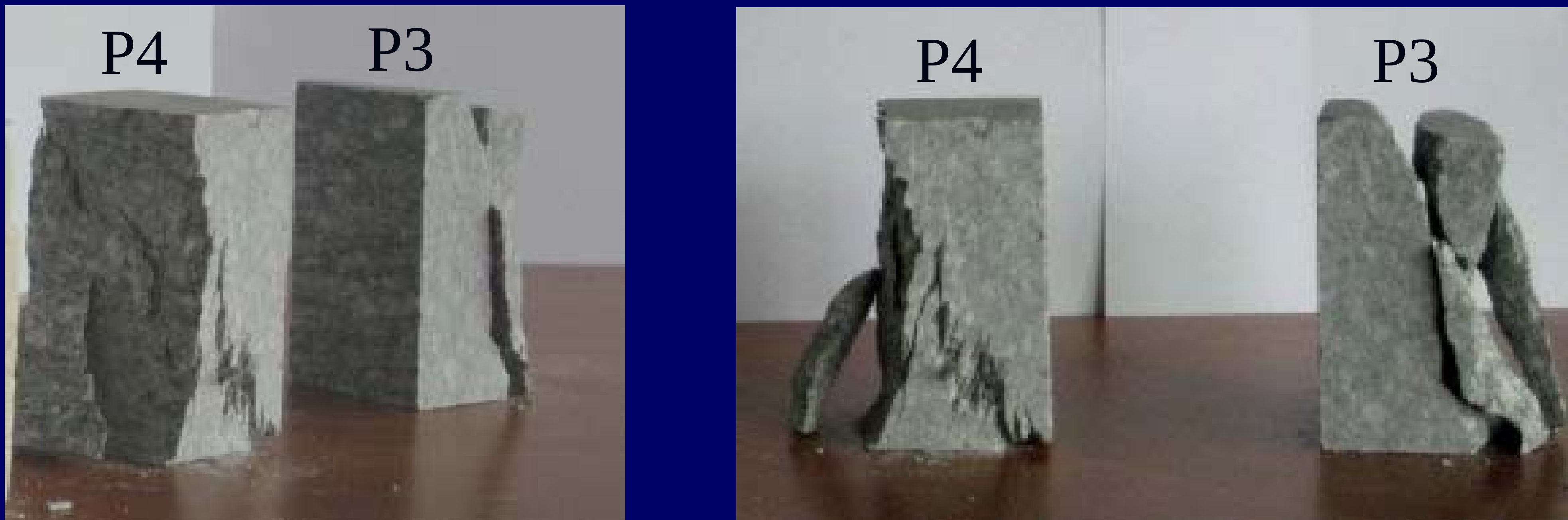

Specimens P3 e P4 in Luserna granite following compression failure.

Brittle Fracture Experiment on Carrara Marble specimen

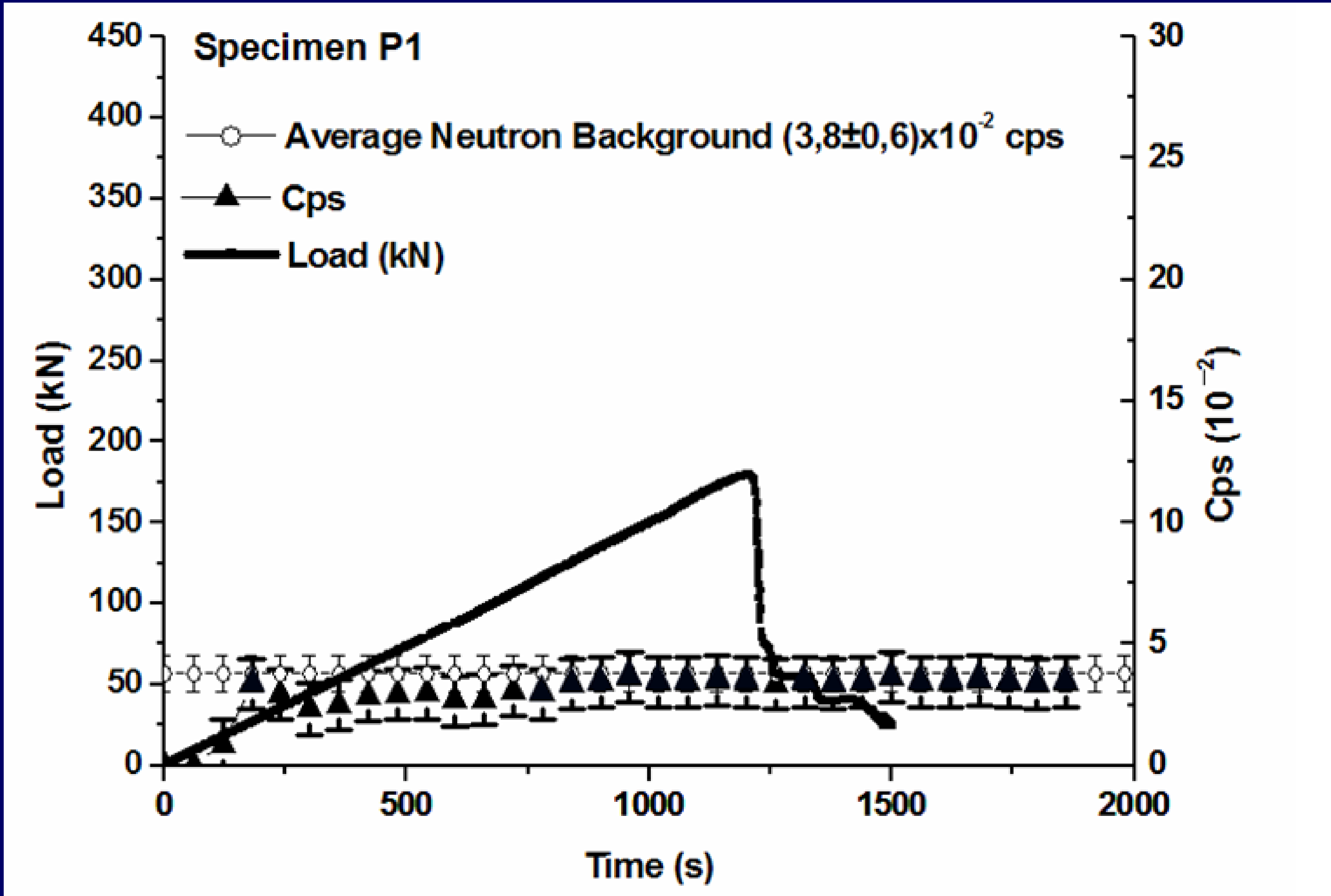

Load vs. time and cps curve for P1 test specimen of Carrara marble.

Brittle Fracture Experiment on granite specimen

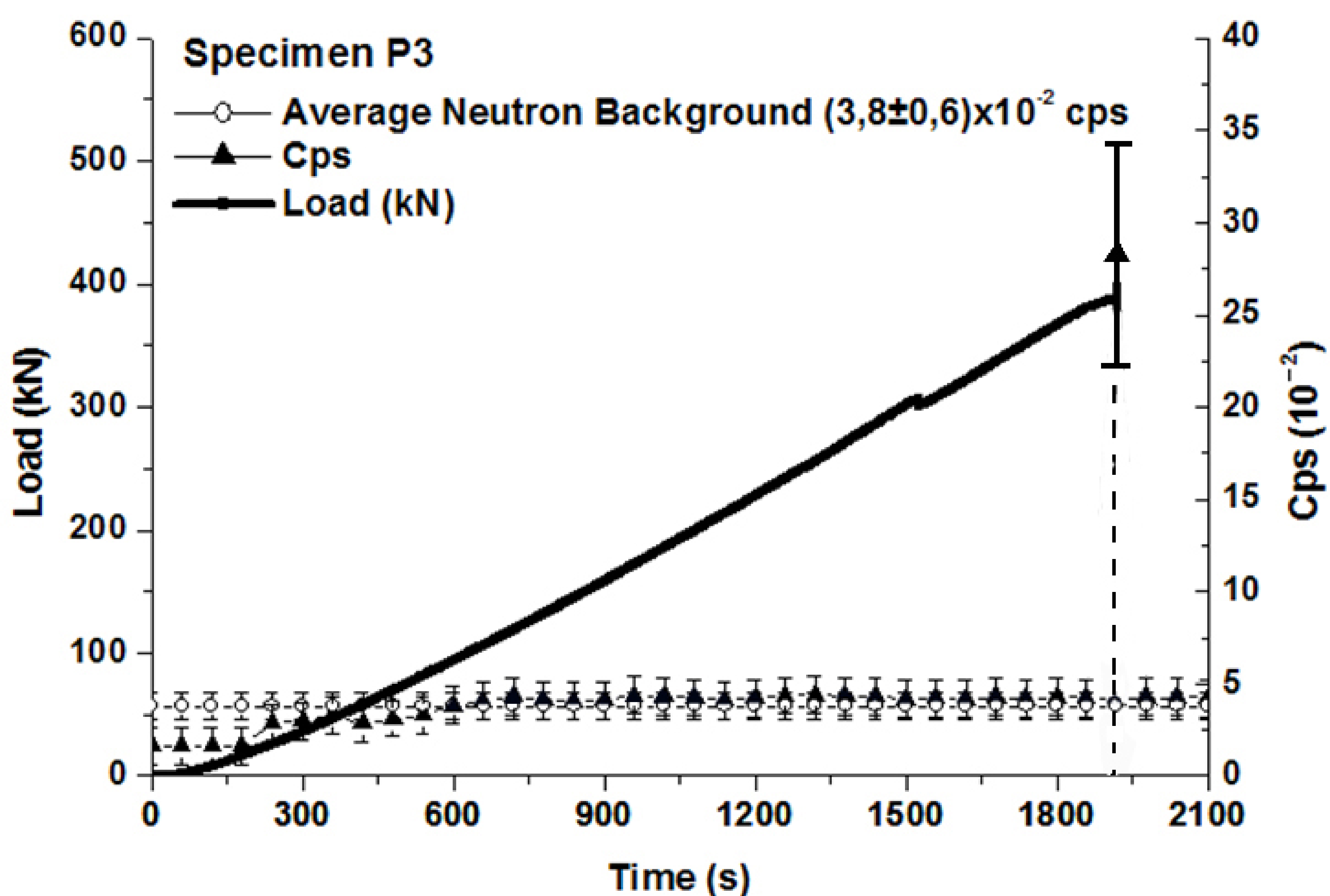

Load vs. time and cps curve for P3 test specimen of granite.

NEUTRON EMISSION FROM CAVITATION IN LIQUIDS AND FRACTURE IN SOLIDS

MATERIAL		NEUTRON EMISSION
LIQUIDS – Cavitation		
Iron chloride	→	**up to 2.5 times the Background Level**
SOLIDS – Fracture		
Steel	→	**up to 2.5 times the Background Level**
Granite (Fe ~ 1.5%)	→	**up to 10^1 times the Background Level**
Basalt (Fe ~ 15%)	→	**up to 10^2 times the Background Level**
Magnetite (Fe ~ 75%)	→	**up to 10^3 times the Background Level**
Marble	→	**Background Level**

Cyclic Loading Experiments on Basaltic Rocks

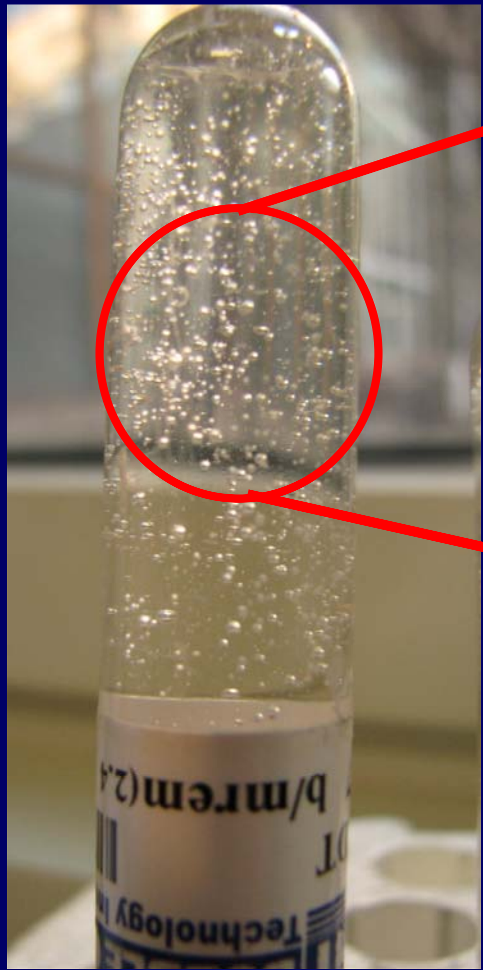

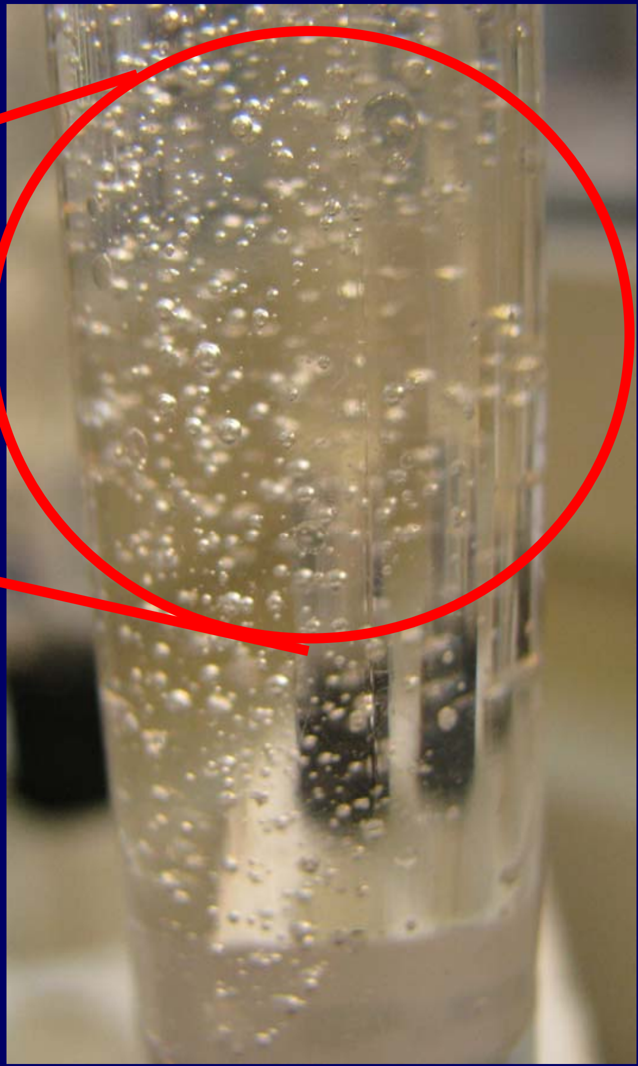

The equivalent neutron dose, at the end of the test on basaltic rock, was 2.62 ± 0,53 μSv/h (Average Background Dose = 41.95 ± 0,85 nSv/h).

$$\frac{\text{Effective Neutron Dose}}{\text{Average Background Dose}} \simeq 50$$

OPEN ACCESS
IOP PUBLISHING JOURNAL OF PHYSICS G: NUCLEAR AND PARTICLE PHYSICS

J. Phys. G: Nucl. Part. Phys. **40** (2013) 015006 (8pp) doi:10.1088/0954-3899/40/1/015006

Neutron production from the fracture of piezoelectric rocks

A Widom[1], J Swain[1] and Y N Srivastava[2]

[1] Physics Department, Northeastern University, Boston MA, USA
[2] Department of Physics & INFN, University of Perugia, Perugia, Italy

E-mail: John.Swain@cern.ch

Received 2 March 2012
Published 14 December 2012
Online at stacks.iop.org/JPhysG/40/015006

Abstract

A theoretical explanation is provided for the experimental evidence that fracturing piezoelectric rocks produces neutrons. The elastic energy micro-crack production ultimately yields the macroscopic fracture. The mechanical energy is converted by the piezoelectric effect into electric field energy. The electric field energy decays via radio frequency (microwave) electric field oscillations. The radio frequency electric fields accelerate the condensed matter electrons which then collide with protons producing neutrons and neutrinos.

IRON DEPLETION

vs

CARBON POLLUTION

TECTONIC ACTIVITY vs CHEMICAL EVOLUTION

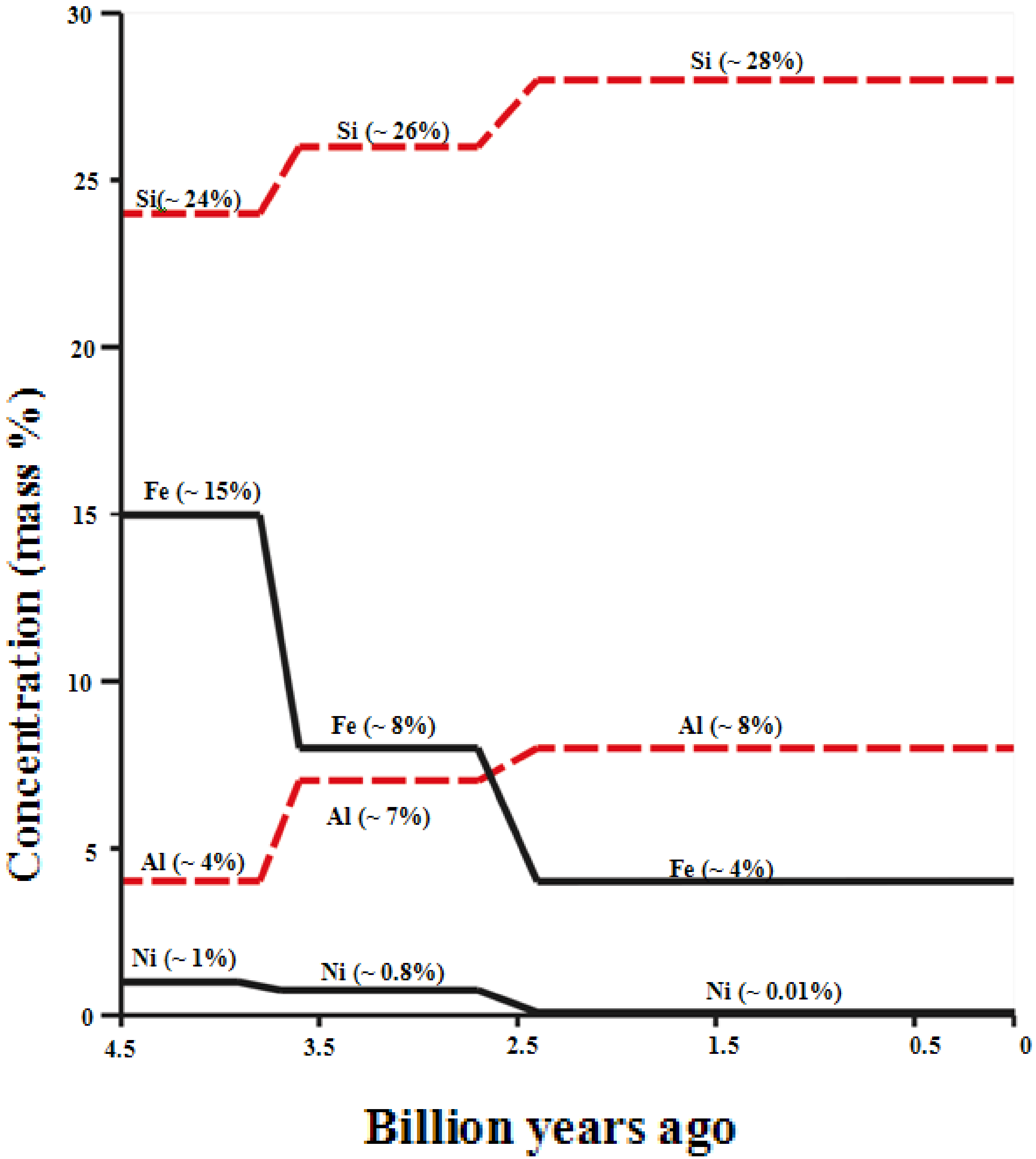

Tectonic plate formation

(3.8 Billion years ago):

Fe (–7%) + Ni (–0.2%) =

=Al (+3%) + Si (+2.2%) + Mg (+2%)

Most severe tectonic activity

(2.5 Billion years ago):

Fe (–4%) + Ni (–0.8%) =

=Al (+1%) + Si (+2.3%) + Mg (+1.5%)

Conjecture about ferrous elements' transformations in the Earth Crust

(1) $Fe_{26}^{56} \rightarrow 2\,Al_{13}^{27} + 2n$

(2) $Fe_{26}^{56} \rightarrow Si_{14}^{28} + Mg_{12}^{24} + 4n$

(3) $Fe_{26}^{56} \rightarrow Ca_{20}^{40} + C_{6}^{12} + 4n$

(4) $Co_{27}^{59} \rightarrow Si_{14}^{28} + Al_{13}^{27} + 4n$

(5) $Ni_{28}^{59} \rightarrow 2\,Si_{14}^{28} + 3n$

(6) $Ni_{28}^{59} \rightarrow Na_{11}^{23} + Cl_{17}^{35} + 1n$

Photo-Disintegration of the Iron Nucleus in Fractured Magnetite Rocks with Magnetostriction

A. Widom and J. Swain
Physics Department, Northeastern University, Boston MA USA

Y.N. Srivastava
Physics Department & INFN, University of Perugia, Perugia IT

There has been considerable interest in recent experiments on iron nuclear disintegrations observed when rocks containing such nuclei are crushed and fractured. The resulting nuclear transmutations are particularly strong for the case of magnetite rocks, i.e. loadstones. We argue that the fission of the iron nucleus is a consequence of photo-disintegration. The electro-strong coupling between electromagnetic fields and nuclear giant dipole resonances are central for producing observed nuclear reactions. The large electron energies produced during the fracture of piezomagnetic rocks are closely analogous to the previously discussed case of the fracture of piezoelectric rocks. In both cases electro-weak interactions can produce neutrons and neutrinos from energetic protons and electrons thus inducing nuclear transmutations. The electro-strong condensed matter coupling discussed herein represents new many body collective nuclear photo-disintegration effects.

PACS numbers: 62.20.mm, 81.40.Np, 03.75.Be, 14.20.Dh

EVIDENCE FOR PHOTOFISSION OF IRON*

C. B. Fulmer, I. R. Williams, and T. H. Handley
Oak Ridge National Laboratory, Oak Ridge, Tennessee

and

G. F. Dell and L. N. Blumberg†
Cambridge Electron Accelerator, Cambridge, Massachusetts
(Received 4 August 1967)

Studies of proton-induced reactions in the GeV energy region[1,2] have given evidence that fission occurs in nuclei at least as light as silver. It has been pointed out that any nucleus can be made to undergo fission provided it is supplied with sufficient excitation energy.[3,4] In this note we present evidence of photofission in iron foils that were bombarded with high-energy electrons.

that were bombarded with 3-GeV electrons an appreciable yield of ^{7}Be was observed.[5] Careful examination of the gamma spectra obtained from the iron targets yielded no evidence for ^{7}Be. A radiochemical separation also yielded no evidence for ^{7}Be in an iron foil that was bombarded with 3-GeV electrons. Studies of proton- and alpha-induced reactions[6] have shown that emission of ^{7}Be is enhanced by rotation-

PHYSICAL REVIEW VOLUME 82, NUMBER 5 JUNE 1, 1951

Fission of Medium Weight Elements*

ROGER E. BATZEL AND GLENN T. SEABORG
Radiation Laboratory and Department of Chemistry, University of California, Berkeley, California
(Received February 19, 1951)

Evidence is presented here which indicates that large fragments (much larger than alpha-particles) are emitted among the competitive products of transmutation throughout the entire range of atomic numbers of the elements. Threshold considerations for the observed nuclear reactions show that the reactions are observed with small cross sections well below the threshold for spallation reactions in which the maximum number of alpha-particles are considered as being emitted from the excited nucleus. The calculated thresholds include the mass difference between the reactants and the products and the excitation energy which the product particles or fragments must have in order to pass over the coulombic barrier. Preliminary experiments on the ranges of recoil fragments from copper irradiated with 340-Mev protons give additional evidence for the emission of heavy fragments. It is suggested that the term "fission" is proper for such reactions, throughout the entire range of atomic numbers, in which the nucleus is split essentially into pieces of comparable weight.

I. INTRODUCTION

THE fission reaction has been observed with high energy accelerator projectiles for elements as light as tantalum,[1] but has not been reported for medium weight elements. Evidence is presented here for occurrence of reactions which are probably most

an example, the extreme reaction $Cu^{63}+p\rightarrow Cl^{38}+Al^{25}+n$, which is energetically most economical but still endoergic, has a threshold of about 50 Mev.

This result made it seem worthwhile to investigate another such reaction in copper and to extend the threshold studies to other elements in the middle portion

JANUARY, 1927 *PHYSICAL REVIEW* *VOLUME 29*

THE BREAKDOWN OF ATOMS AT HIGH PRESSURES

By P. W. Bridgman

Abstract

Thermodynamic evidence supports the experimental suggestion of a previous paper that at ordinary temperatures sufficiently high pressures are capable of breaking down the quantum structure of atoms, reducing matter to an electrical gas of electrons and protons. We may, therefore look for atomic dissociation under two sorts of conditions: high temperatures and comparatively low pressures, such as we have in the stellar atmospheres, and high pressures and comparatively low temperatures, which we may surmize we have in the interiors of stars, possibly in stars like the sun, and almost certainly in stars of the enormous density of the dark Sirius type. The possibility of two sorts of dissociation, together with the more rapid increase of pressure than density when the diameter of a star is reduced, offers the possibility of a critical condition determining whether a star is of the dark Sirius type or not.

IN THE Physical Review for January 1926 I called attention to a reversal in the behavior of certain properties of potassium (the atom of which has an abnormally loose structure) at high pressures and room temperature, which I suggested might indicate the initiation of an ulti-

Localization of iron mines

(*) World Iron Ore producers. Available at http://www.mapsofworld.com/minerals/world-iron-ore-producers.html.

(**) World Mineral Resources Map. Available at http://www.mapsofworld.com/world-mineral-map.html.

Localization of Aluminum mines

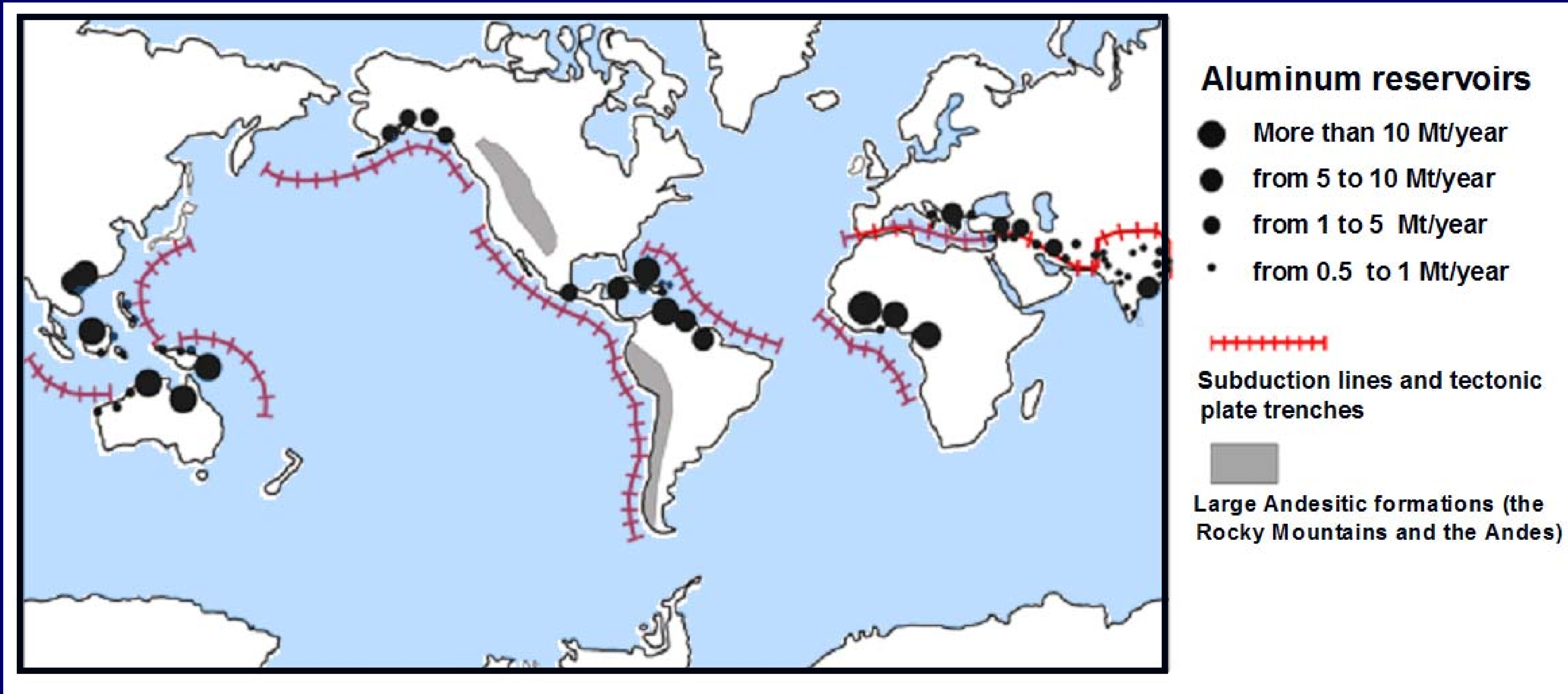

(*) World Iron Ore producers. Available at http://www.mapsofworld.com/minerals/world-iron-ore-producers.html.

(**) World Mineral Resources Map. Available at http://www.mapsofworld.com/world-mineral-map.html.

Salinity level in the Mediterranean Sea

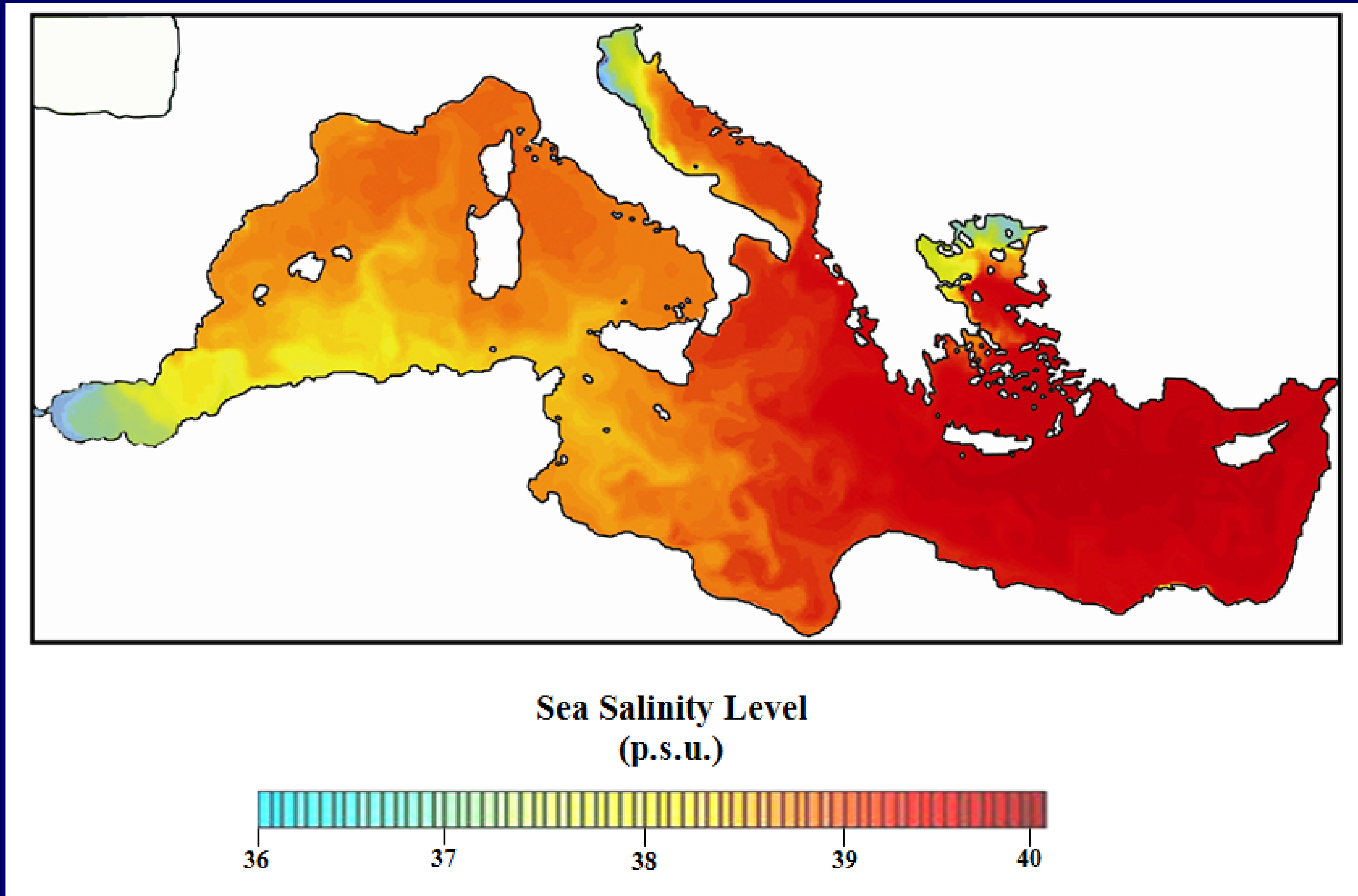

Map of the salinity level in the Mediterranean Sea expressed in p.s.u.
The Mediterranean basin is characterized by the highest sea salinity level in the World.

Map of the major earthquakes in the last fifteen years

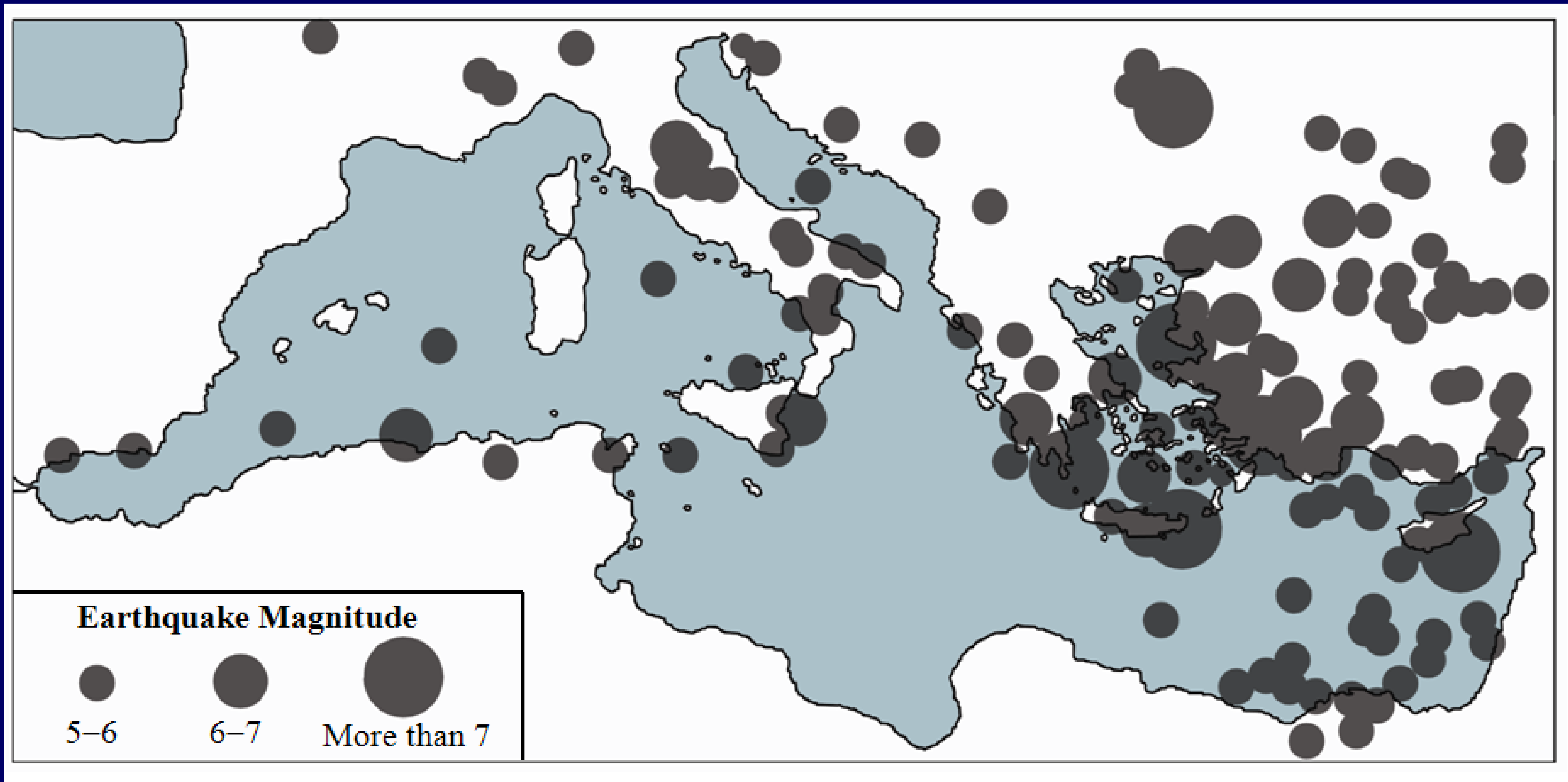

Nickel Depletion: $Ni_{28}^{59} \rightarrow Na_{11}^{23} + Cl_{17}^{35} + 1n$

Magnesium depletion and Carbon concentration in the primordial atmosphere

The estimated Mg increase (~3.5%) is equivalent to the Carbon content in the primordial atmosphere:

$$Fe^{56}_{26} \rightarrow Mg^{24}_{12} + Si^{28}_{14} + 4n$$
$$Mg^{24}_{12} \rightarrow 2C^{12}_{6}$$

Assuming a mean density of the Earth Crust equal to 3.6 g/cm^3 and a thickness of ~60 km, the mass increase in Mg (~3.5×10^{21} kg), and therefore in C, implies a very high atmospheric pressure

Primordial atmospheric pressure due to C increase = ~650 atm ⟷ **Primordial atmospheric pressure reported by other authors = ~650 atm (Liu, 2004)**

Liu, L., "The inception of the oceans and CO2-atmosphere in the early history of the Earth". *Earth Planet. Sci. Lett.*, 227, 179–184 (2004)

theguardian

Friday 8 March 2013 10.55 GMT

News | Sport | Comment | Culture | Business | Money | Life & style

Environment > Climate change

Large rise in CO2 emissions sounds climate change alarm

Hopes for 'safe' temperature increase within 2C fade as Hawaii station documents second-greatest emissions increase

"What is disturbing scientists is he acceleration of CO_2 concentrations in the atmosphere, which are occurring in spite of attempts by governments to restrain fossil fuel emissions"

CALCIUM DEPLETION
vs
OCEAN FORMATION

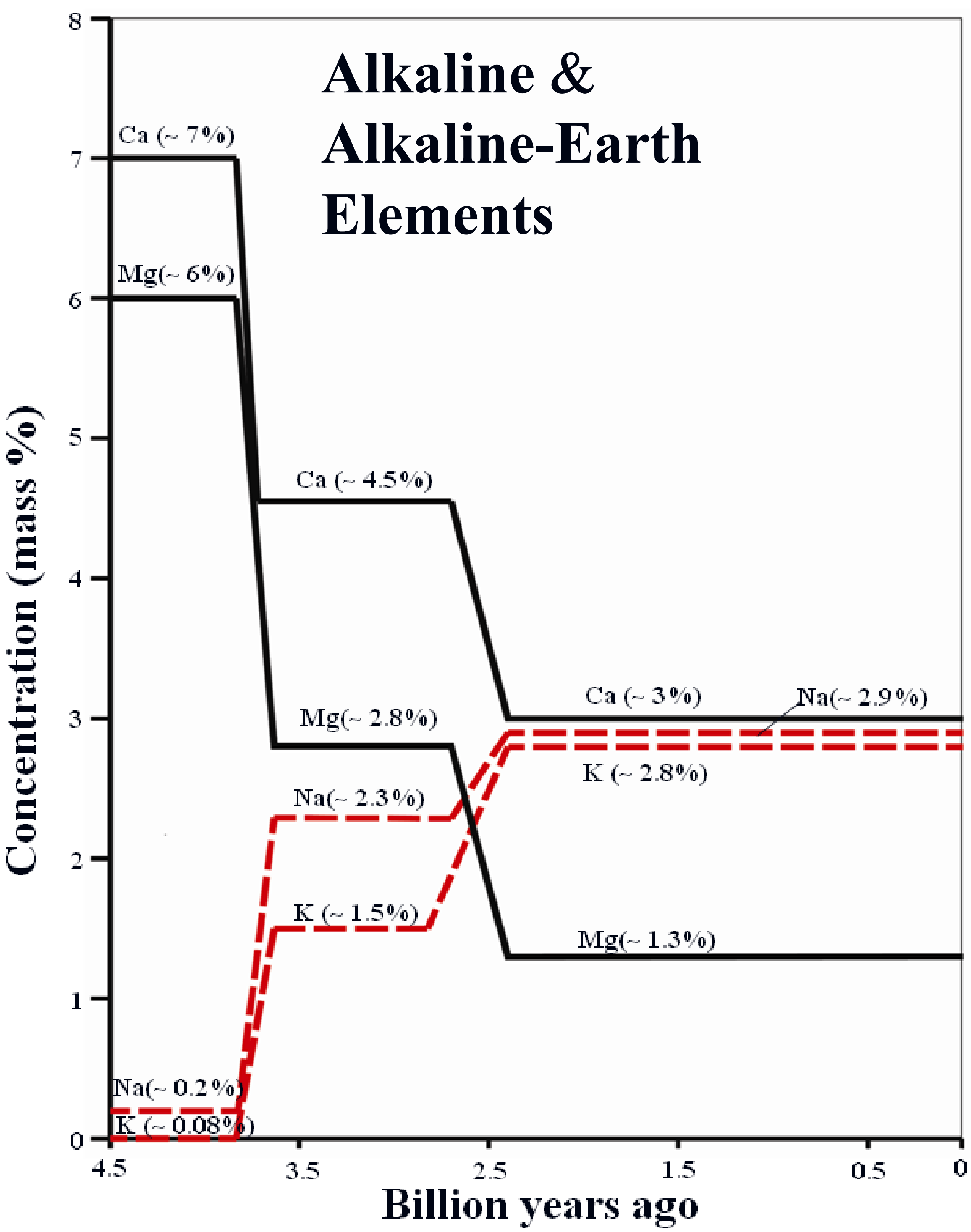

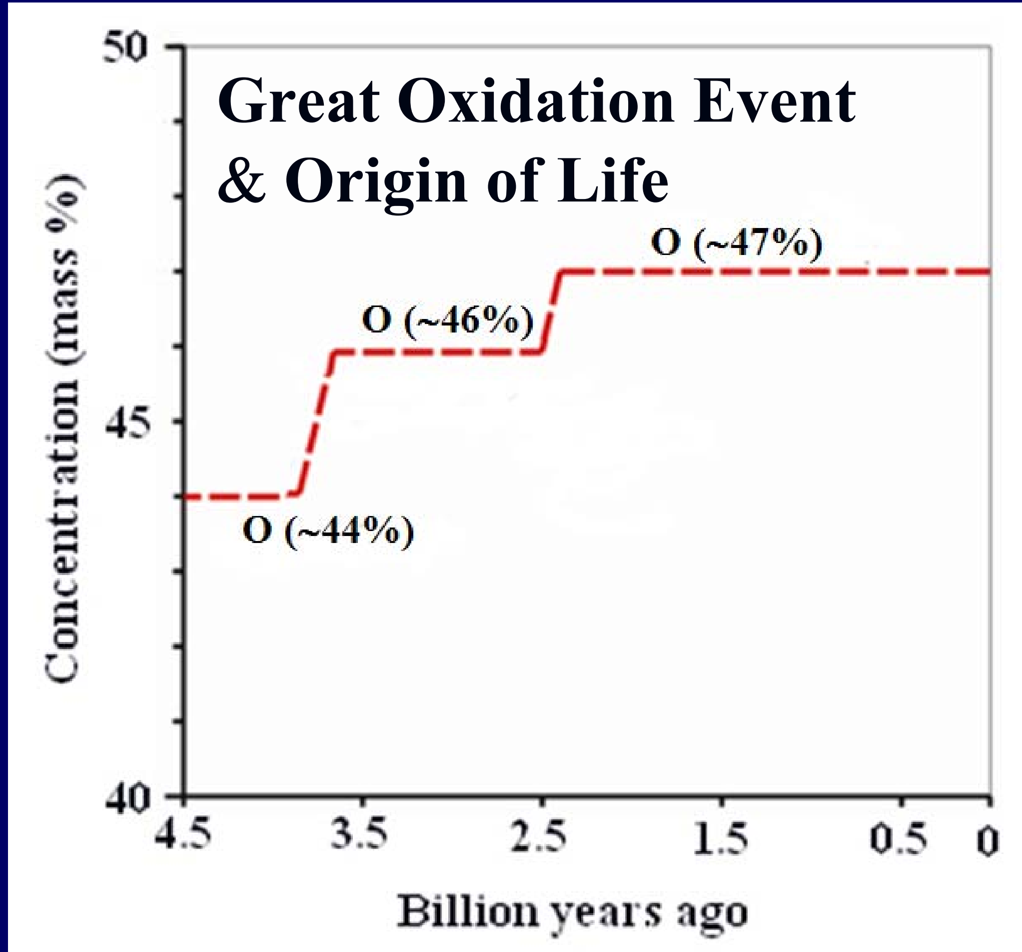

3.8 Billion years ago:
Ca (–2.5%) + Mg(–3.2%) =
= K (+1.4%) + Na (+2.1%) + O (+2.2%)

2.5 Billion years ago:
Ca (–1.5%) + Mg(–1.5%) =
=K (+1.3%) + Na (+0.6%) + O (+1.1%)

Conjecture about Alkaline-Earth elements' transformations

(7) $Mg_{12}^{24} \rightarrow Na_{11}^{23} + H_1^1$

(8) $Mg_{12}^{24} \rightarrow O_8^{16} + 2H_1^1 + He_2^4 + 2n$

(9) $Mg_{12}^{24} \rightarrow 2C_6^{12}$

(10) $Ca_{20}^{40} \rightarrow K_{19}^{39} + H_1^1$

(11) $Ca_{20}^{40} \rightarrow 2O_8^{16} + 4H_1^1 + 4n$

(12) $Ca_{20}^{40} \rightarrow 3C_6^{12} + He_2^4$

Conjecture about Alkaline-Earth elements' transformations

$$(7)\quad Mg_{12}^{24} \rightarrow Na_{11}^{23} + H_1^1$$

$$(8)\quad Mg_{12}^{24} \rightarrow O_8^{16} + 2H_1^1 + He_2^4 + 2n$$

$$(9)\quad Mg_{12}^{24} \rightarrow 2C_6^{12}$$

$$(10)\quad Ca_{20}^{40} \rightarrow K_{19}^{39} + H_1^1$$

$$(11)\quad Ca_{20}^{40} \rightarrow 2O_8^{16} + 4H_1^1 + 4n$$

$$(12)\quad Ca_{20}^{40} \rightarrow 3C_6^{12} + He_2^4$$

Primordial Atmosphere

Conjecture about Alkaline-Earth elements' transformations

(7) $$Mg_{12}^{24} \rightarrow Na_{11}^{23} + H_1^1$$

(8) $$Mg_{12}^{24} \rightarrow O_8^{16} + 2H_1^1 + He_2^4 + 2n$$

(9) $$Mg_{12}^{24} \rightarrow 2C_6^{12}$$

(10) $$Ca_{20}^{40} \rightarrow K_{19}^{39} + H_1^1$$

(11) $$Ca_{20}^{40} \rightarrow 2O_8^{16} + 4H_1^1 + 4n$$

(12) $$Ca_{20}^{40} \rightarrow 3C_6^{12} + He_2^4$$

Ocean Formation

Calcium depletion and ocean formation

Global decrease in Ca (–4.0%) is counterbalanced by an increase in K (+2.7%) and in H_2O (+1.3%).

$$Ca_{20}^{40} \rightarrow K_{19}^{39} + H_1^1$$
$$Ca_{20}^{40} \rightarrow 2O_8^{16} + 4H_1^1 + 4n$$

Assuming a mean density of the Earth Crust equal to 3.6 g/cm3 and a thickness of ~60 km, the partial mass decrease in Ca due to the second reaction is about 1.41×10^{21} kg.

Considering a global ocean surface of 3.61×10^{14} m^2, and an average depth of 3950 m, we obtain a mass of water of about 1.35×10^{21} kg

Partial decrease in Ca
1.41×10^{21} kg

$\Leftrightarrow$

Mass of H_2O in the oceans today
1.35×10^{21} kg

CHEMICAL COMPOSITION CHANGES AT THE LABORATORY SCALE

ENERGY DISPERSIVE X-RAY SPECTROSCOPY: COMPOSITIONAL ANALYSIS OF PRODUCT ELEMENTS

Two different kinds of samples were examined: (i) polished thin sections from the external surface; (ii) small portions from the fracture surface.

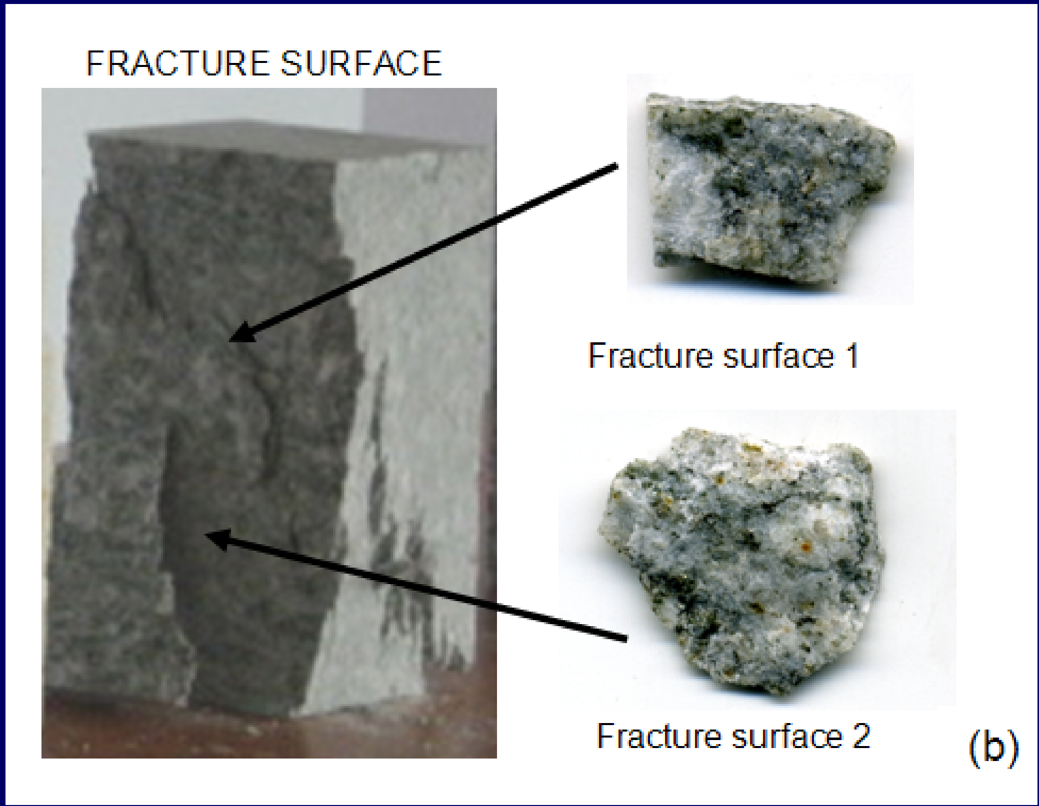

A quantitative analysis was performed on the collected spectra in order to recognize specific **variations in each element between external and fracture surfaces**.

Phengite (Granite)

	External surface mean value (wt%)	Fracture surface mean value (wt%)	Increase/ decrease with respect to phengite	Increase/ decrease with respect to the same element
Fe	6.2	4.0	–2.2%	–35%
Al	12.5	14.5	+2.0%	+16%
Si	28.0	27.8	NO VARIATIONS	NO VARIATIONS
Mg	0.7	0.8	NO VARIATIONS	NO VARIATIONS
K	8.0	7.7	NO VARIATIONS	NO VARIATIONS

$$Fe_{26}^{56} \rightarrow 2\,Al_{13}^{27} + 2\,n$$

Biotite (Granite)

	External surface mean value (wt%)	Fracture surface mean value (wt%)	Increase/ decrease with respect to biotite	Increase/ decrease with respect to the same element
Fe	21.2	18.2	–3.0 %	–14%
Al	8.1	9.6	+1.5 %	+18%
Si	18.4	19.6	+1.2 %	+6%
Mg	1.5	2.2	+0.7 %	+46%
K	6.9	7.1	NO VARIATIONS	NO VARIATIONS

$$Fe_{26}^{56} \rightarrow 2\,Al_{13}^{27} + 2n$$

$$Fe_{26}^{56} \rightarrow Si_{14}^{28} + Mg_{12}^{24} + 4n$$

Olivine (Basalt)

	External surface mean value (wt%)	Fracture surface mean value (wt%)	Increase/decrease with respect to Olivine	Increase/decrease with respect to the same element
Fe	18.4	14.4	−4.0%	−21%
Si	18.3	20.5	+2.2%	+12%
Mg	21.2	22.8	+1.6%	+7%
Ca	0.5	0.5	NO VARIATIONS	NO VARIATIONS

$$Fe^{56}_{26} \rightarrow Si^{28}_{14} + Mg^{24}_{12} + 4n$$

Magnetite

	External surface mean value (wt%)	Fracture surface mean value (wt%)	Increase/decrease with respect to Magnetite	Increase/decrease with respect to the same element
Fe	64.8	36.8	–27.9%	–56%
Al	–	10.1	+10.1%	BEFORE ABSENT
Mn	–	2.2	+2.2%	BEFORE ABSENT
Si	1.6	10.3	+8.7%	+540%
O	31.8	38.5	+6.7%	+21%

$$Fe_{26}^{56} \rightarrow 2\,Al_{13}^{27} + 2\,n$$

$$Fe_{26}^{56} \rightarrow Mn_{25}^{55} + H_{1}^{1}$$

$$Fe_{26}^{56} \rightarrow Si_{14}^{28} + O_{8}^{16} + 2He_{2}^{4} + 4n$$

Carrara Marble

	External surface mean value (wt%)	Fracture surface mean value (wt%)	Increase/ decrease with respect to Carrara Marble	Increase/ decrease with respect to the same element
Ca	13.4	9.8	–3.6 %	–26%
Mg	0.7	0.3	–0.4 %	–57%
O	45.8	36.8	–9.0 %	–19%
C	40.1	53.1	+13.0%	+32%

$$Ca^{40}_{20} \rightarrow 3C^{12}_{6} + He^{4}_{2}$$

$$Mg^{24}_{12} \rightarrow 2C^{12}_{6}$$

$$O^{16}_{8} \rightarrow C^{12}_{6} + He^{4}_{2}$$

SOLAR SYSTEM EVOLUTION: THE PLANET MARS

THREE DIFFERENT INVESTIGATIONS

Mars Odissey, Nasa 2001
Mars Global Surveyor, Nasa 1996

- **<u>Seismicity</u> monitoring by laser altimeter analysis**
- **<u>Elemental Abundance</u> by Gamma-Ray Spectrometer**
- **<u>Neutron</u> Emissions**

Knapmeyer M. et al. “Working Models for Spatial Distribution and Level of Mars Seismicity” *J. of Geophys. Res*., 111, E11006, (2006).

Hahn, B., McLennan, S., “Gamma-Ray Spectometer Elemental Abundance Correlation with Martian Surface Age: Implication for Martian Crustal Evolution”. *Lunar and Planet. Sci.* 37,1904 (2006).

Mitrofanov, I. et al., “Maps of Subsurface Hydrogen from the High Energy Neutron Detector, Mars Odyssey”, *Science*, 297, 78-81, (2002).

Faults

Iron (≥ 15%)

Neutrons (> 0.18 cps)

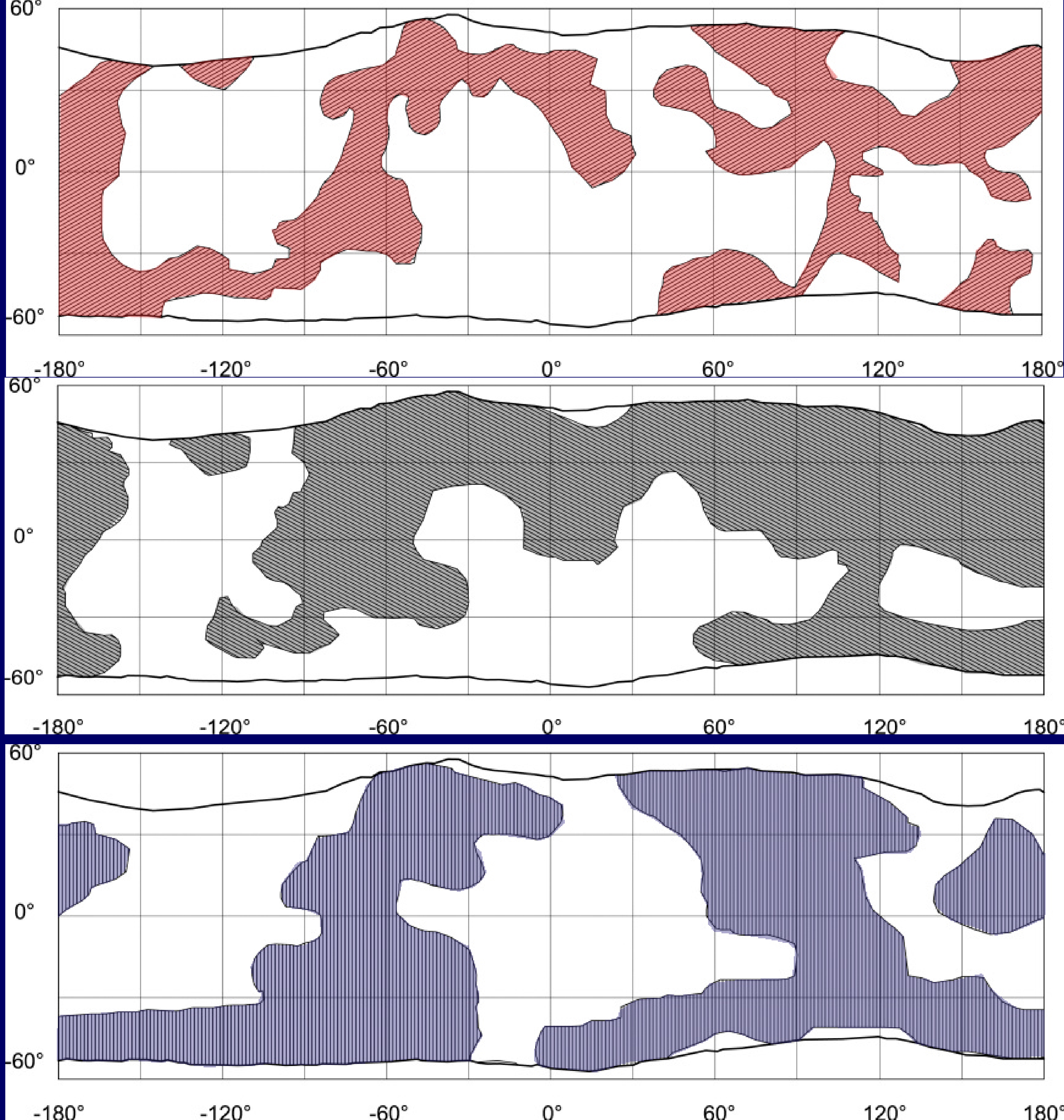

Faults vs Iron

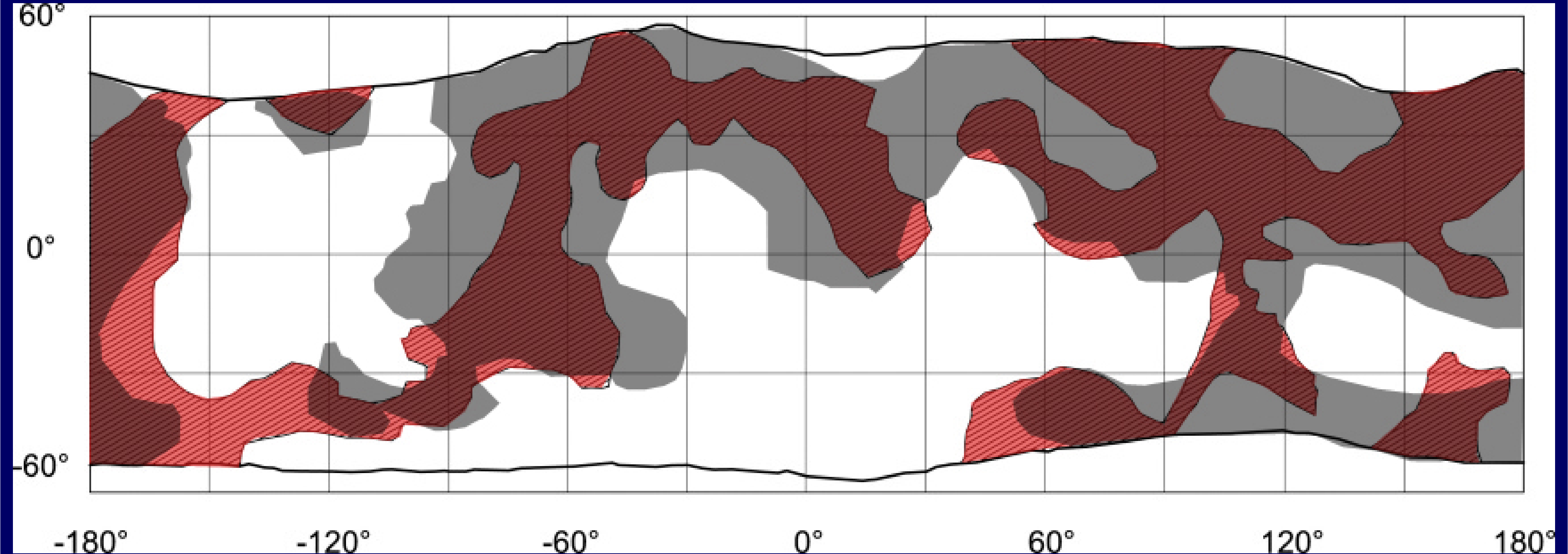

Faults

Iron (≥ 15%)

Faults vs Neutrons

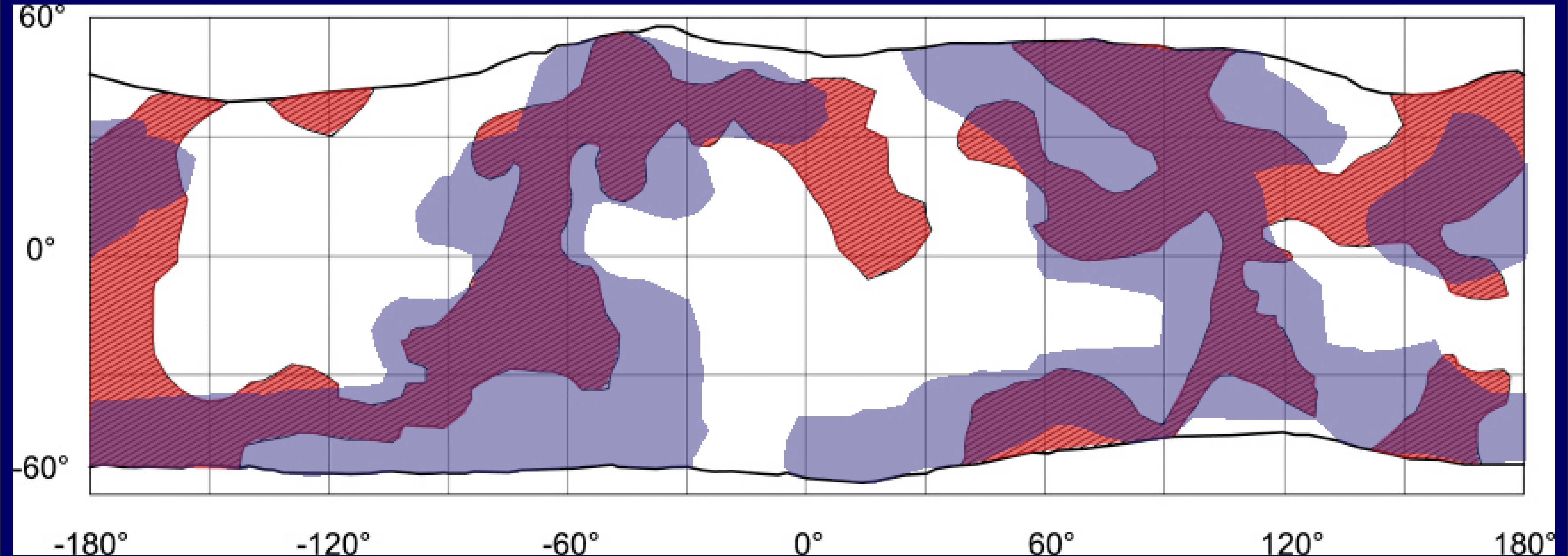

Faults

Neutrons (> 0.18 cps)

Iron vs Neutrons

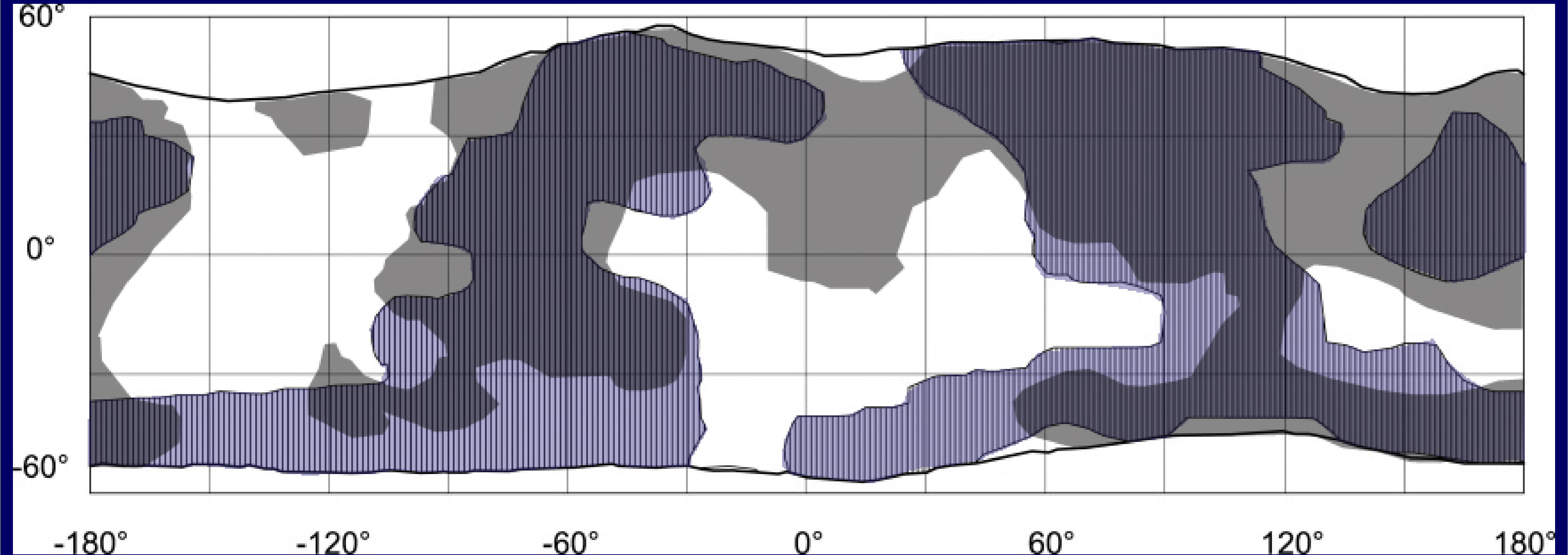

Iron (≥ 15%)

Neutrons (> 0.18 cps)

Element evolution: Ni-Fe transformation

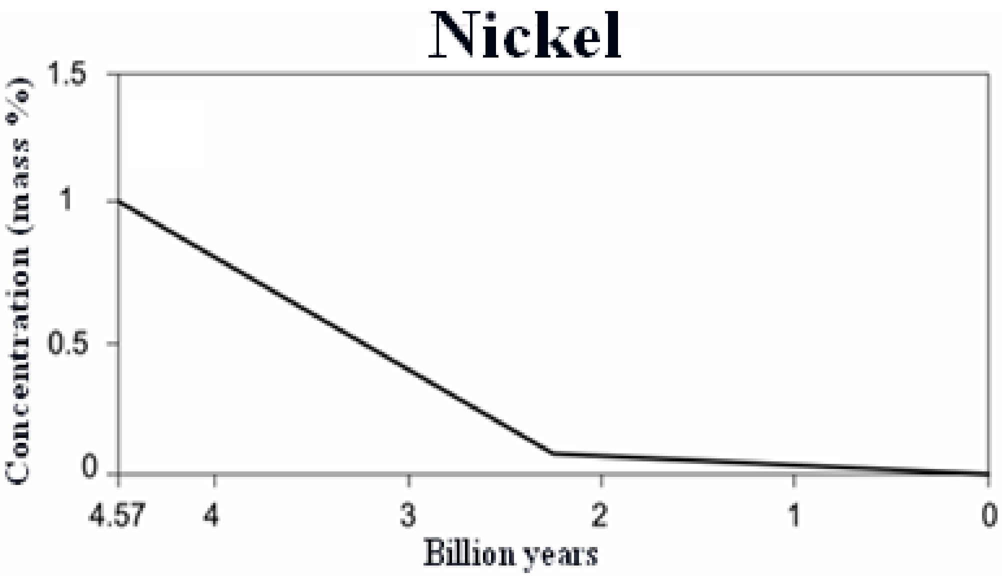

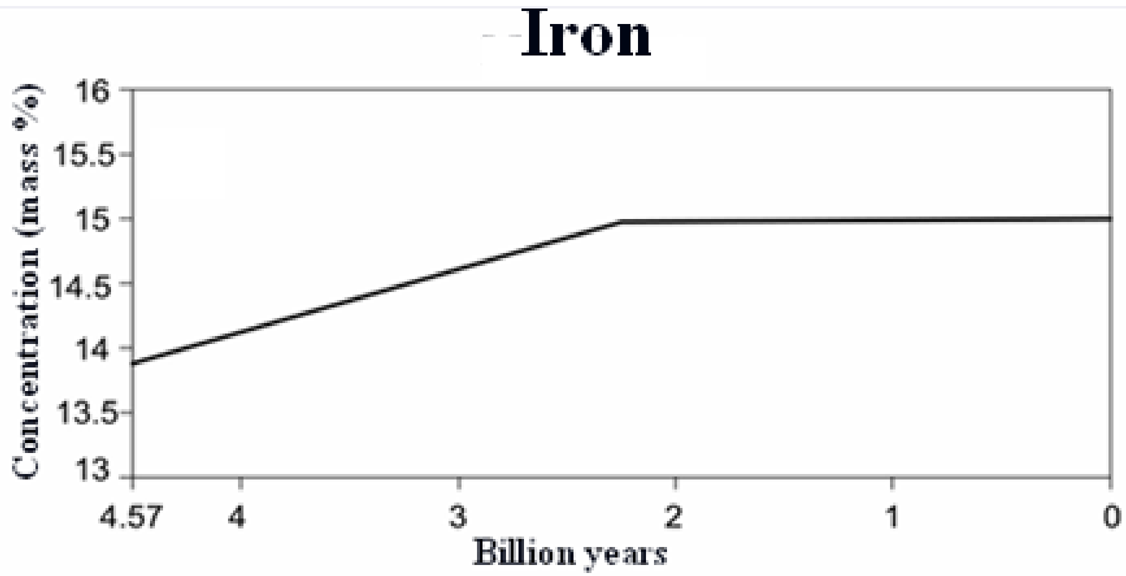

Ni decrease ~ Fe increase ~ 1.0%

$$Ni^{59}_{28} \rightarrow Fe^{56}_{26} + 2H^{1}_{1} + 1n$$

Hahn B. C., McLennan S. M. (2006) Gamma-Ray Spectometer Elemental Abundance Correlation with Martian Surface Age: Implication for Martian Crustal Evolution. *Lunar and Planetary Science* XXXVII.

Element evolution: K-Cl and K-Ar transformations

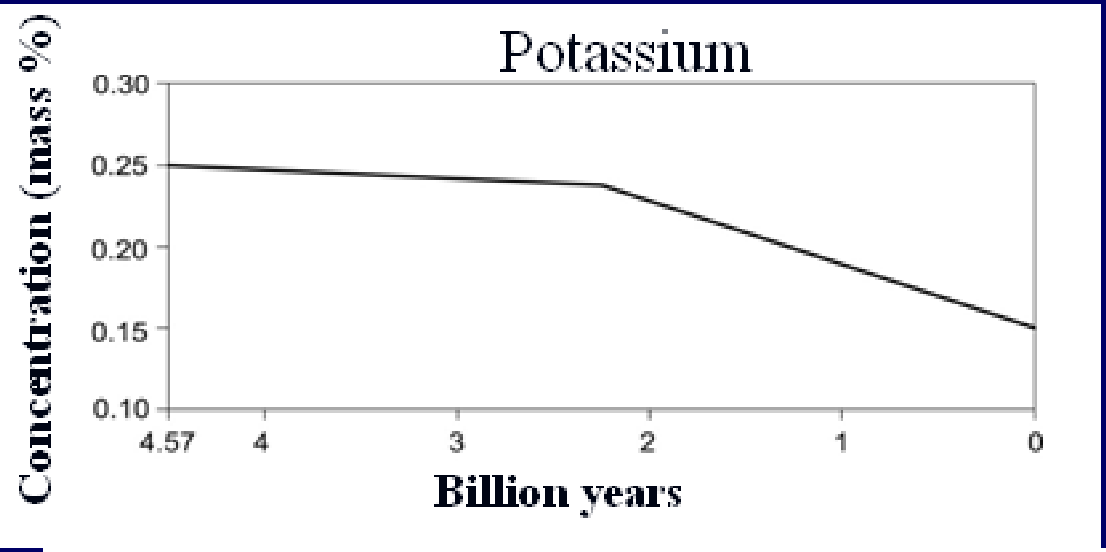

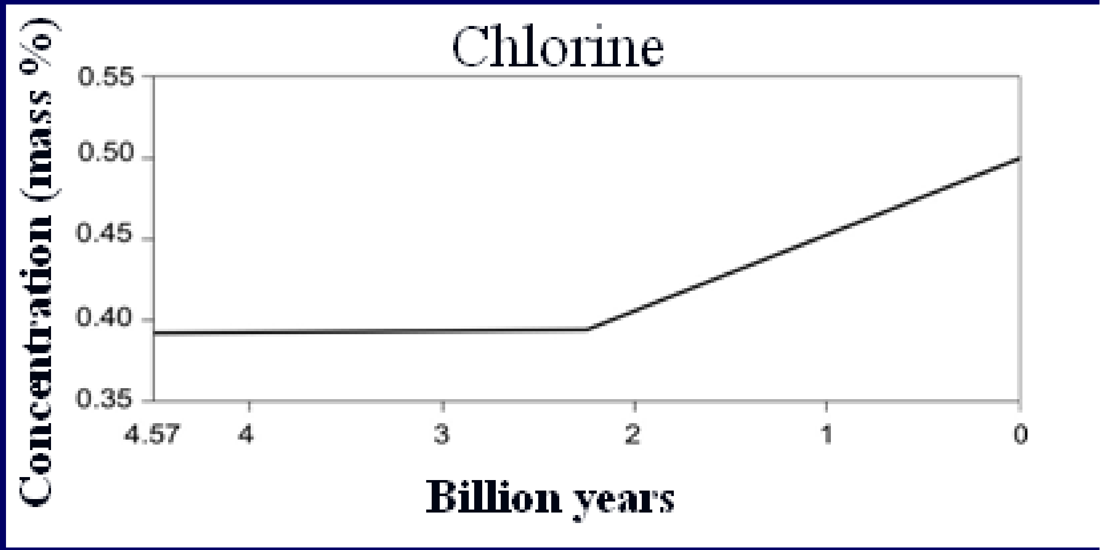

$$K_{19}^{39} \rightarrow Cl_{17}^{35} + 2H_{1}^{1} + 2n$$

A small quantity of the K decrease may be responsible for the Ar concentration evolution in the Mars athmosphere.

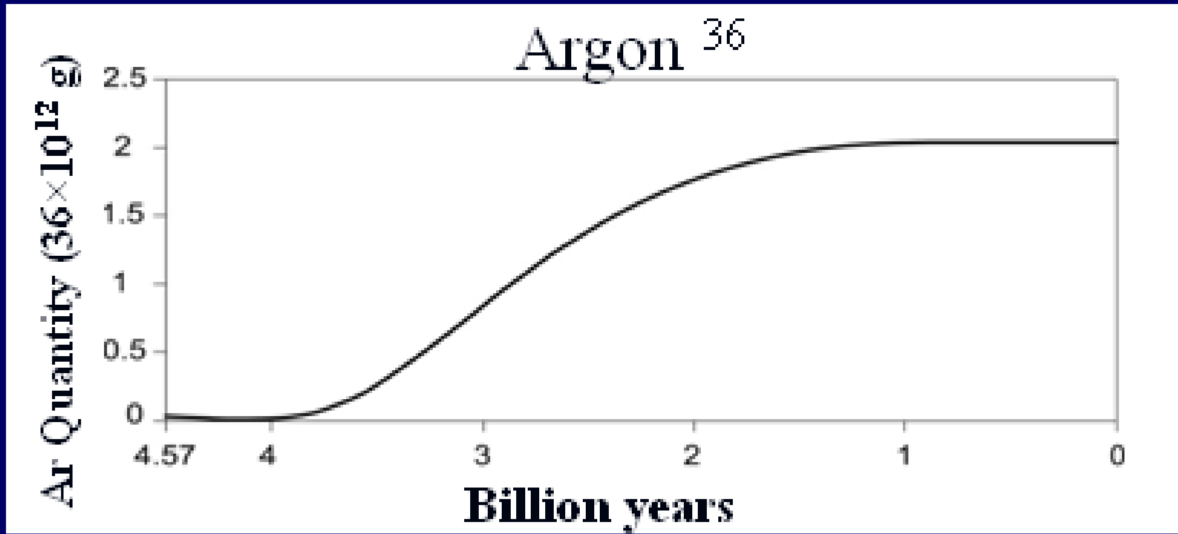

$$K_{19}^{39} \rightarrow Ar_{18}^{36} + H_{1}^{1} + 2n$$

HYDROGEN EMBRITTLEMENT, MICRO-CRACKING, AND FRACTURE IN “COLD FUSION” EXPERIMENTS

CHARACTERISTIC PHENOMENA IN THE SO-CALLED COLD FUSION (CF)

- 1989 - Fleishman & Pons → Heat Generation
- 1998 - Mizuno → Heat Generation, Neutron Emission, Compositional changes
- 2008 - Mosier-Boss et al. → Heat Generation, Neutron Emission, Compositional changes, Alpha particle emissions

---

Fleischmann, Pons, Hawkins, 1989. J. Electroanalitical Chemistry

Mizuno, 1998. Infinite Energy Press.

Mosier-Boss, P.A., et al., 2008. Eur. J. of Applied Physics

Cold Fusion vs Piezonuclear Reactions

"A unified interpretation and theory of these phenomena has not been accepted and their comprehension still remains unresolved" (***Preparata 1991***)

Is there a relation between the experimental evidence of the so-called "Cold Fusion", observed during the last two decades, and the Piezonuclear evidence recently observed from fracture of inert and nonradioactive materials?

Phenomena in common :

Neutron Emission

Alpha Emission

Compositional Changes

Micro-cracking and Fracture

Experimental Set-up

Electrolytic Cell

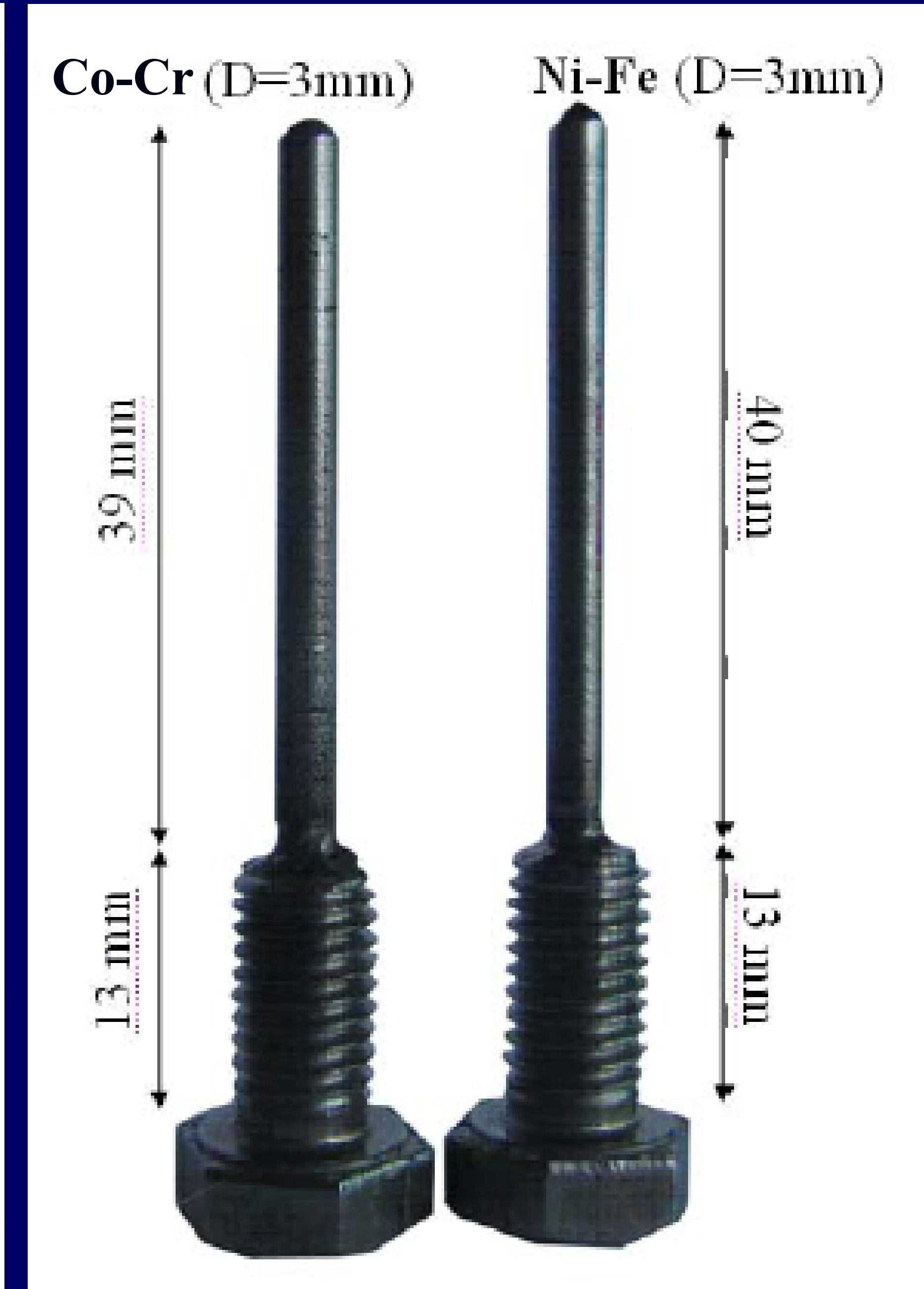

Electrodes

Neutron Emissions

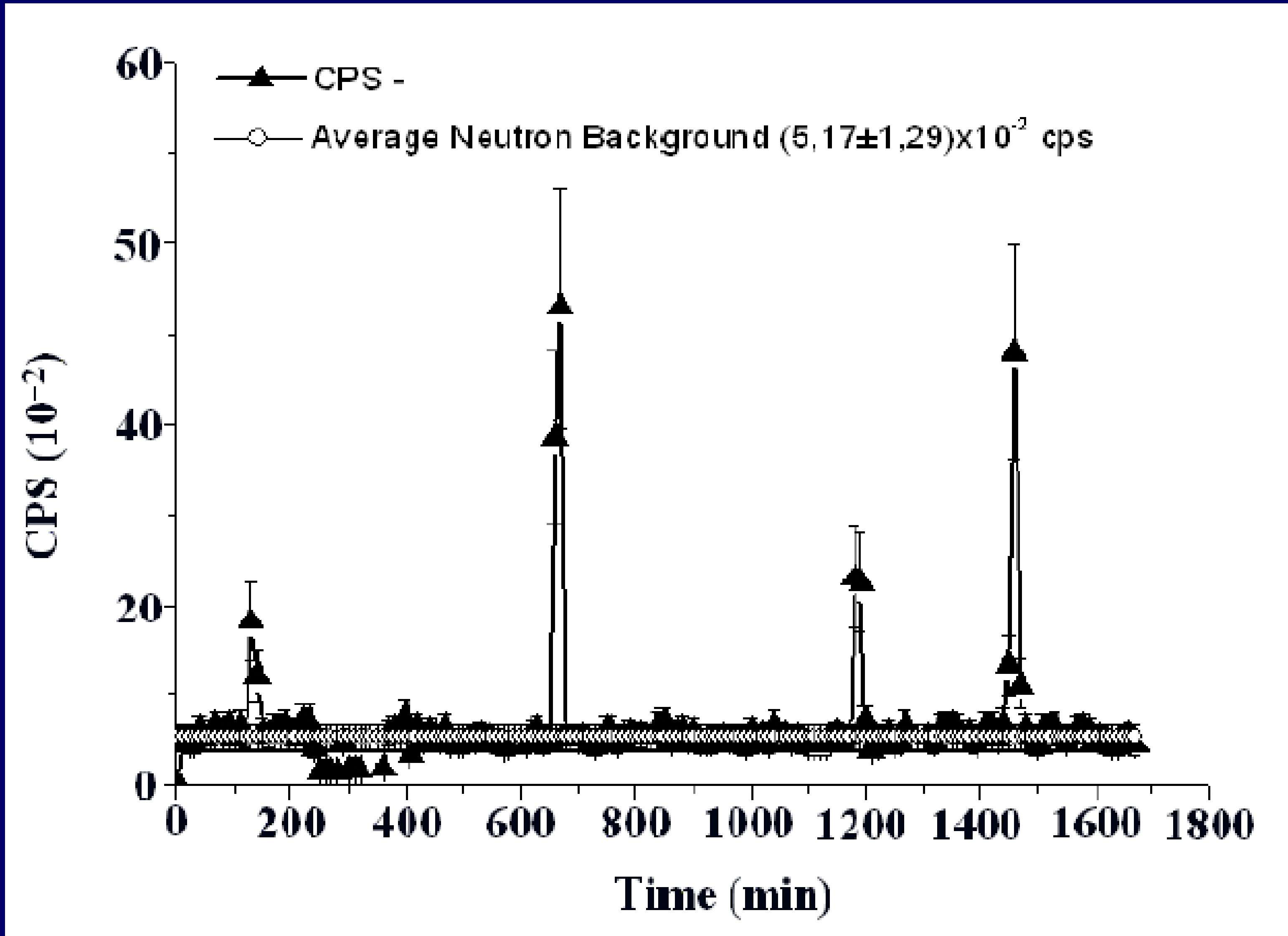

Instantaneous Neutron Emission between 4 and 10 times the background level

Alpha Particle Emissions

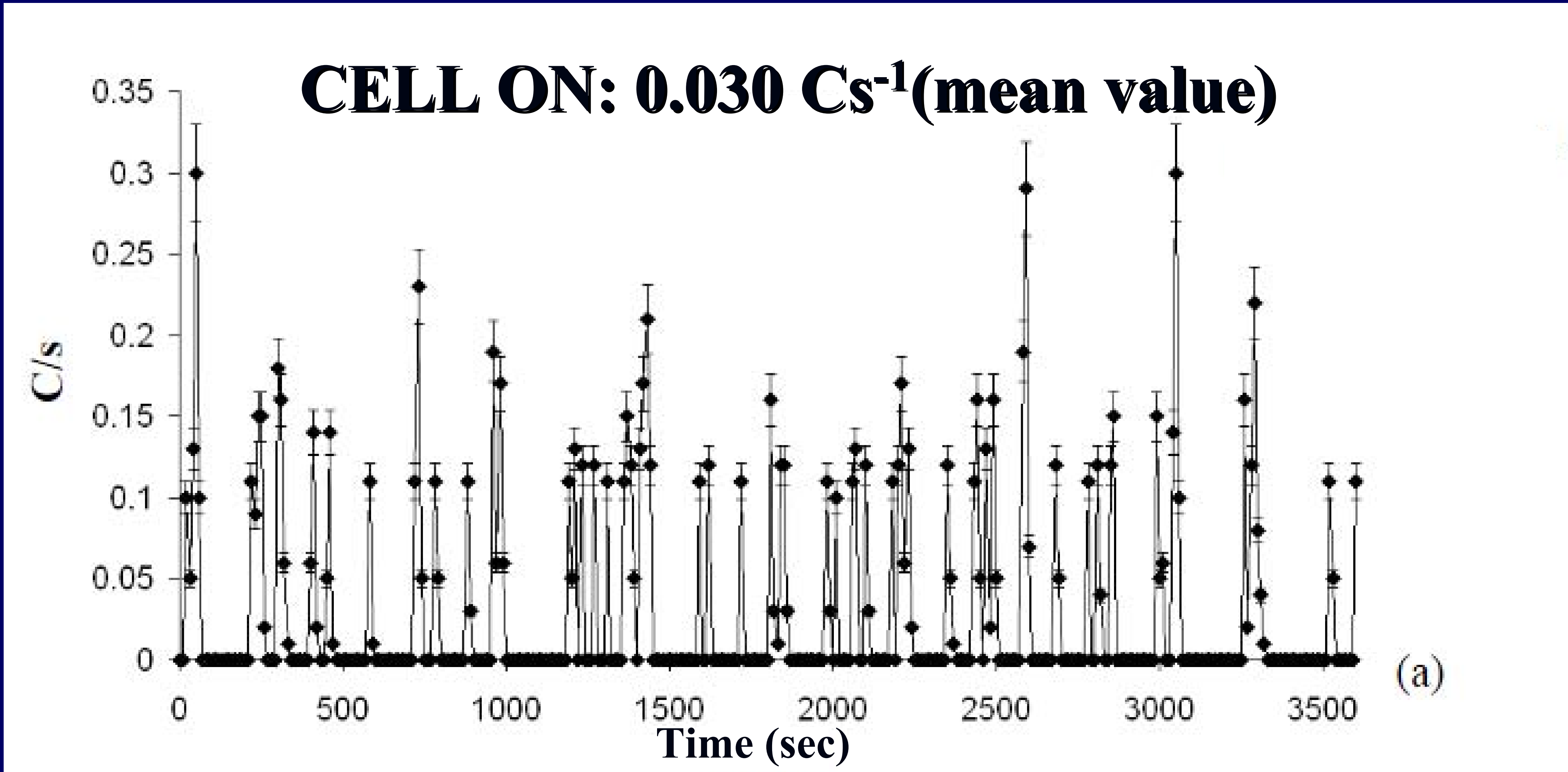

Total acquisition time: 1 hour

Alpha Particle Emissions

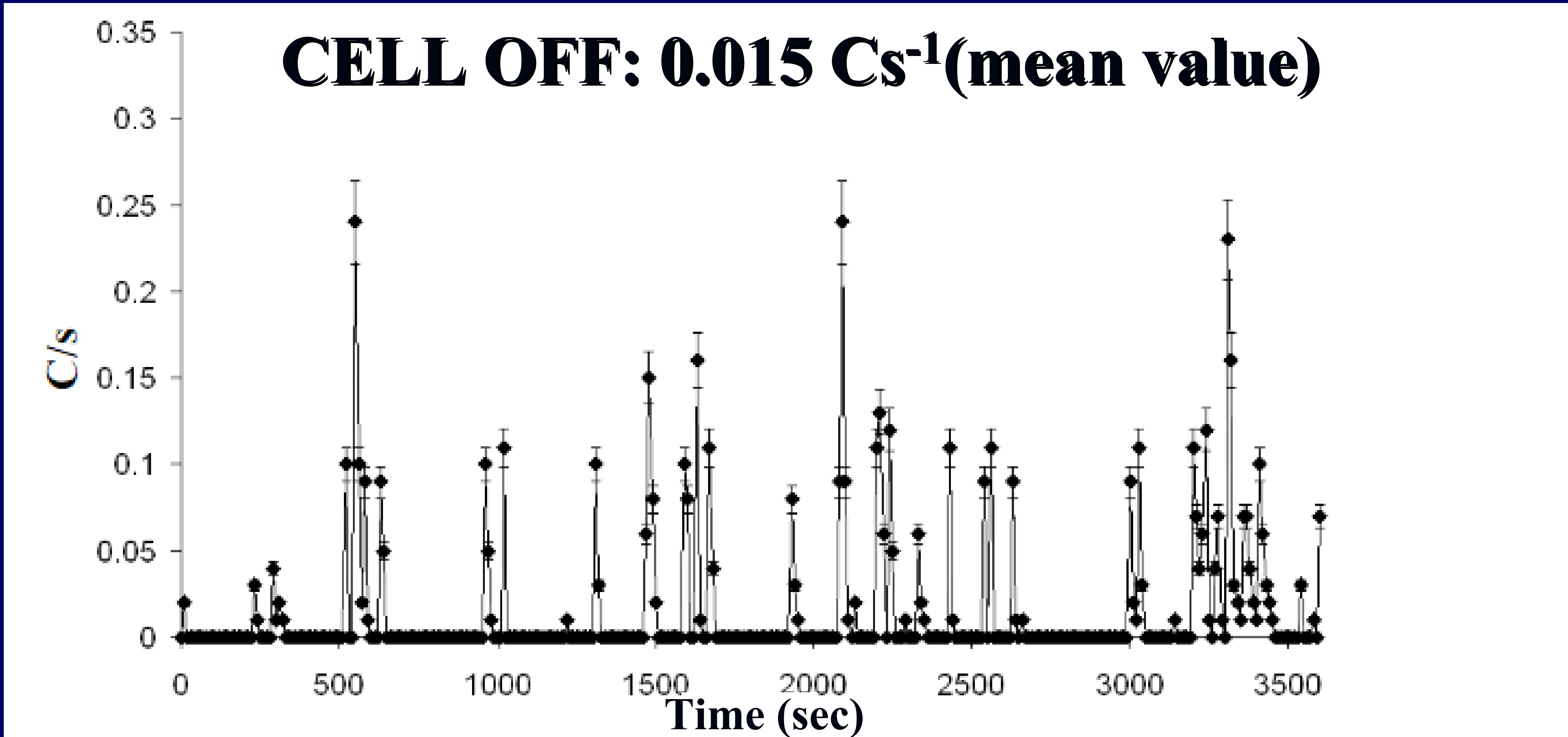

Total acquisition time: 1 hour

Cumulative Curves for the Alpha Emissions

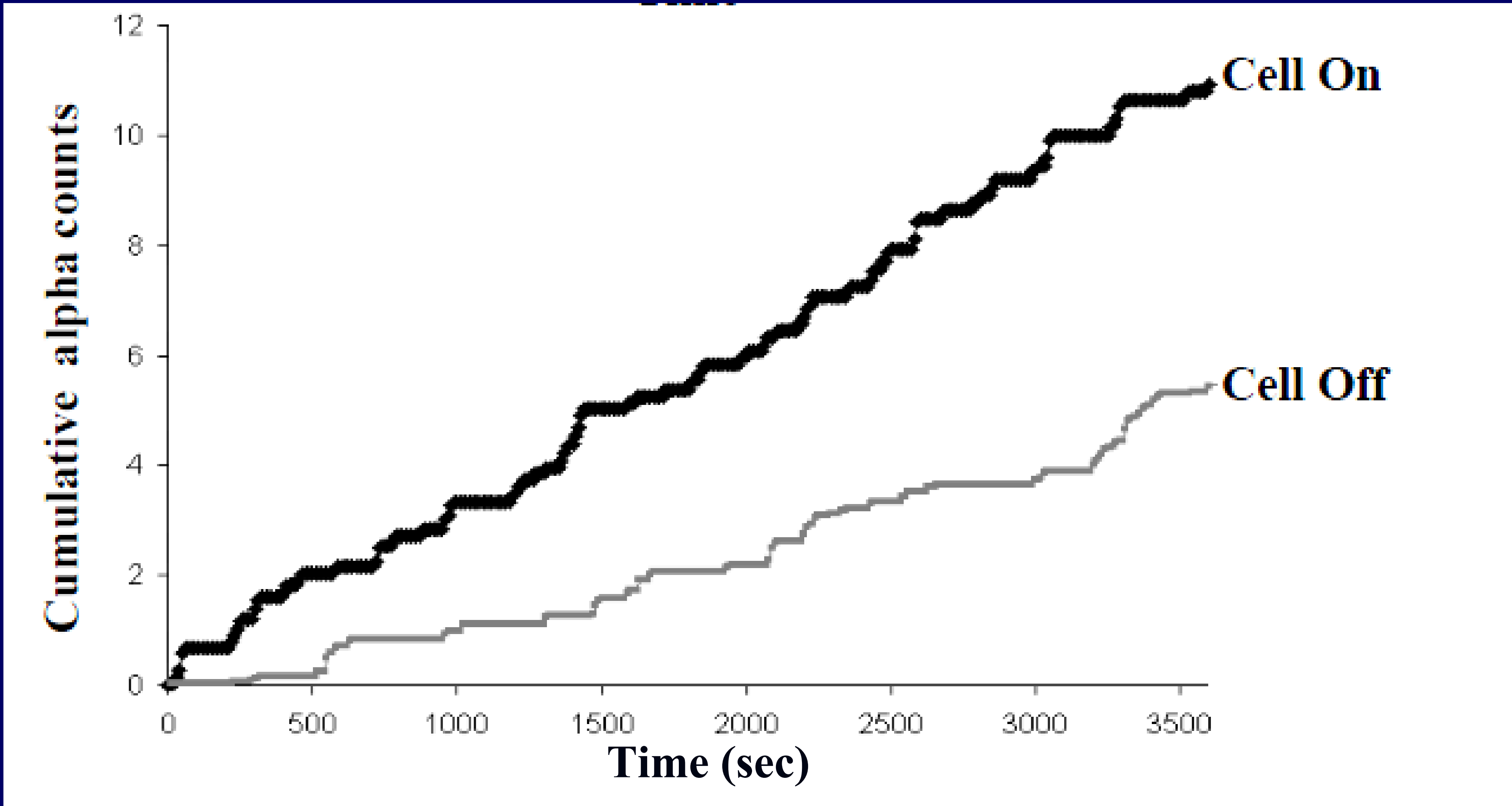

Co-Cr electrode surface BEFORE the test

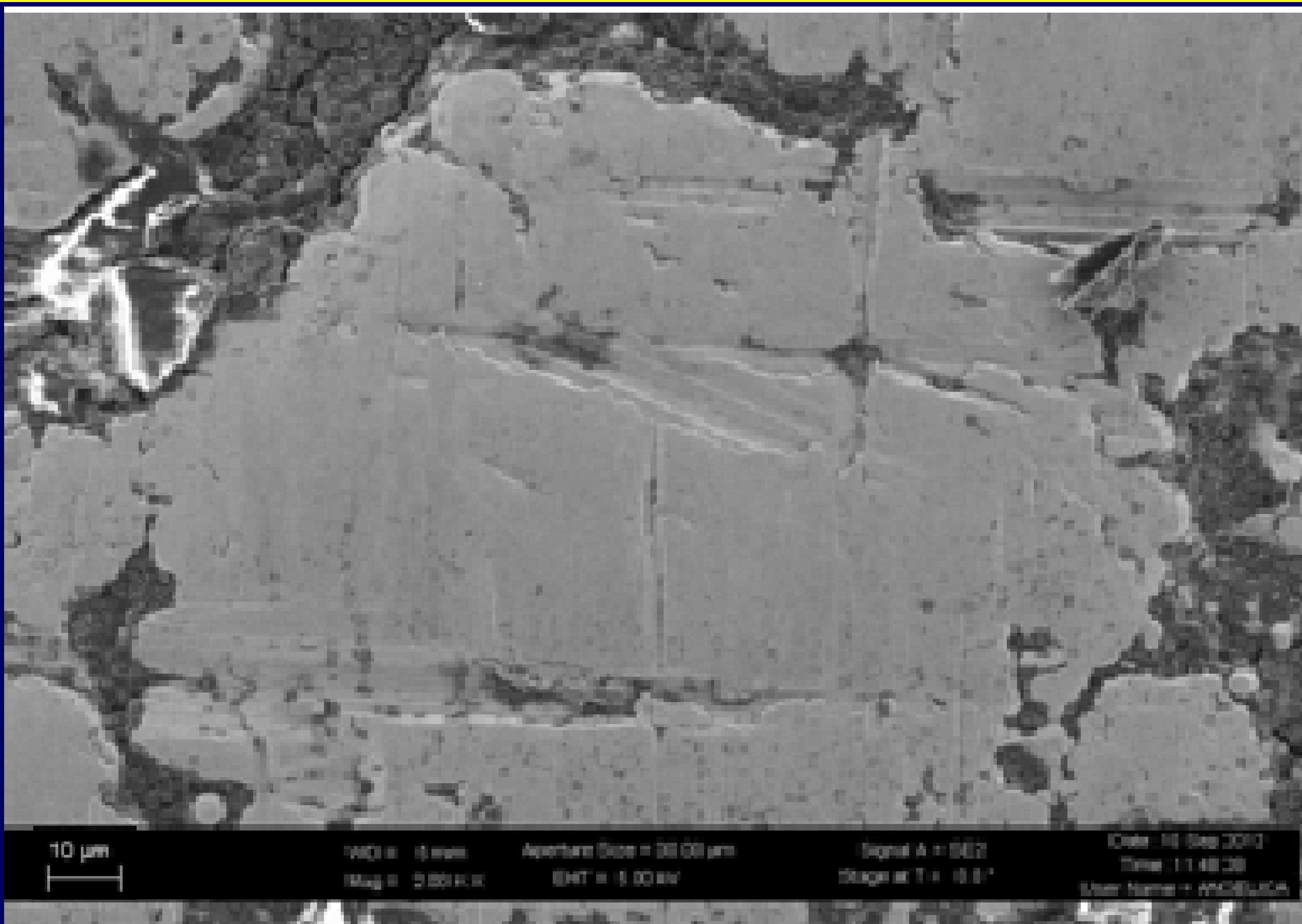

Co-Cr electrode surface AFTER the test

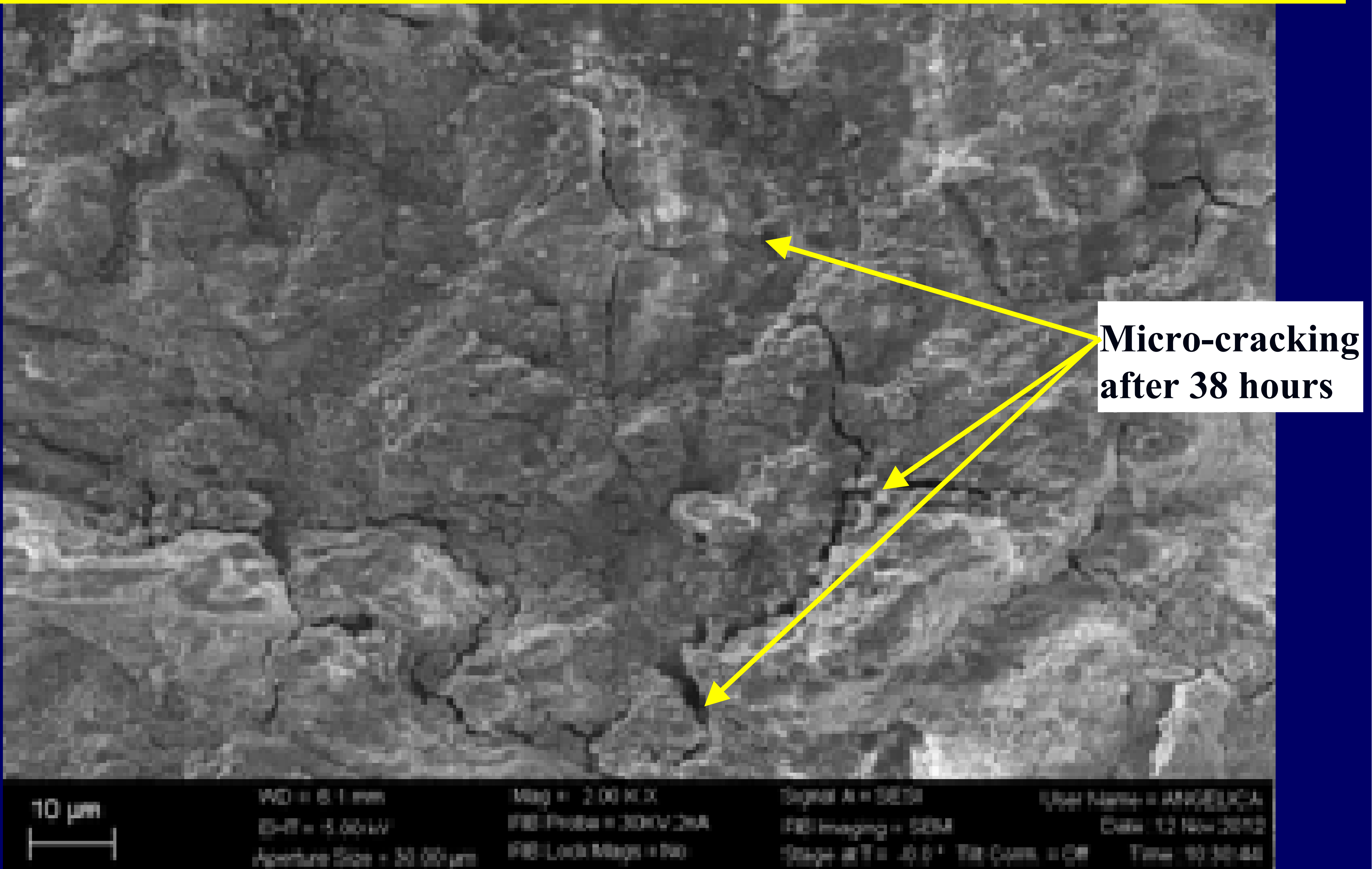

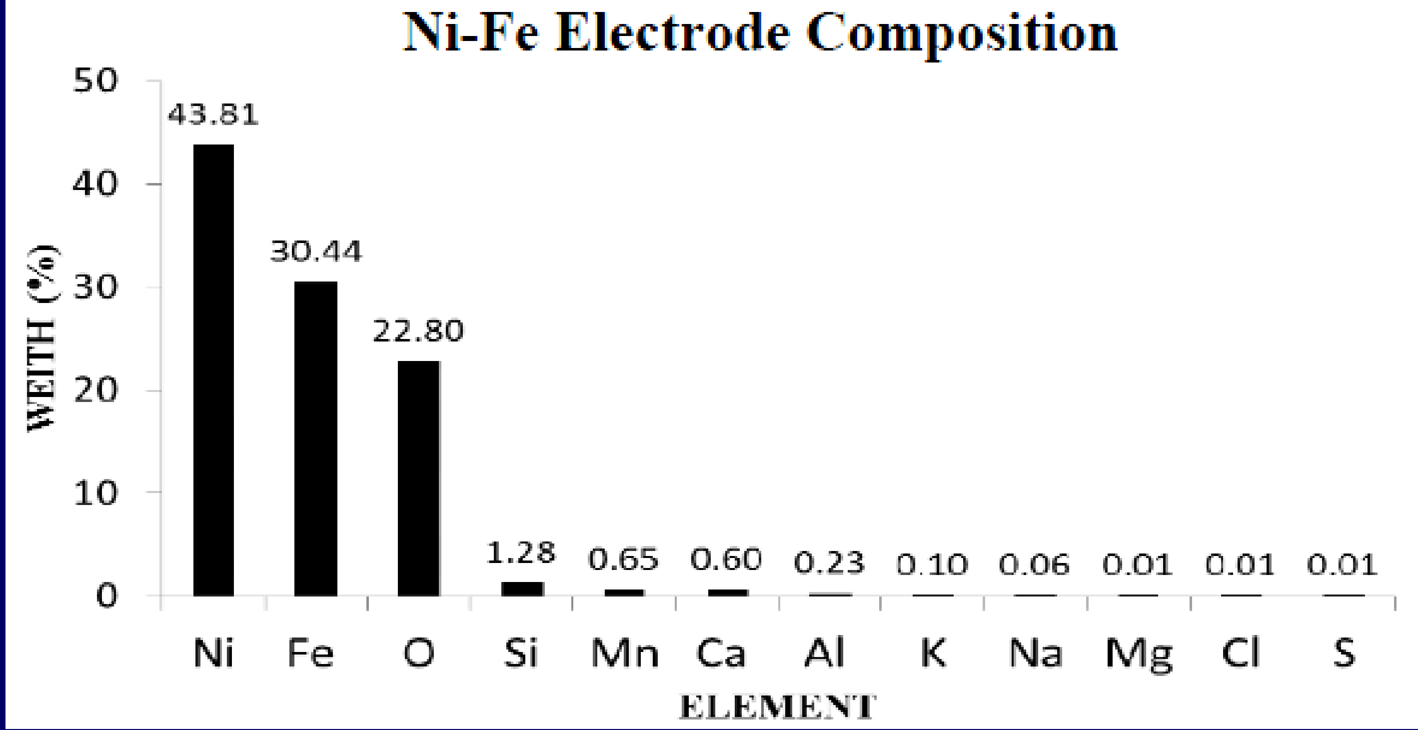
Ni-Fe Electrode Composition
WEITH (%)
ELEMENT
43.81
30.44
22.80
1.28
0.65
0.60
0.23
0.10
0.06
0.01
0.01
0.01
Ni Fe O Si Mn Ca Al K Na Mg Cl S
0 10 20 30 40 50

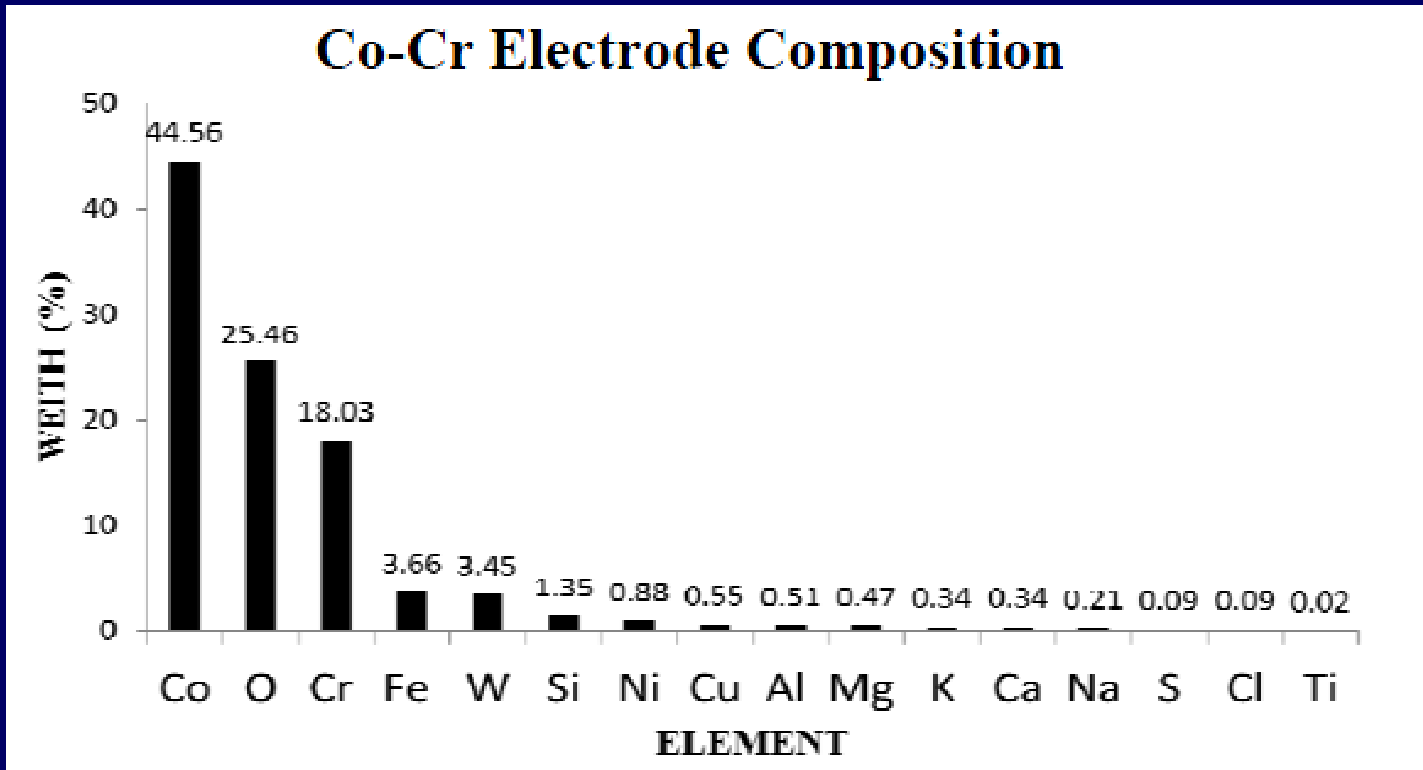
Co-Cr Electrode Composition
WEITH (%)
ELEMENT
44.56
25.46
18.03
3.66
3.45
1.35
0.88
0.55
0.51
0.47
0.34
0.34
0.21
0.09
0.09
0.02
Co O Cr Fe W Si Ni Cu Al Mg K Ca Na S Cl Ti
0 10 20 30 40 50

Ni-Fe Electrode : Compositional Changes

	Mean Values*				
Experiment	**Ni**	**Si**	**Mg**	**Fe**	**Cr**
After 0 h	43.9%	1.1%	0.1%	30.5%	-
After 4h	43.6%	0.5%	0.4%	30.7%	-
After 32h	35.2%	$\boxed{5.0\%}$	0.2%	27.9%	-
After 38h	$\boxed{35.3\%}$	1.5%	$\boxed{4.8\%}$	$\boxed{27.3\%}$	$\boxed{3.0\%}$

Ni (–8.6%) = Si (+3.9%) +Mg (+4.7%)

$$Ni^{58}_{28} \rightarrow 2Si^{28}_{14} + 2n$$

$$Ni^{58}_{28} \rightarrow 2Mg^{24}_{12} + 2He^{4}_{2} + 2n$$

Ni-Fe Electrode : Compositional Changes

	Mean Values*				
Experiment	Ni	Si	Mg	Fe	Cr
After 0 h	43.9%	1.1%	0.1%	30.5%	-
After 4h	43.6%	0.5%	0.4%	30.7%	-
After 32h	35.2%	$\boxed{5.0\%}$	0.2%	27.9%	-
After 38h	$\boxed{35.3\%}$	1.5%	$\boxed{4.8\%}$	$\boxed{27.3\%}$	$\boxed{3.0\%}$

Ni (–8.6%) = Si (+3.9%) +Mg (+4.7%)

$$Ni_{28}^{58} \rightarrow 2Si_{14}^{28} + 2n$$

$$Ni_{28}^{58} \rightarrow 2Mg_{12}^{24} + 2He_{2}^{4} + 2n$$

Fe (–3.2%) = Cr (+3.0%)

$$Fe_{26}^{56} \rightarrow Cr_{24}^{52} + He_{2}^{4}$$

Co-Cr Electrode : Compositional Changes

Experiment	Co	Fe	Cr	K
After 0 h	44.1%	3.1%	17.8%	0.5%
After 4h	43.7%	1.6%	17.8%	2.2%
After 32h	20.6%	26.3%	9.7%	12.9%

Co (–23.5%) = Fe (+23.2%)

$$Co_{27}^{59} \rightarrow Fe_{26}^{56} + H_1^1 + 2n$$

Co-Cr Electrode : Compositional Changes

Experiment	Co	Fe	Cr	K
After 0 h	44.1%	3.1%	17.8%	0.5%
After 4h	43.7%	1.6%	17.8%	2.2%
After 32h	20.6%	26.3%	9.7%	12.9%

Co (–23.5%) = Fe (+23.2%)

$$Co_{27}^{59} \rightarrow Fe_{26}^{56} + H_1^1 + 2n$$

Cr (–8.1%) + K_2CO_3 (–4.3%) = K (+12.4%)

$$Cr_{24}^{52} \rightarrow K_{19}^{39} + 2He_2^4 + H_1^1 + 4n$$

CONCLUSIONS

Two piezonuclear fission reaction jumps typical of the Earth Crust:

$$Fe_{26}, Co_{27}, Ni_{28} \longrightarrow Mg_{12}, Al_{13}, Si_{14} \longrightarrow C_6, N_7, O_8$$

Explanation for:

- Production of **NEUTRONS** (Rn, CO_2) during earthquakes
- **STEP-WISE TIME VARIATIONS** in the most abundant elements (including Na_{11}, K_{19}, Ca_{20})
- **SPACE LOCALIZATION** of the resources on the Earth's Crust
- Very high **CARBON** content in the primordial atmosphere
- Great Oxidation Event (2.5 Billion years ago), **OCEAN FORMATION** and origin of life

- Evolution of the planets of the **SOLAR SYSTEM**: Mercury, Mars, Jupiter, Saturn (and the Sun itself)

- The so-called **COLD NUCLEAR FUSION** may be explained by piezonuclear fission reactions occurring in the electrodes and due to **HYDROGEN EMBRITTLEMENT,** rather than by fusion of hydrogen isotopes

POSSIBLE APPLICATIONS

- Precurring and monitoring of **Earthquakes**
- Correct evaluation of **Carbon Pollution** & **Climate Changes**
- Production of **Clean energy** (?)

APPENDIX A

Phengite (Granite) : Fe concentrations

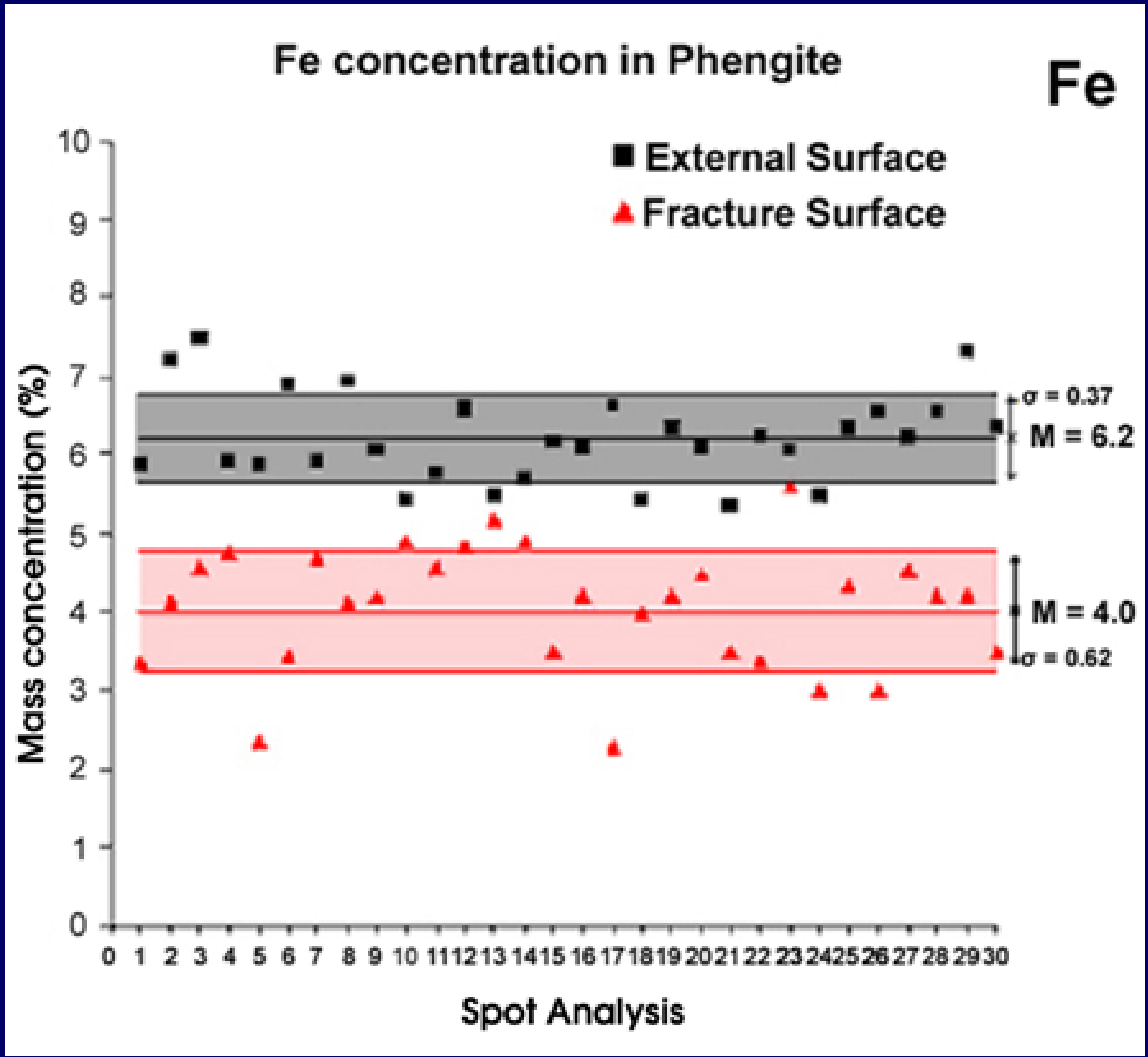

External Surf.:

Fe content = <u>6.2%</u>

Fracture Surf.:

Fe content = <u>4.0%</u>

Fe content decrease

–2.2%

Phengite (Granite) : Al concentrations

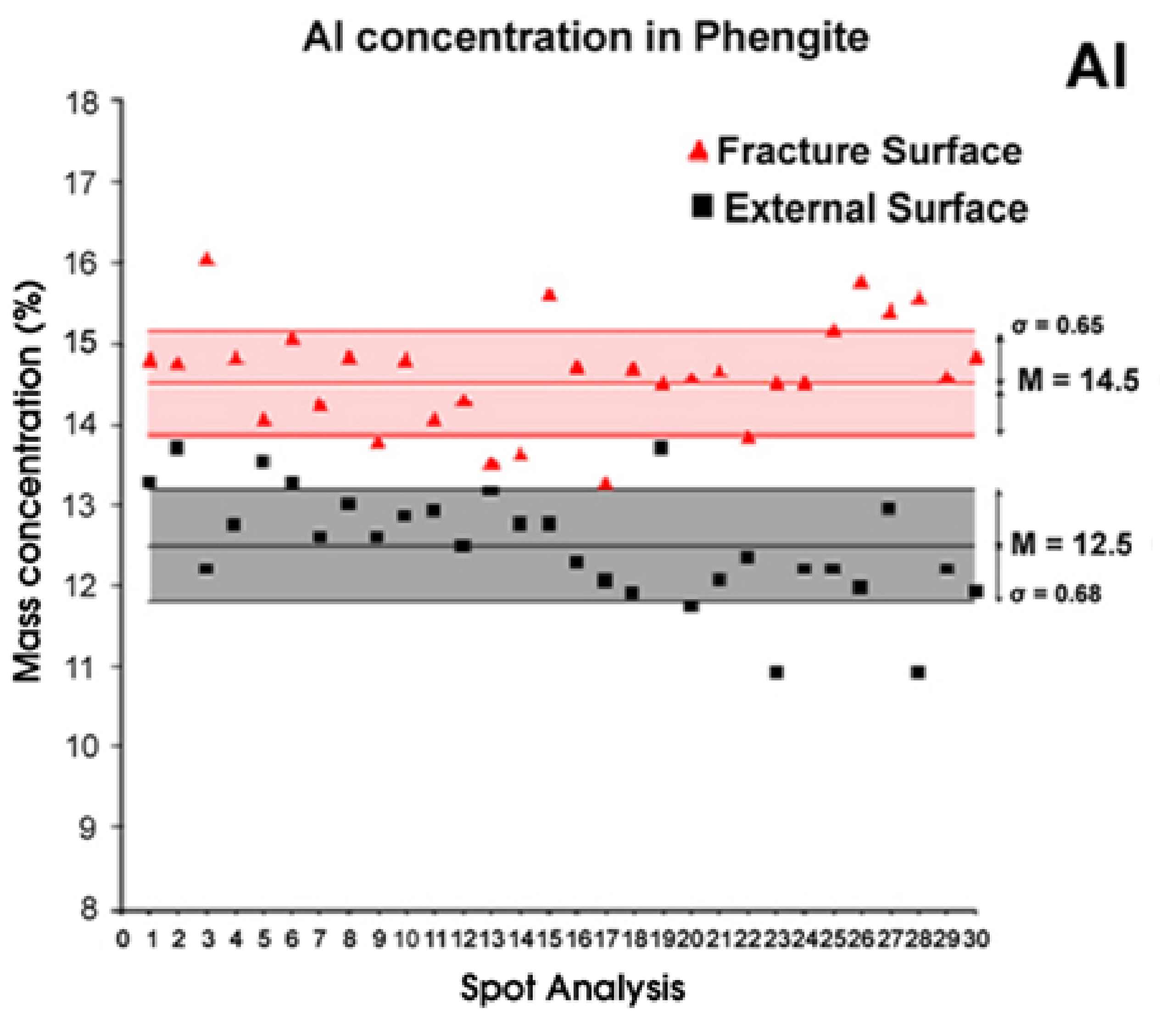

Fracture Surf.:

Al content = 14.5%

External Surf.:

Al content = 12.5%

Al content increase

+2.0%

Phengite (Granite) : Si, Mg and K concentrations

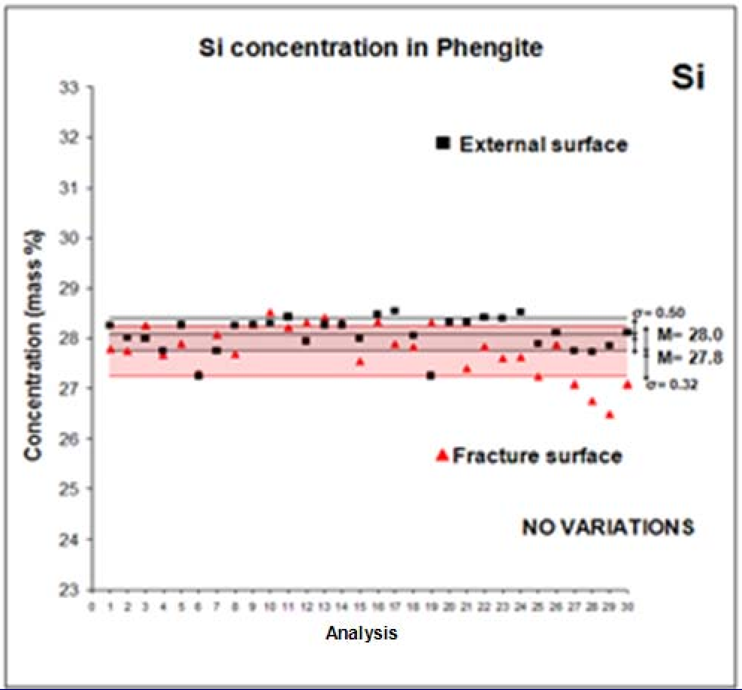

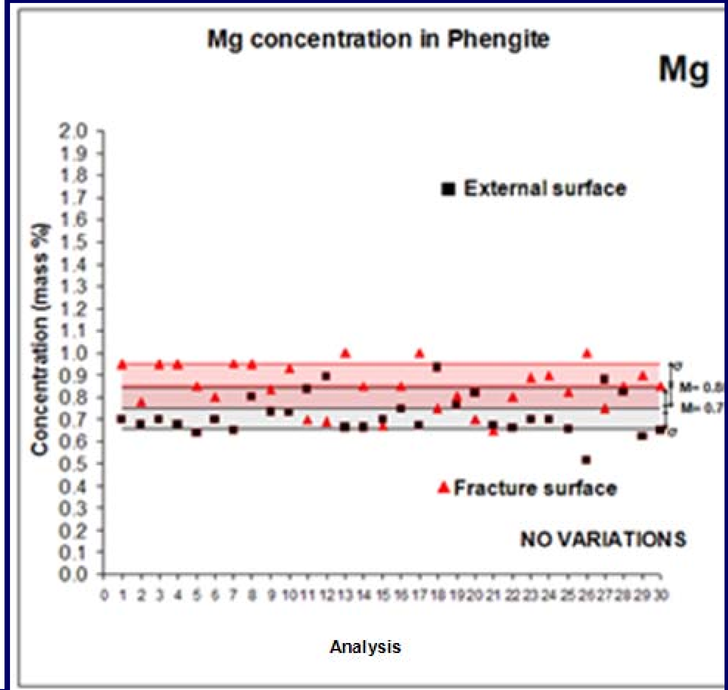

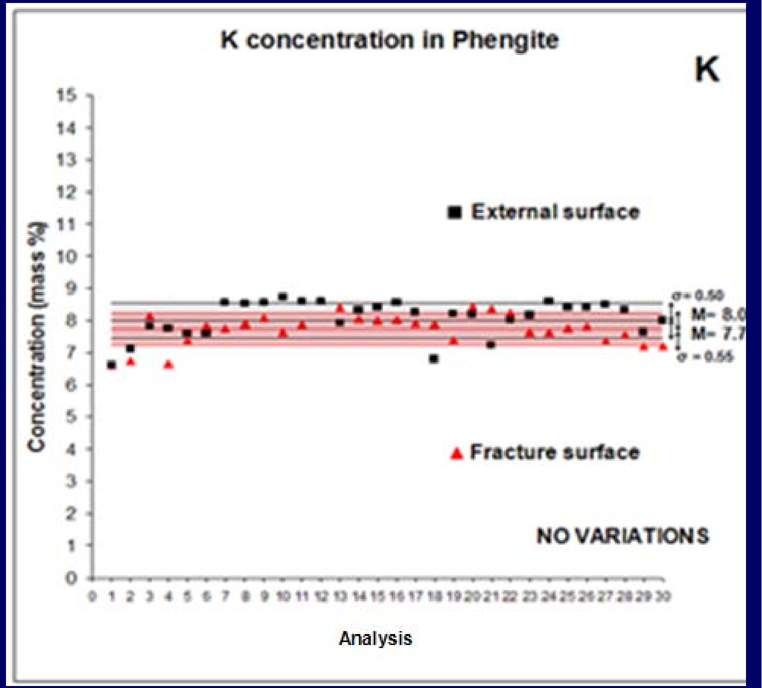

No appreciable variations can be recognized between the average values

Phengite (Granite)

	External surface mean value (wt%)	Fracture surface mean value (wt%)	Increase/ decrease with respect to phengite	Increase/ decrease with respect to the same element
Fe	6.2	4.0	–2.2%	–35%
Al	12.5	14.5	+2.0%	+16%
Si	28.0	27.8	NO VARIATIONS	NO VARIATIONS
Mg	0.7	0.8	NO VARIATIONS	NO VARIATIONS
K	8.0	7.7	NO VARIATIONS	NO VARIATIONS

$$Fe_{26}^{56} \rightarrow 2\,Al_{13}^{27} + 2\,n$$

Biotite (Granite): Fe concentrations

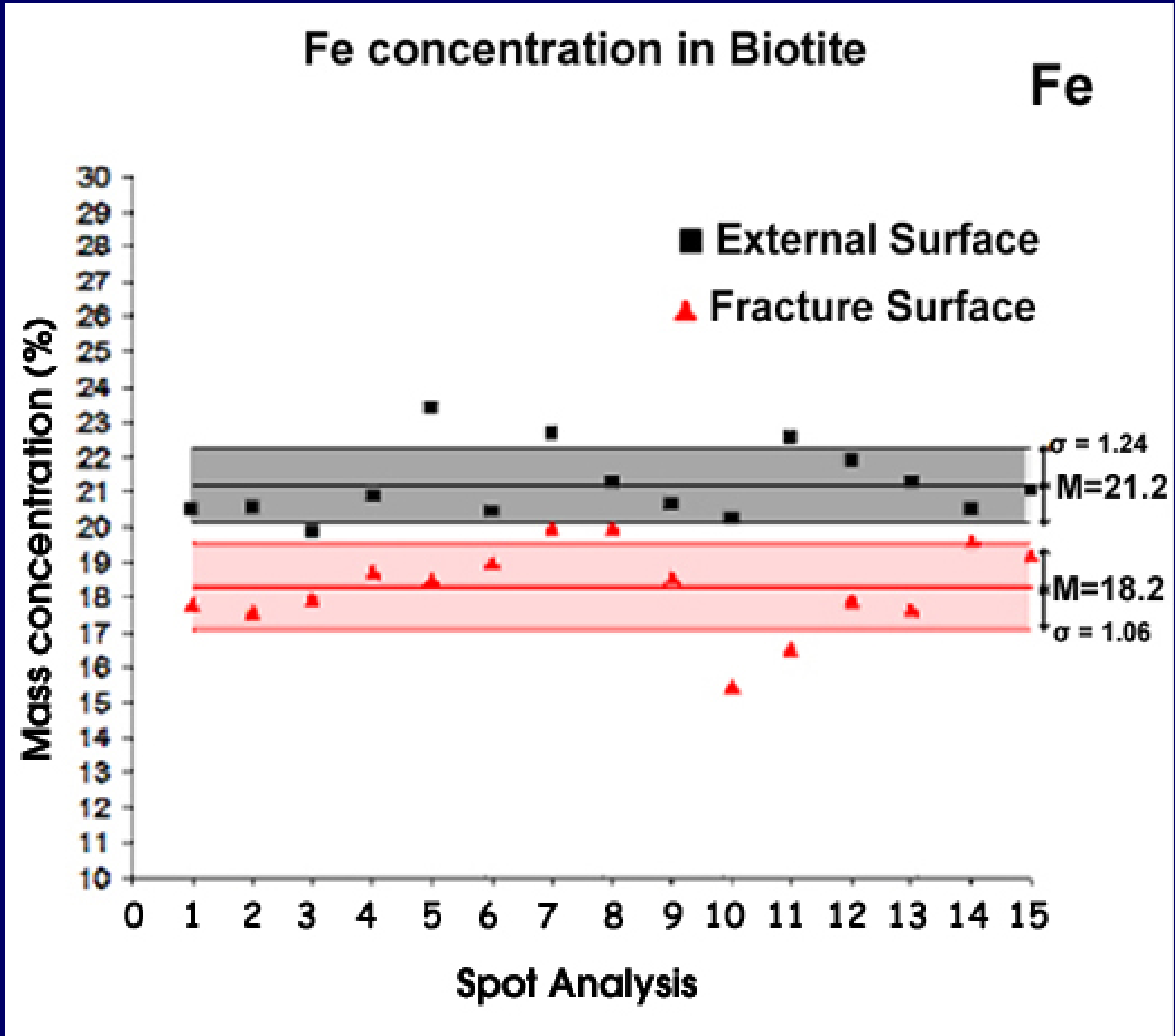

External Surf.:

Fe content = 21.2%

Fracture Surf.:

Fe content = 18.2%

Fe content decrease

–3.0%

Biotite (Granite) : Al concentrations

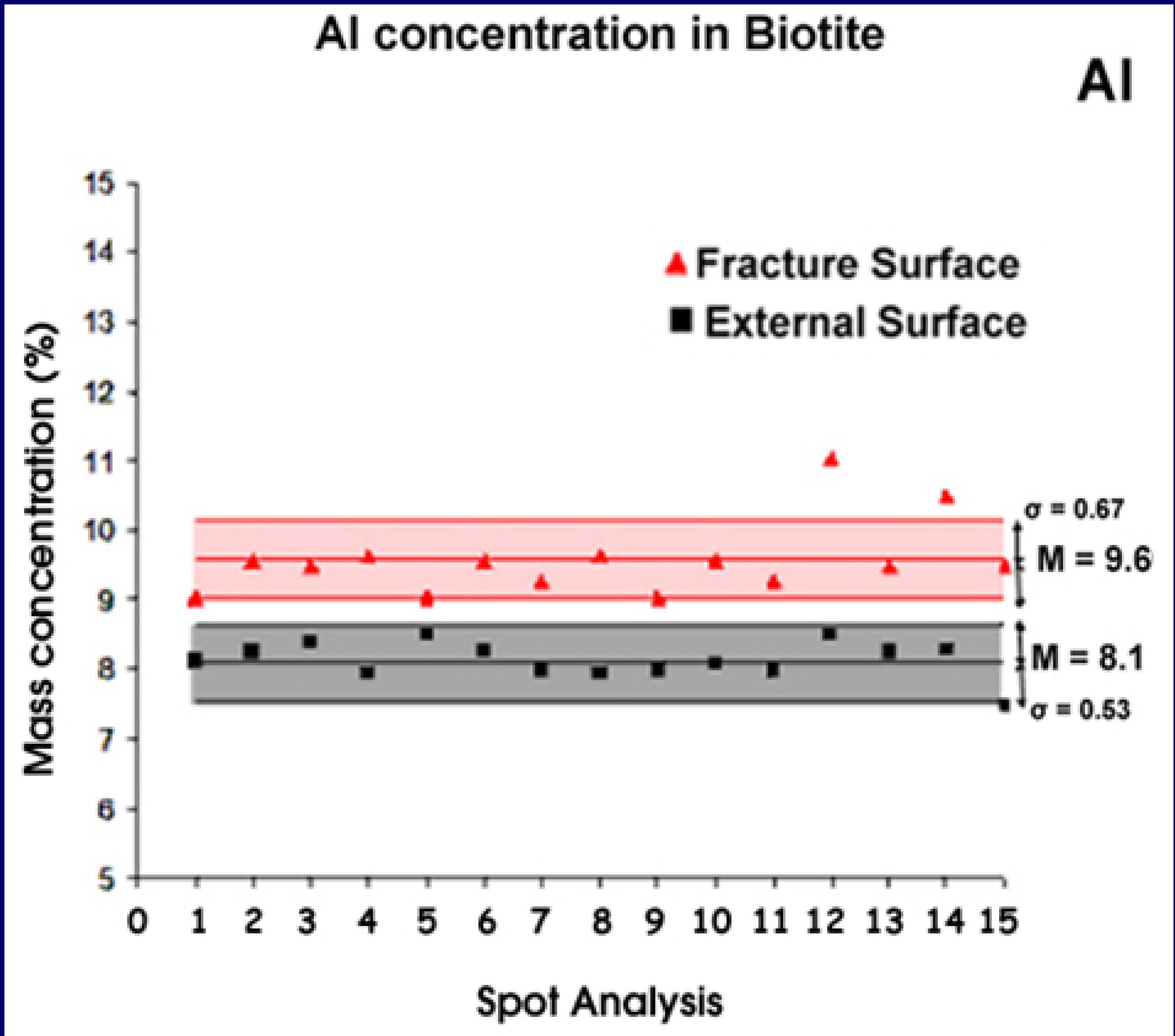

Fracture Surf.:

Al content = 9.6%

External Surf.:

Al content = 8.1%

Al content increase

+1.5%

Biotite (Granite) : Si concentrations

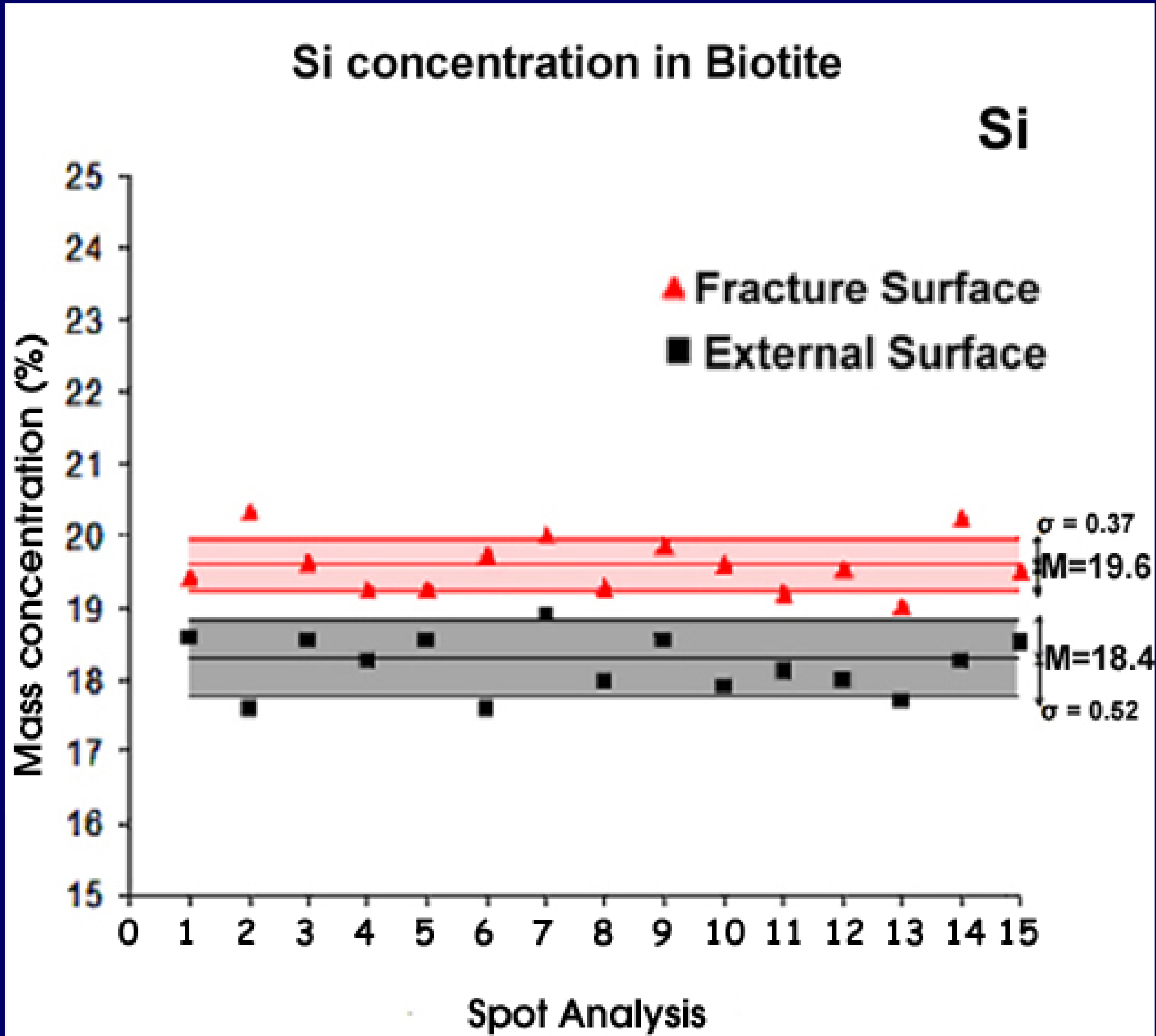

Fracture Surf.:

Si content = 19.6%

External Surf.:

Si content = 18.4%

Si content increase

+1.2%

Biotite (Granite) : Mg concentrations

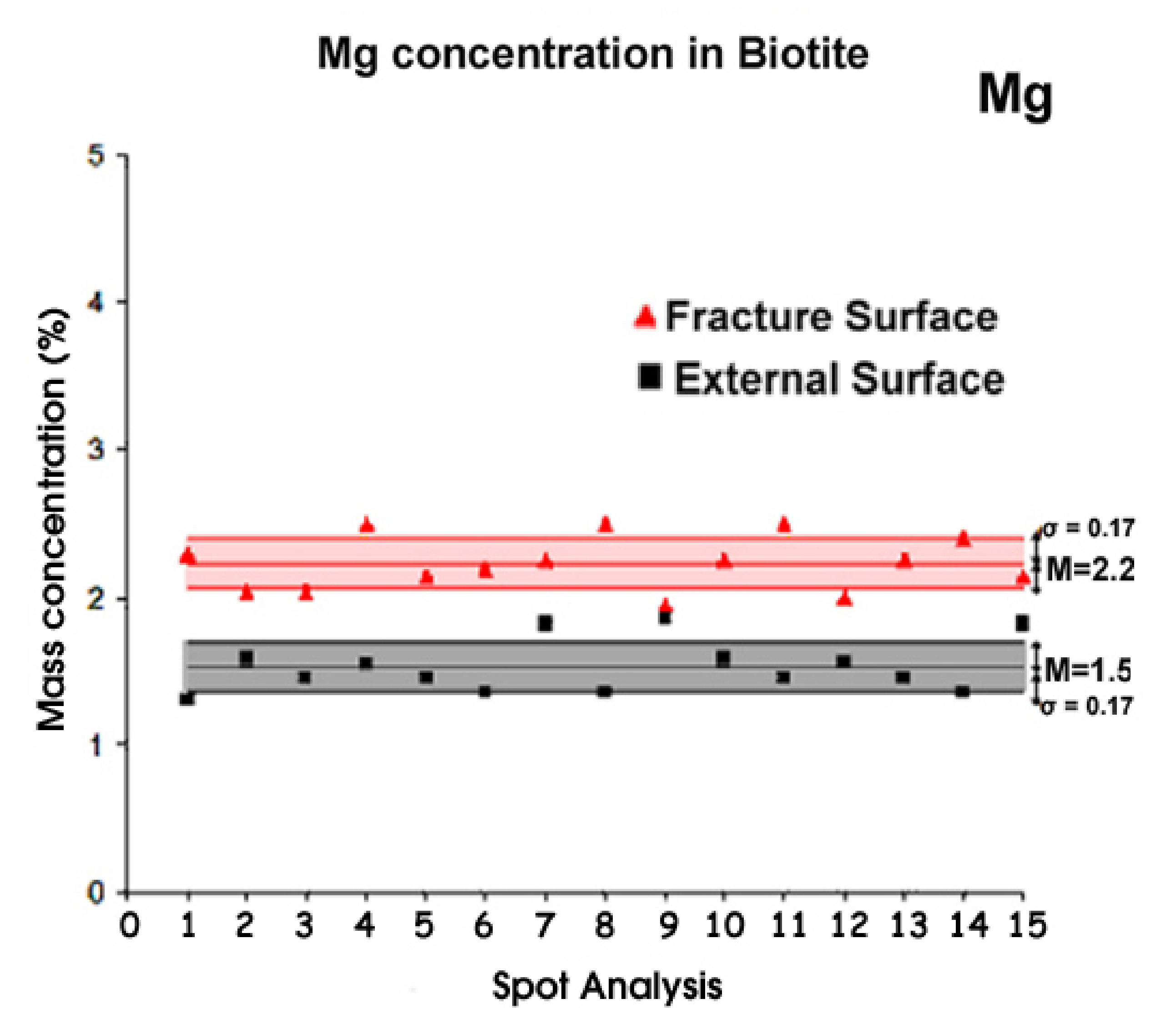

Fracture Surf.:

Mg content = 2.2%

External Surf.:

Mg content = 1.5%

Mg content increase

+0.7%

Biotite (Granite)

	External surface mean value (wt%)	Fracture surface mean value (wt%)	Increase/ decrease with respect to biotite	Increase/ decrease with respect to the same element
Fe	21.2	18.2	–3.0 %	–14%
Al	8.1	9.6	+1.5 %	+18%
Si	18.4	19.6	+1.2 %	+6%
Mg	1.5	2.2	+0.7 %	+46%
K	6.9	7.1	NO VARIATIONS	NO VARIATIONS

$$Fe_{26}^{56} \rightarrow 2\,Al_{13}^{27} + 2n$$

$$Fe_{26}^{56} \rightarrow Si_{14}^{28} + Mg_{12}^{24} + 4n$$

Olivine (Basalt): Fe concentrations

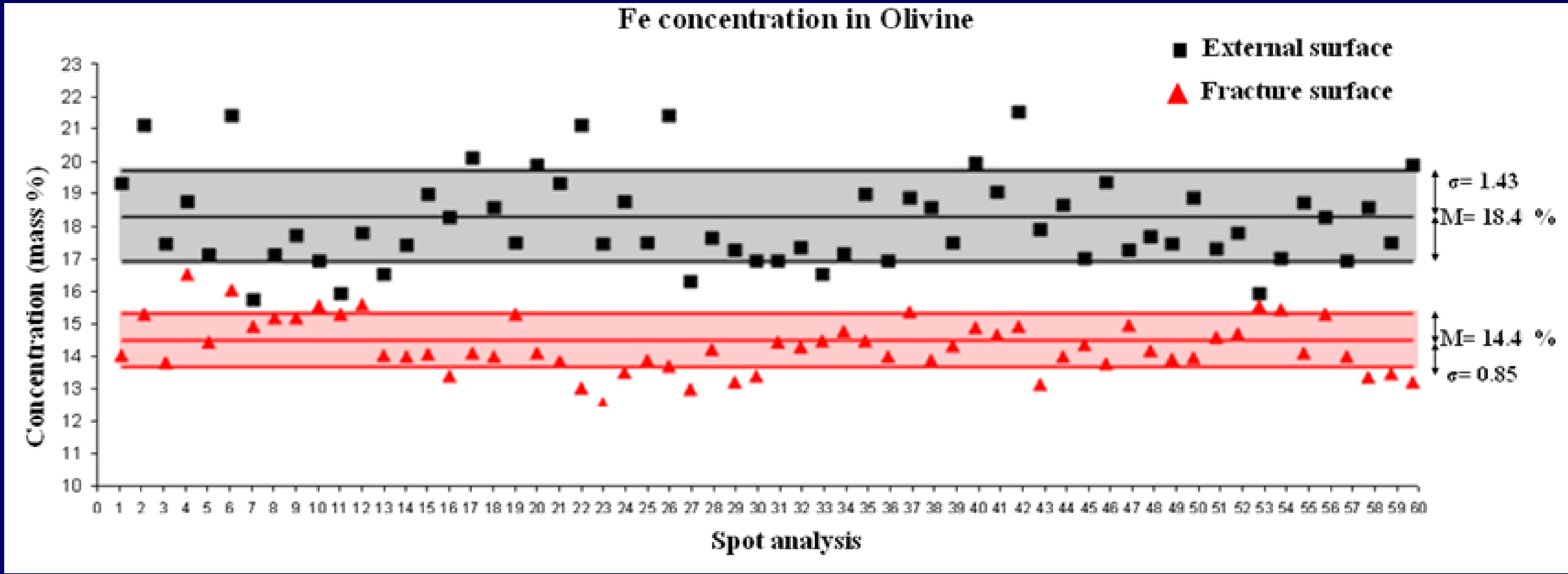

External Surf.: Fe content = 18.4%

Fracture Surf.: Fe content = 14.4%

Fe content decrease

– 4.0%

Olivine (Basalt): Si concentrations

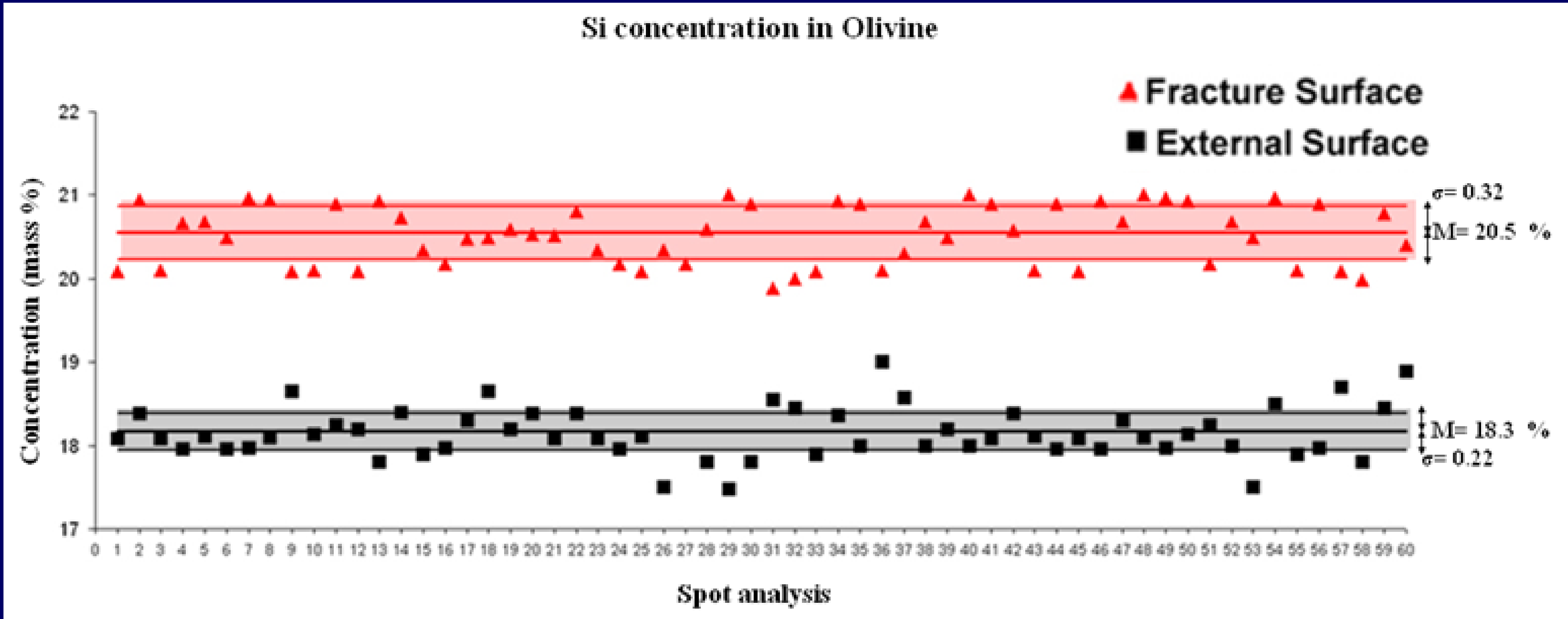

Fracture Surf.: Fe content = 20.5%

External Surf.: Fe content = 18.3%

Si content increase

+ 2.2%

Olivine (Basalt): Mg concentrations

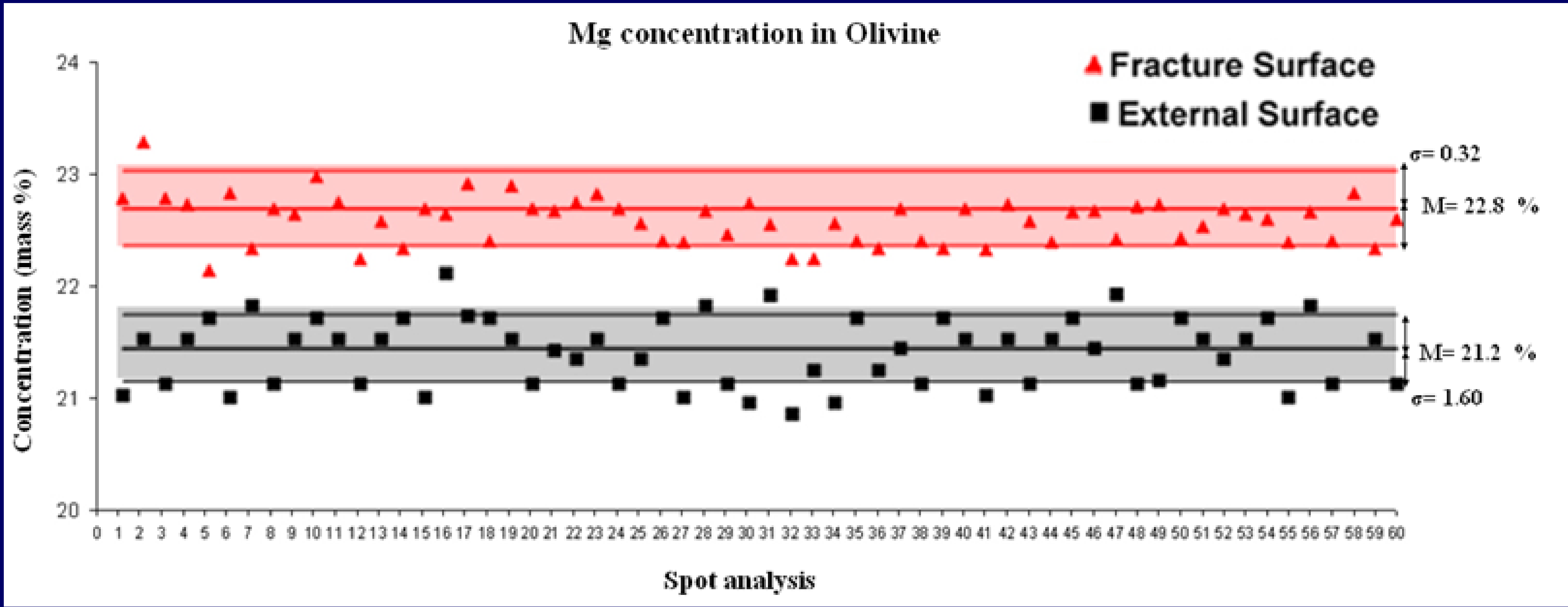

Fracture Surf.: Fe content = 22.8%

External Surf.: Fe content = 21.2%

Si content increase

+ 1.6%

Olivine (Basalt)

	External surface mean value (wt%)	Fracture surface mean value (wt%)	Increase/decrease with respect to Olivine	Increase/decrease with respect to the same element
Fe	18.4	14.4	–4.0%	–21%
Si	18.3	20.5	+2.2%	+12%
Mg	21.2	22.8	+1.6%	+7%
Ca	0.5	0.5	NO VARIATIONS	NO VARIATIONS

$$Fe^{56}_{26} \rightarrow Si^{28}_{14} + Mg^{24}_{12} + 4n$$

Magnetite: Fe concentrations

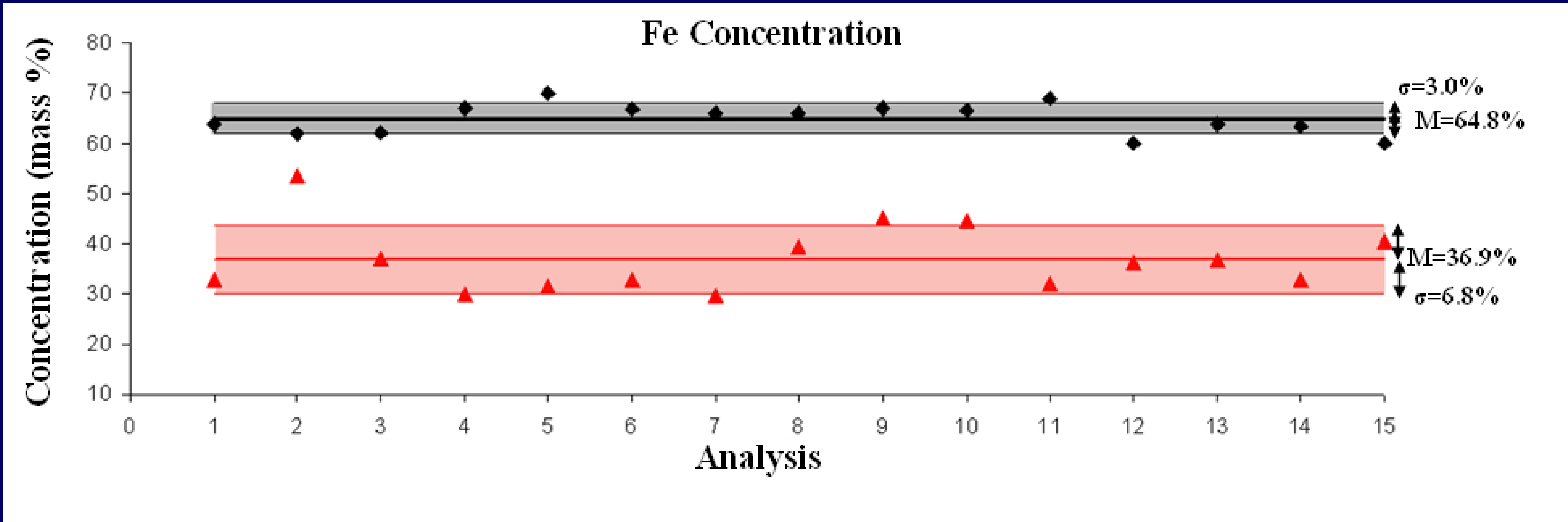

External Surf.: Fe content = 64.8%

Fracture Surf.: Fe content = 36.9%

Fe content decrease

– 27.9%

Magnetite: Al concentration

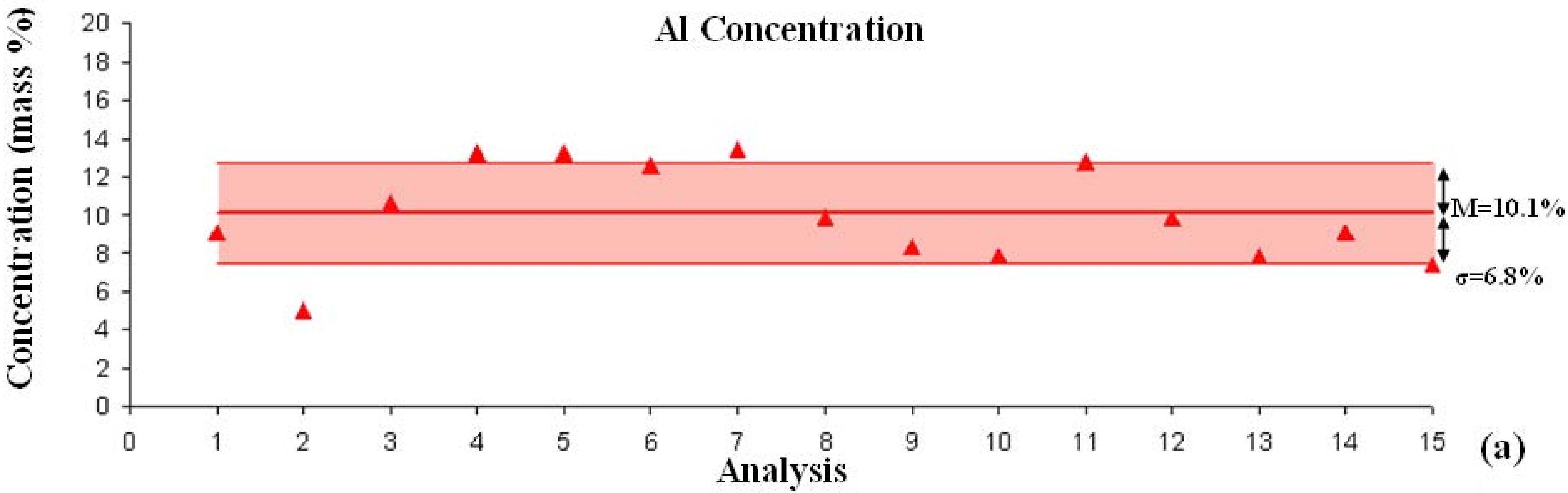

Fracture Surf.: Al content = 10.1%

External Surf.: Al content = ~0.0%

Al content increase

+ 10.1%

Magnetite: Mn concentration

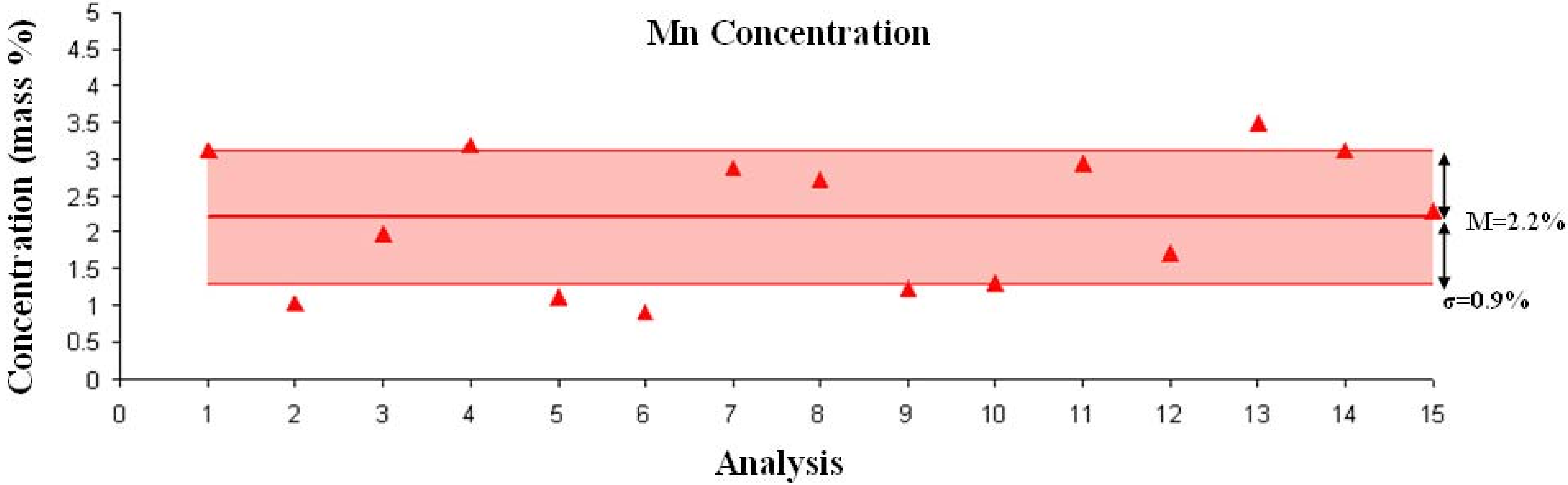

Fracture Surf.: Mn content = 2.2%

External Surf.: Mn content = 0.0%

Mn content increase

+ 2.2%

Magnetite: Si concentration

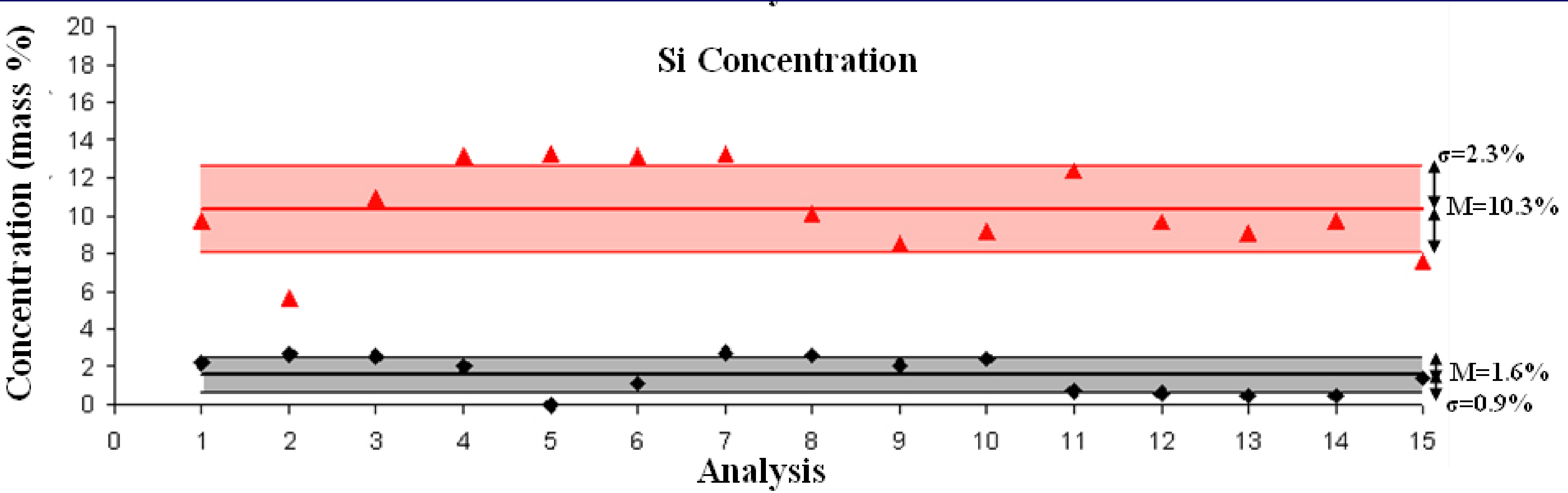

Fracture Surf.: Si content = 10.3%

External Surf.: Si content = 1.6%

Si content increase

+ 8.7%

Magnetite: O concentration

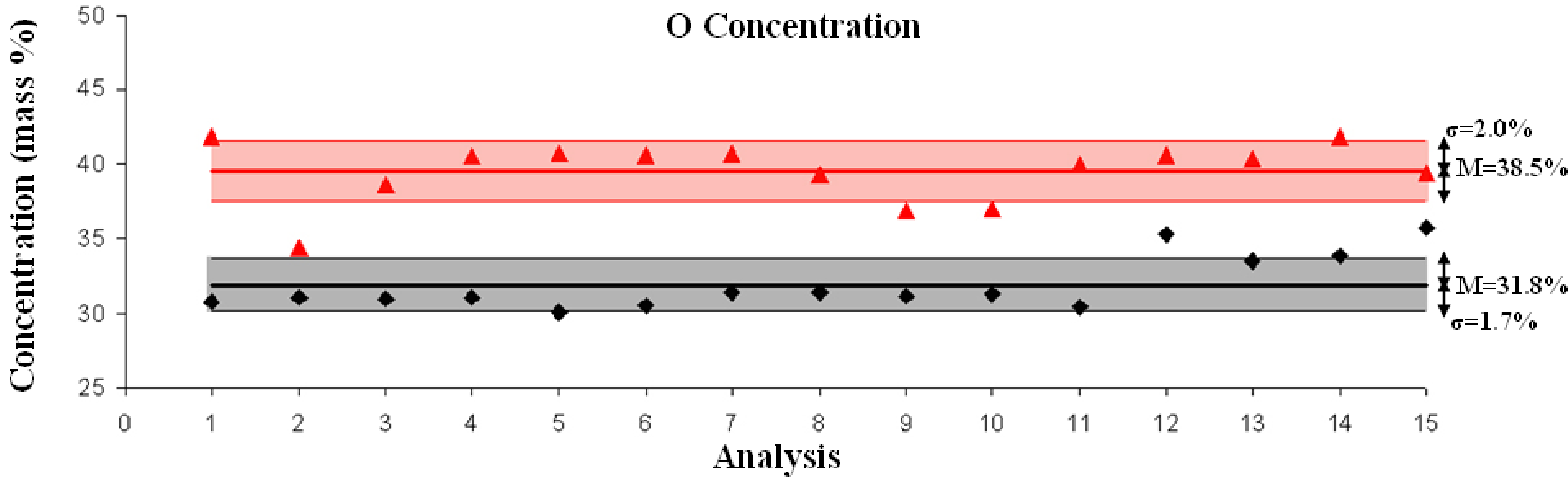

Fracture Surf.: Fe content = 38.5%

External Surf.: Fe content = 31.8%

O content increase

+ 6.7%

Magnetite

	External surface mean value (wt%)	Fracture surface mean value (wt%)	Increase/decrease with respect to Magnetite	Increase/decrease with respect to the same element
Fe	64.8	36.8	–27.9%	–56%
Al	–	10.1	+10.1%	BEFORE ABSENT
Mn	–	2.2	+2.2%	BEFORE ABSENT
Si	1.6	10.3	+8.7%	+540%
O	31.8	38.5	+6.7%	+21%

$$Fe_{26}^{56} \rightarrow 2\,Al_{13}^{27} + 2\,n$$

$$Fe_{26}^{56} \rightarrow Mn_{25}^{55} + H_{1}^{1}$$

$$Fe_{26}^{56} \rightarrow Si_{14}^{28} + O_{8}^{16} + 2He_{2}^{4} + 4n$$

Carrara Marble: Ca concentrations

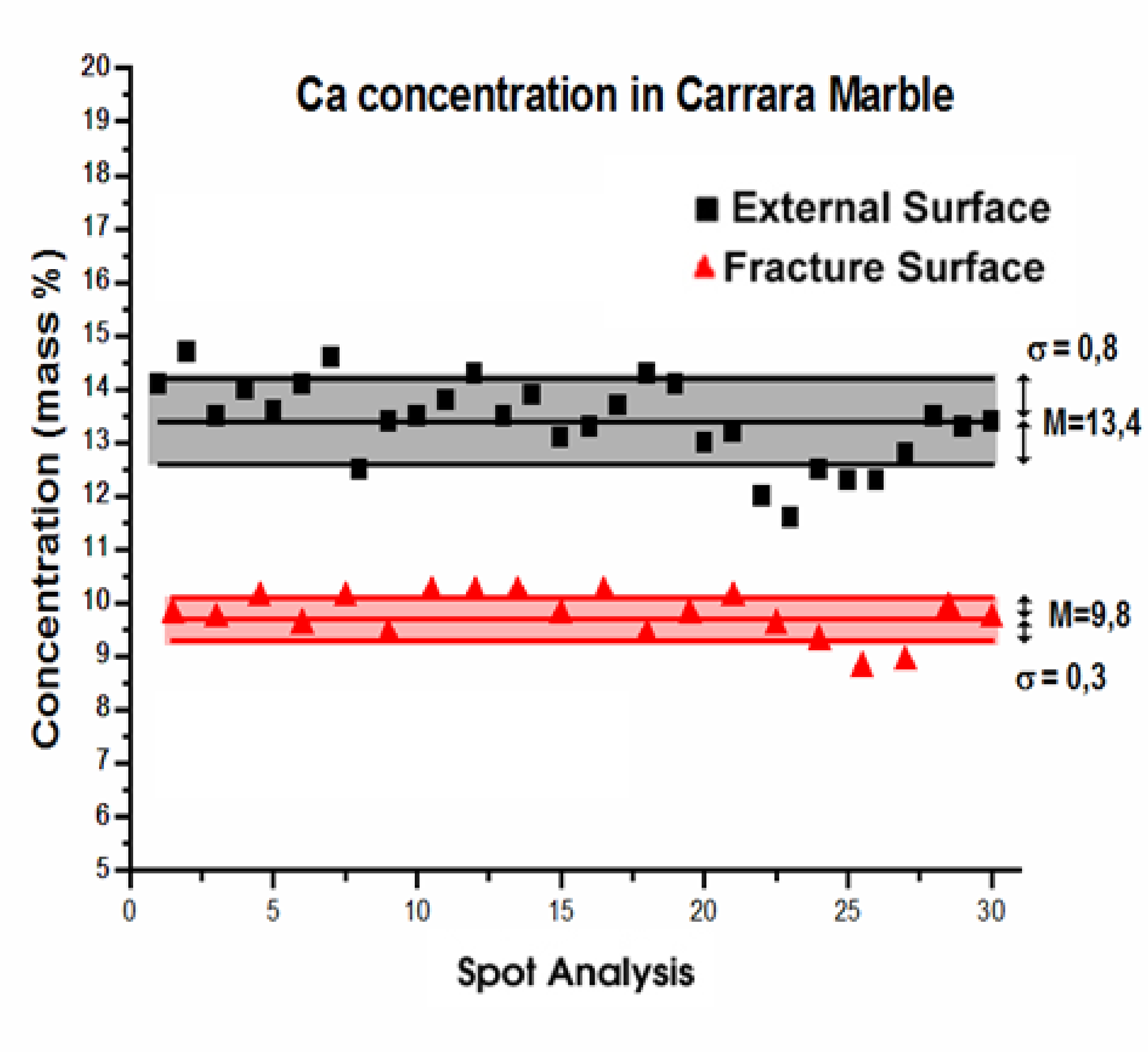

External Surf.:

Ca content = <u>13.4%</u>

Fracture Surf.:

Ca content = <u>9.8%</u>

Ca content decrease

–3.6%

Carrara Marble: Mg concentrations

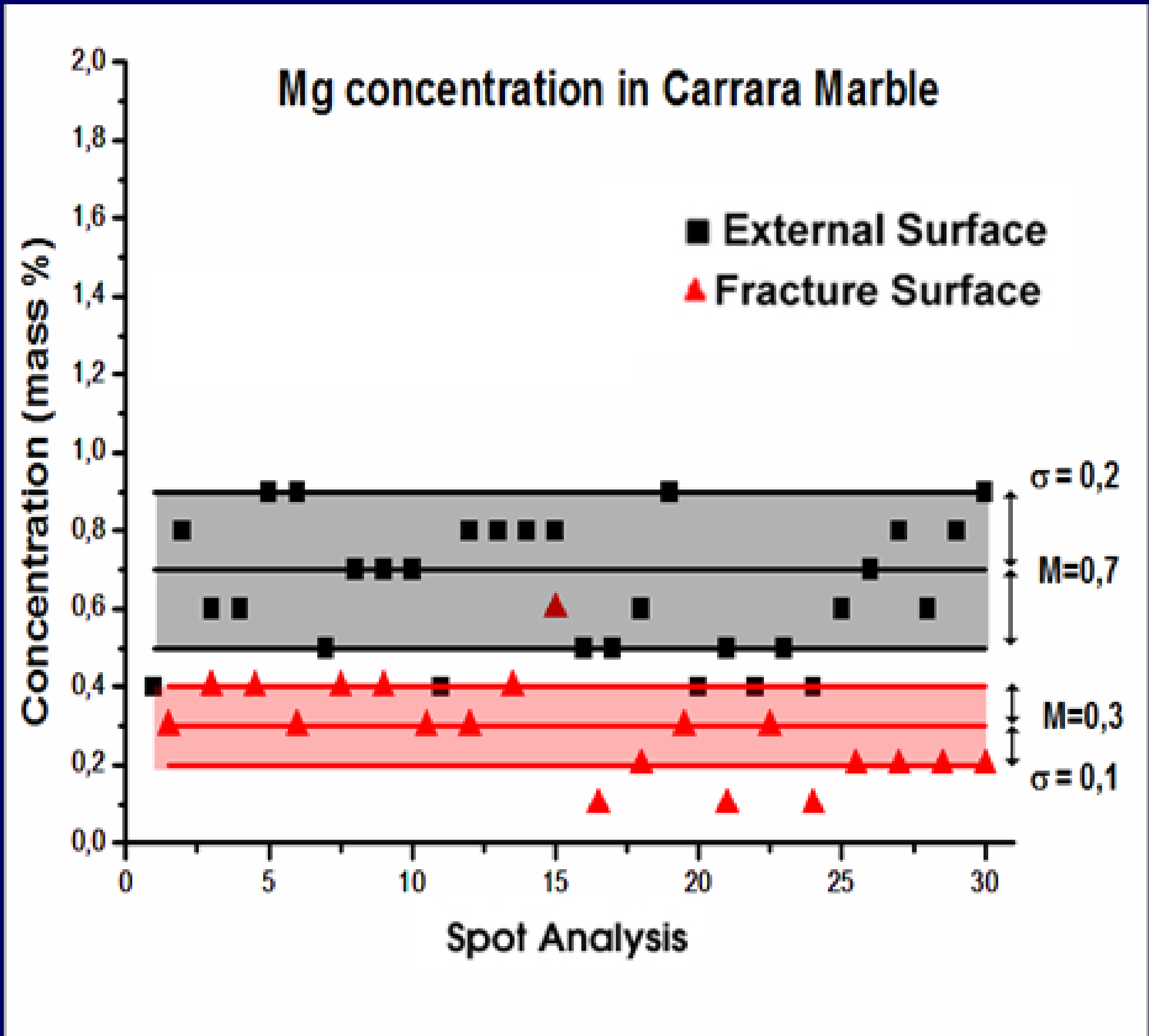

External Surf.:

Mg content = <u>0.7%</u>

Fracture Surf.:

Mg content = <u>0.3%</u>

Mg content decrease

–0.4%

Carrara Marble: O concentrations

X-ray Photoelectron Spectroscopy

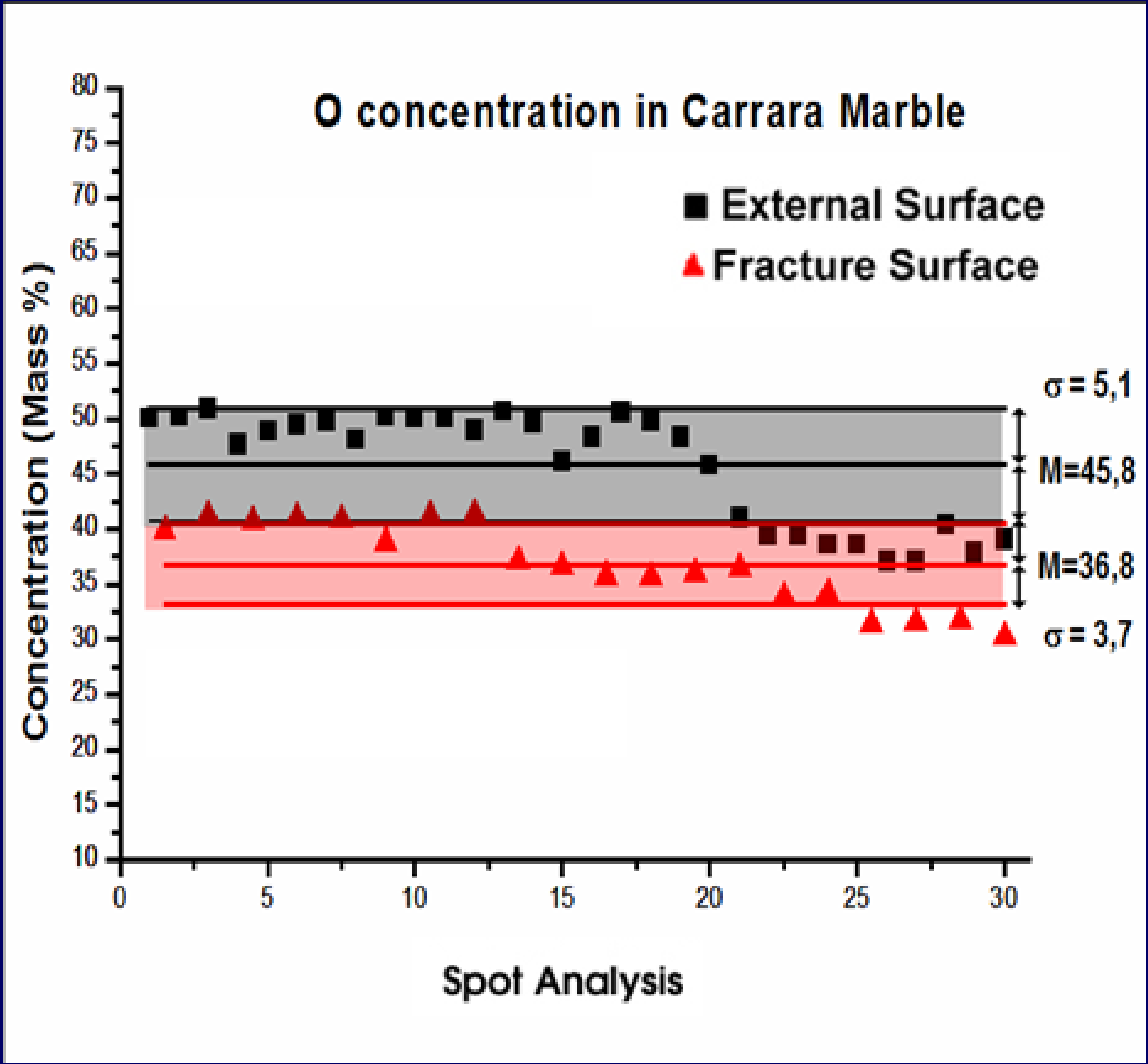

External Surf.:

O content = <u>45.8%</u>

Fracture Surf.:

O content = <u>36.8%</u>

O content decrease

–9.0%

Carrara Marble: C concentrations

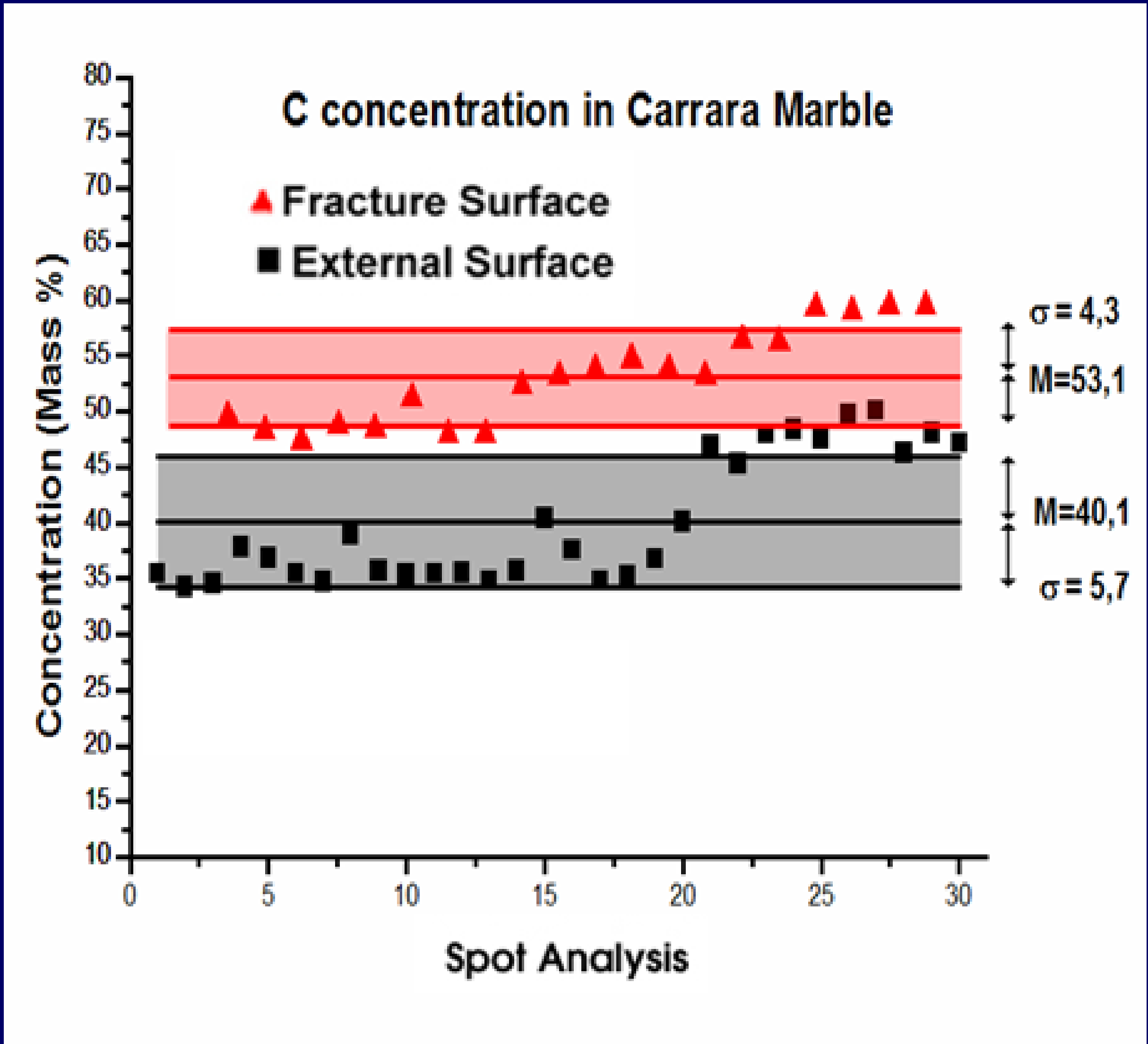

Fracture Surf.:

C content = <u>53.1%</u>

External Surf.:

C content = <u>40.1%</u>

C content increase

+13.0%

Carrara Marble

	External surface mean value (wt%)	Fracture surface mean value (wt%)	Increase/ decrease with respect to Carrara Marble	Increase/ decrease with respect to the same element
Ca	13.4	9.8	–3.6 %	–26%
Mg	0.7	0.3	–0.4 %	–57%
O	45.8	36.8	–9.0 %	–19%
C	40.1	53.1	+13.0%	+32%

$$Ca^{40}_{20} \rightarrow 3C^{12}_{6} + He^{4}_{2}$$

$$Mg^{24}_{12} \rightarrow 2C^{12}_{6}$$

$$O^{16}_{8} \rightarrow C^{12}_{6} + He^{4}_{2}$$

APPENDIX B

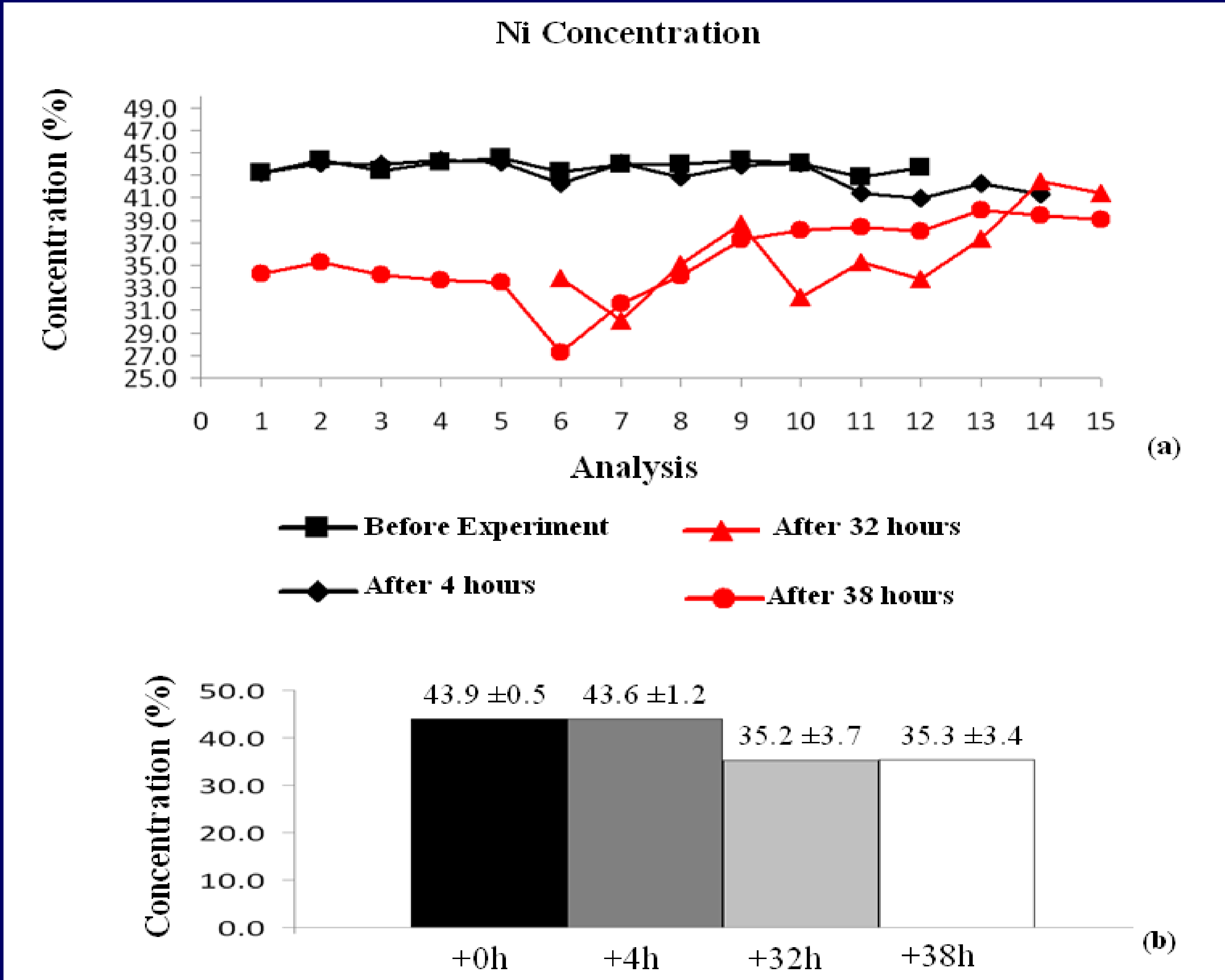

Ni Concentration
Concentration (%)
49.0
47.0
45.0
43.0
41.0
39.0
37.0
35.0
33.0
31.0
29.0
27.0
25.0
0 1 2 3 4 5 6 7 8 9 10 11 12 13 14 15
(a)
Analysis
Before Experiment
After 32 hours
After 4 hours
After 38 hours
Concentration (%)
50.0
40.0
30.0
20.0
10.0
0.0
43.9 ±0.5
43.6 ±1.2
35.2 ±3.7
35.3 ±3.4
+0h
+4h
+32h
+38h
(b)

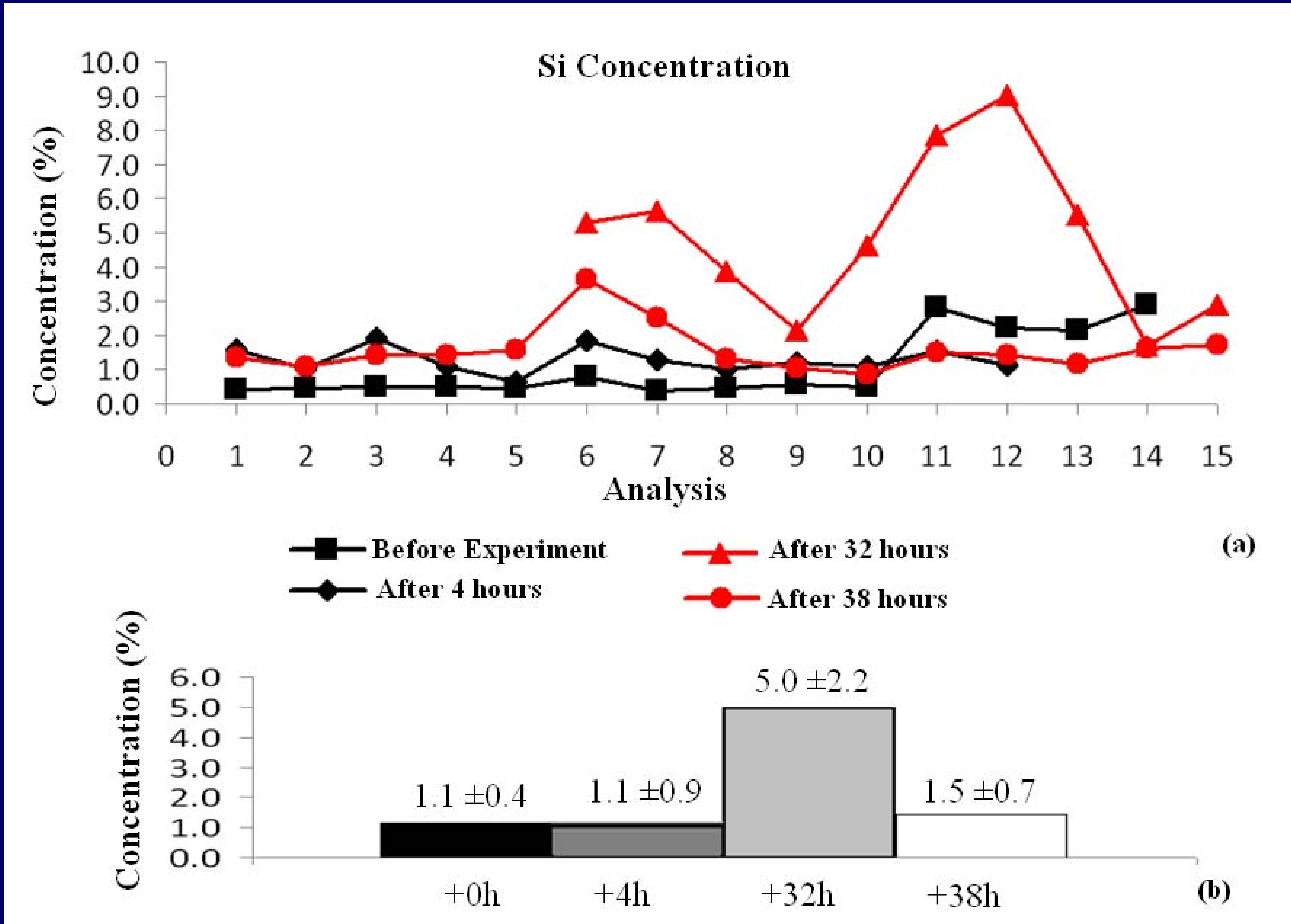

Si Concentration
Concentration (%)
10.0
9.0
8.0
7.0
6.0
5.0
4.0
3.0
2.0
1.0
0.0
0
1
2
3
4
5
6
7
8
9
10
11
12
13
14
15
Analysis
(a)
Before Experiment
After 4 hours
After 32 hours
After 38 hours
Concentration (%)
6.0
5.0
4.0
3.0
2.0
1.0
0.0
1.1 ±0.4
1.1 ±0.9
5.0 ±2.2
1.5 ±0.7
+0h
+4h
+32h
+38h
(b)

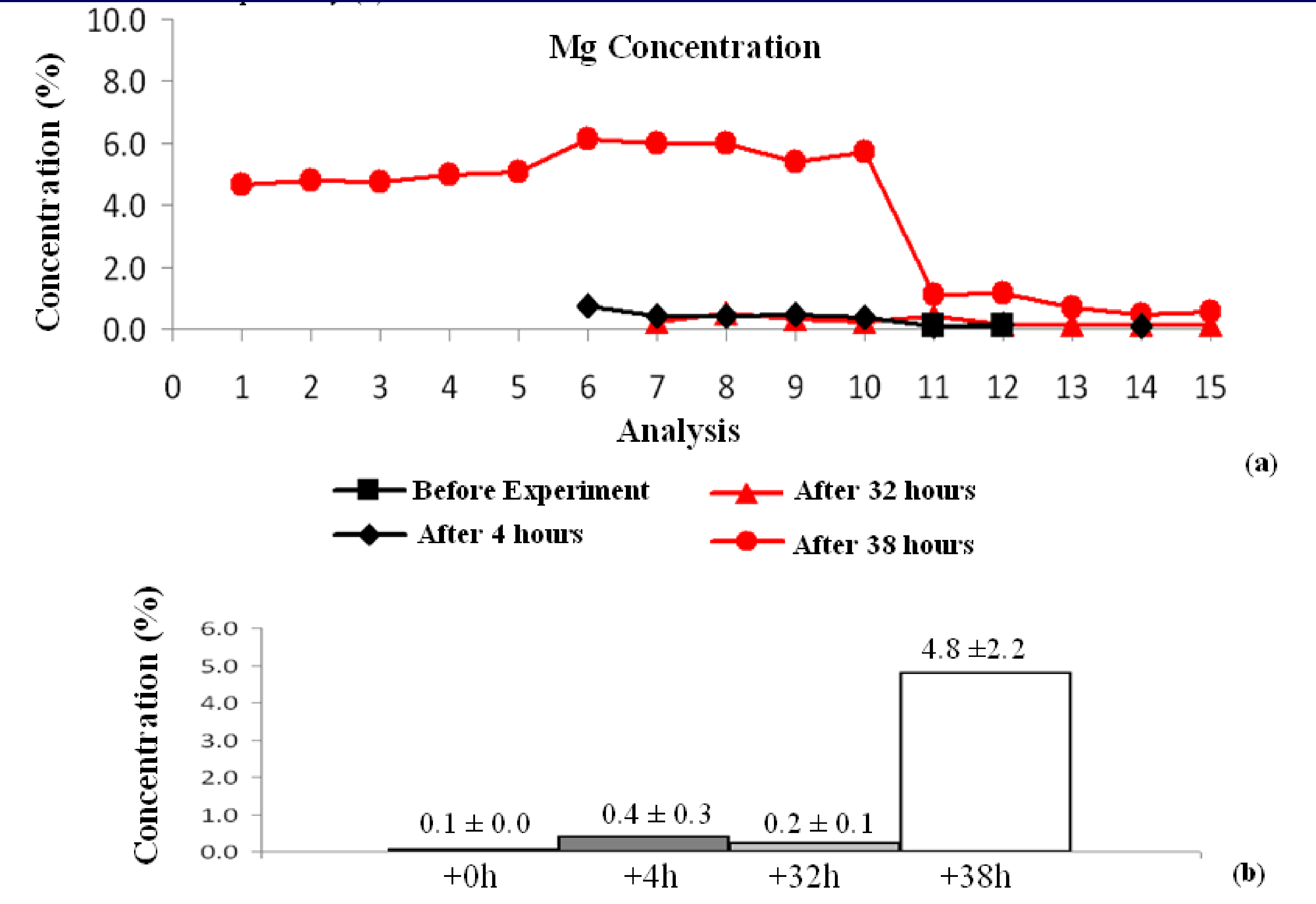
Mg Concentration
Concentration (%)
10.0
8.0
6.0
4.0
2.0
0.0
0
1
2
3
4
5
6
7
8
9
10
11
12
13
14
15
Analysis
(a)
Before Experiment
After 4 hours
After 32 hours
After 38 hours
Concentration (%)
6.0
5.0
4.0
3.0
2.0
1.0
0.0
0.1 ± 0.0
0.4 ± 0.3
0.2 ± 0.1
4.8 ±2.2
+0h
+4h
+32h
+38h
(b)

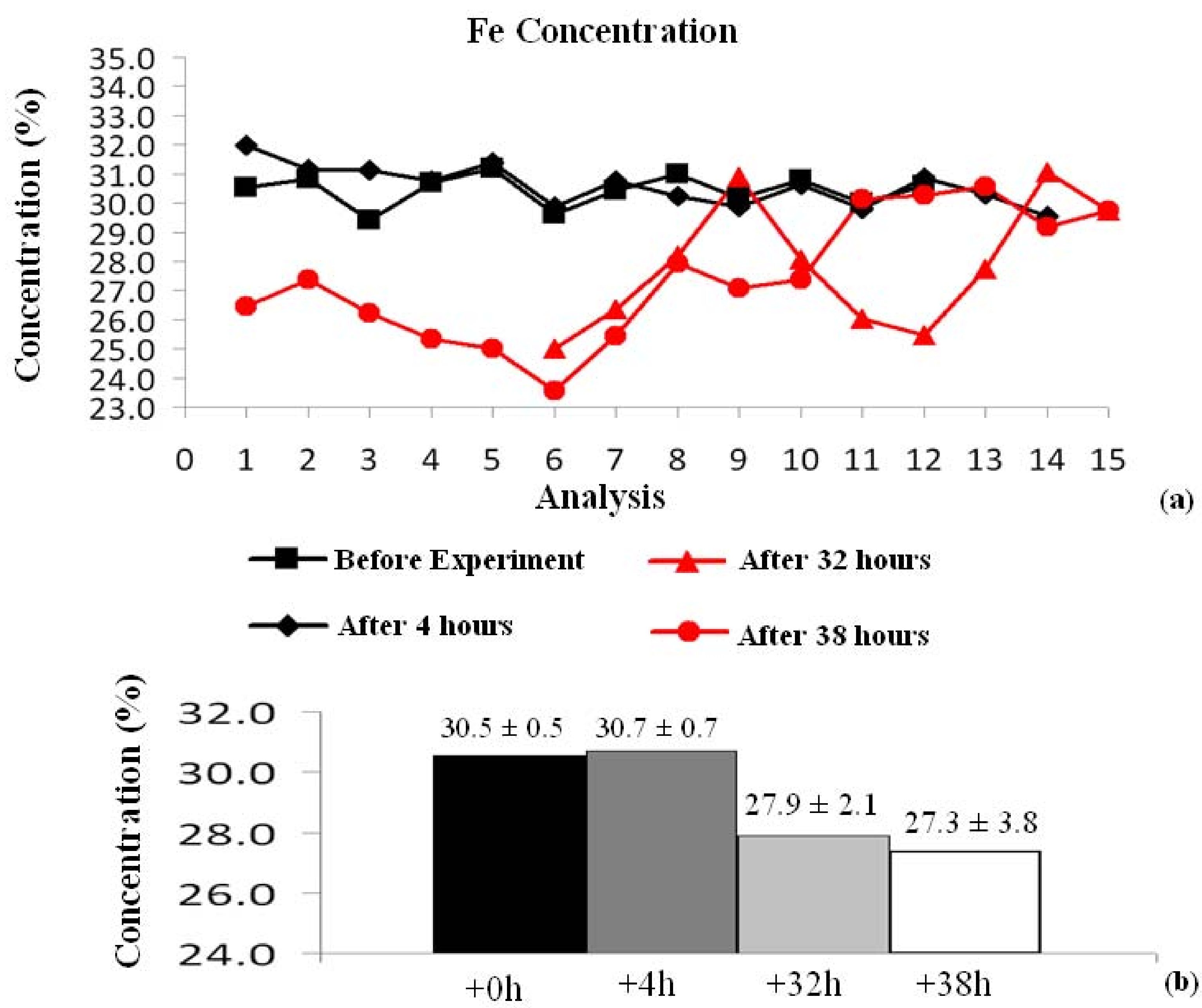

Fe Concentration
Concentration (%)
35.0
34.0
33.0
32.0
31.0
30.0
29.0
28.0
27.0
26.0
25.0
24.0
23.0
0
1
2
3
4
5
6
7
8
9
10
11
12
13
14
15
Analysis
(a)
Before Experiment
After 32 hours
After 4 hours
After 38 hours
Concentration (%)
32.0
30.0
28.0
26.0
24.0
30.5 ± 0.5
30.7 ± 0.7
27.9 ± 2.1
27.3 ± 3.8
+0h
+4h
+32h
+38h
(b)

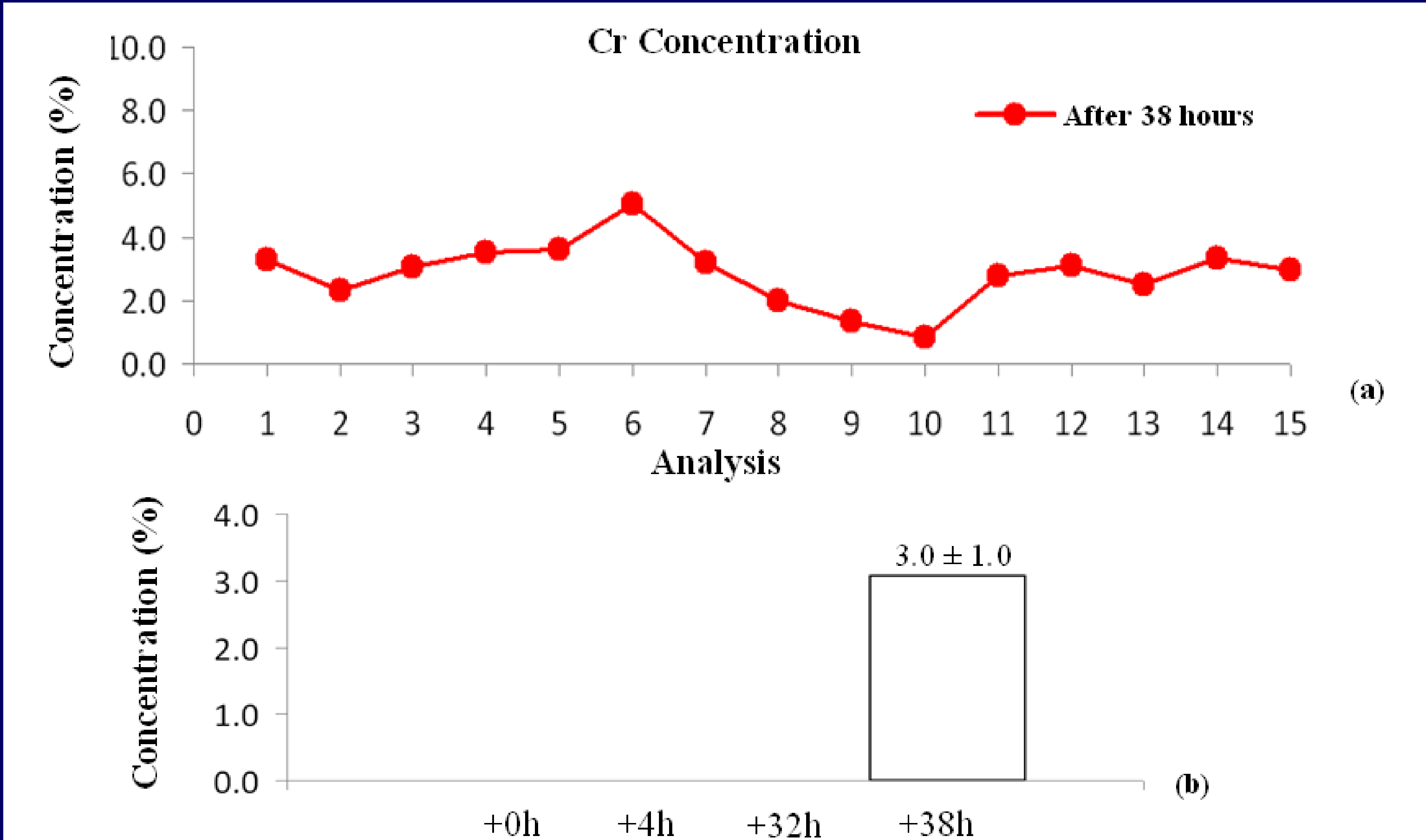
Cr Concentration
Concentration (%)
10.0
8.0
6.0
4.0
2.0
0.0
After 38 hours
(a)
0 1 2 3 4 5 6 7 8 9 10 11 12 13 14 15
Analysis
Concentration (%)
4.0
3.0
2.0
1.0
0.0
3.0 ± 1.0
(b)
+0h +4h +32h +38h

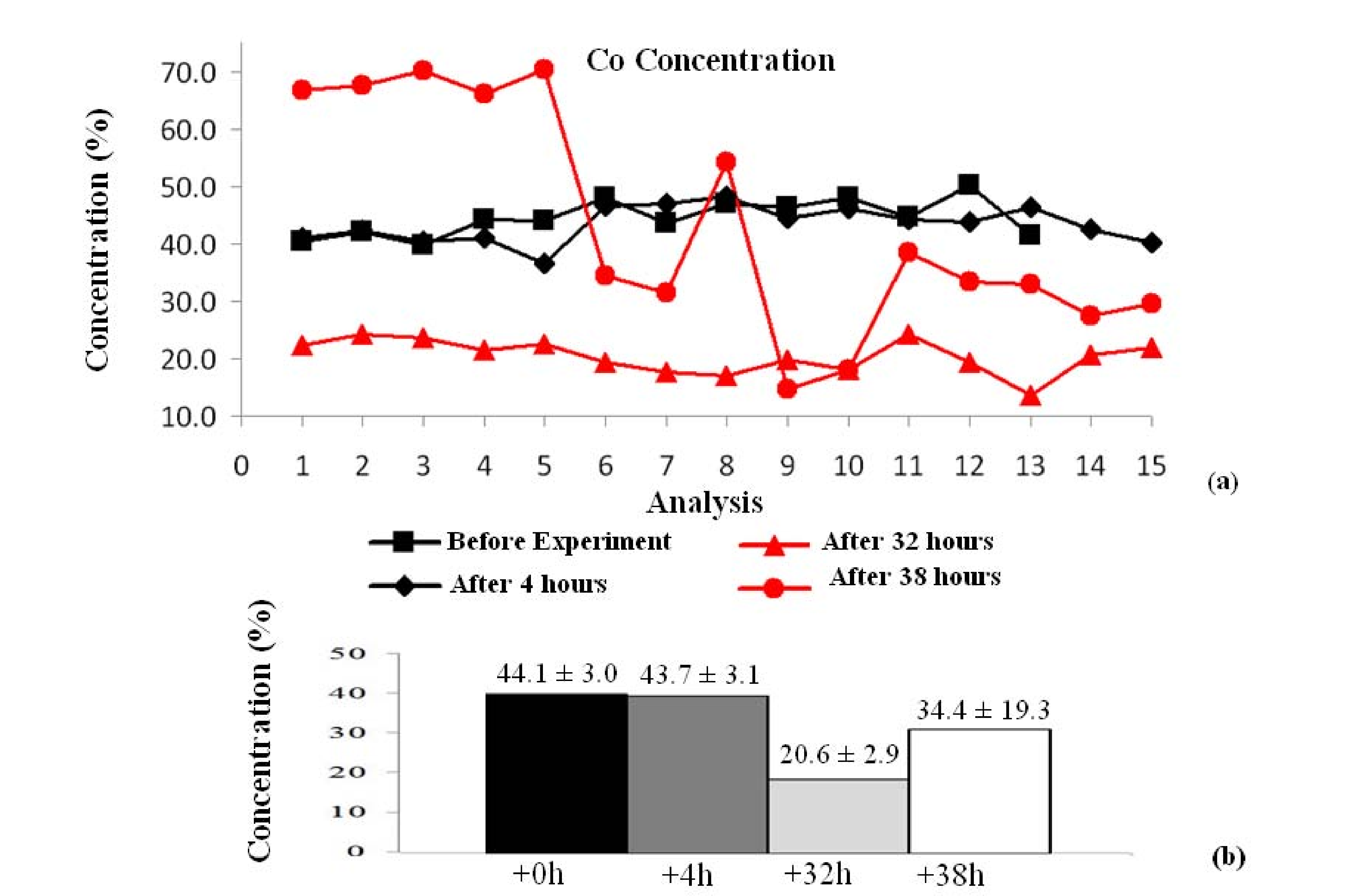

Co Concentration
Concentration (%)
70.0
60.0
50.0
40.0
30.0
20.0
10.0
0
1
2
3
4
5
6
7
8
9
10
11
12
13
14
15
Analysis
(a)
Before Experiment
After 4 hours
After 32 hours
After 38 hours
Concentration (%)
50
40
30
20
10
0
44.1 ± 3.0
43.7 ± 3.1
20.6 ± 2.9
34.4 ± 19.3
+0h
+4h
+32h
+38h
(b)

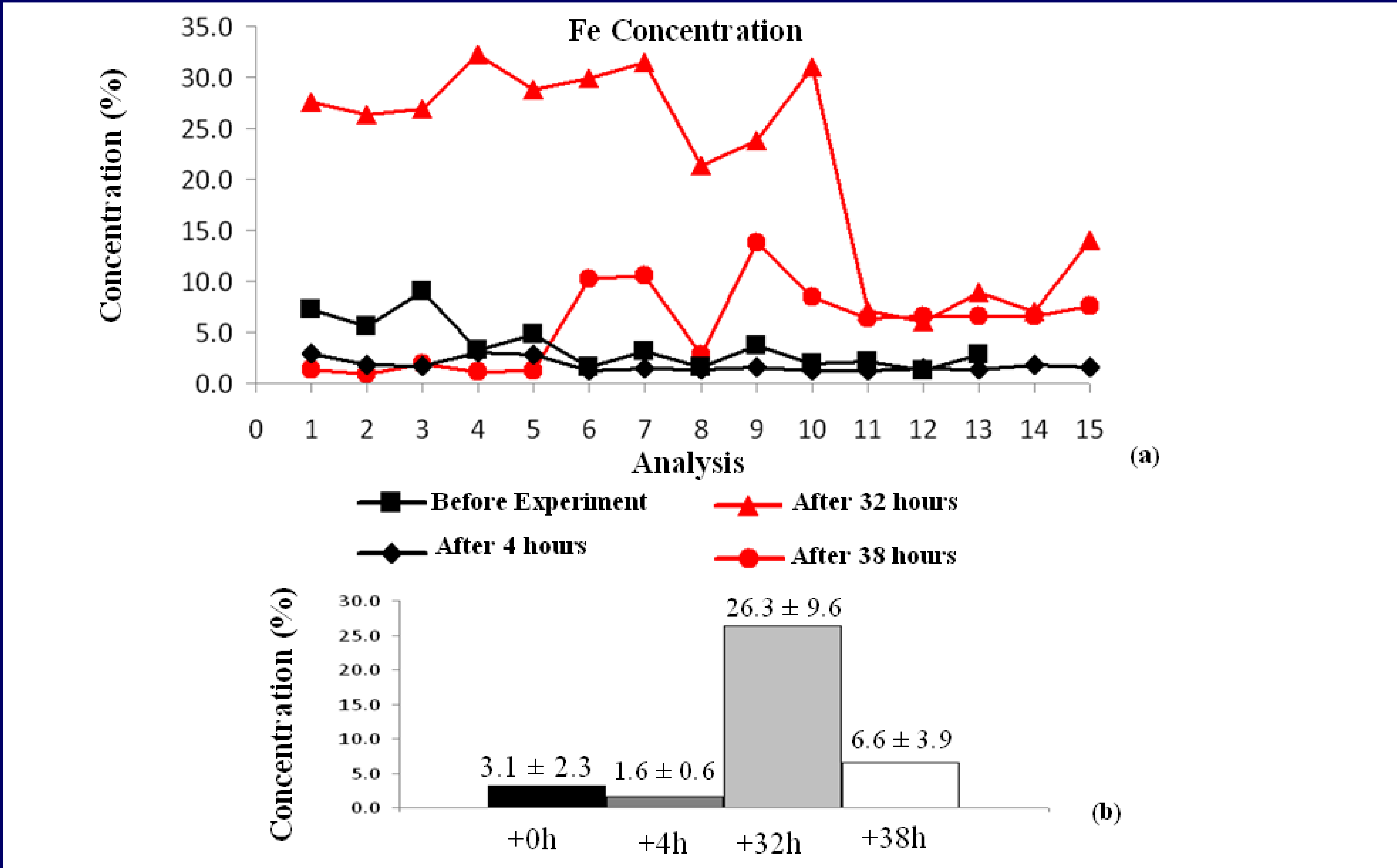

Fe Concentration
Concentration (%)
35.0
30.0
25.0
20.0
15.0
10.0
5.0
0.0
0 1 2 3 4 5 6 7 8 9 10 11 12 13 14 15
Analysis
(a)
Before Experiment
After 32 hours
After 4 hours
After 38 hours
Concentration (%)
30.0
25.0
20.0
15.0
10.0
5.0
0.0
3.1 ± 2.3
1.6 ± 0.6
26.3 ± 9.6
6.6 ± 3.9
+0h
+4h
+32h
+38h
(b)

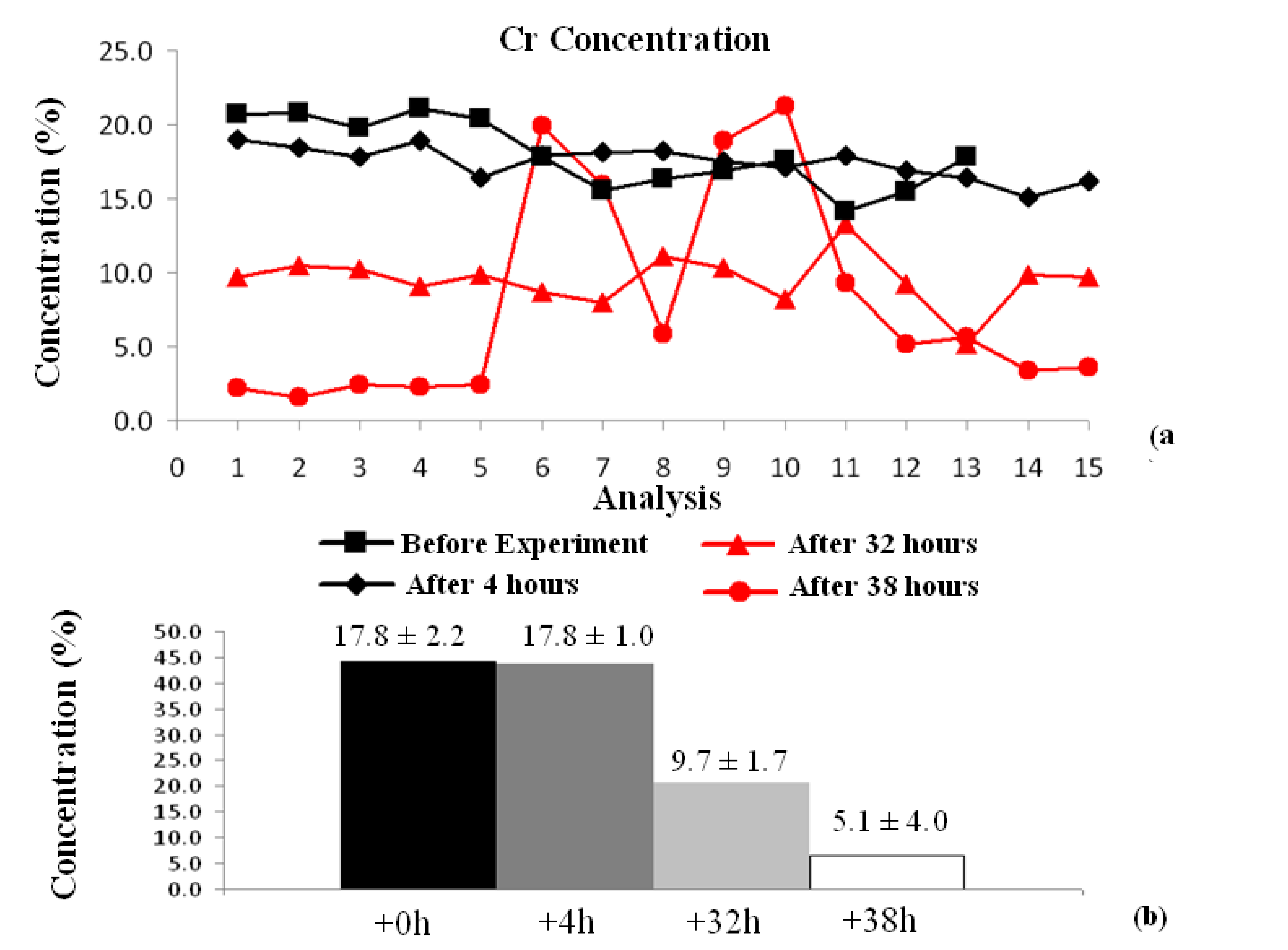

Cr Concentration
Concentration (%)
25.0
20.0
15.0
10.0
5.0
0.0
0 1 2 3 4 5 6 7 8 9 10 11 12 13 14 15
Analysis
(a
Before Experiment
After 4 hours
After 32 hours
After 38 hours
Concentration (%)
50.0
45.0
40.0
35.0
30.0
25.0
20.0
15.0
10.0
5.0
0.0
17.8 ± 2.2
17.8 ± 1.0
9.7 ± 1.7
5.1 ± 4.0
+0h
+4h
+32h
+38h
(b)

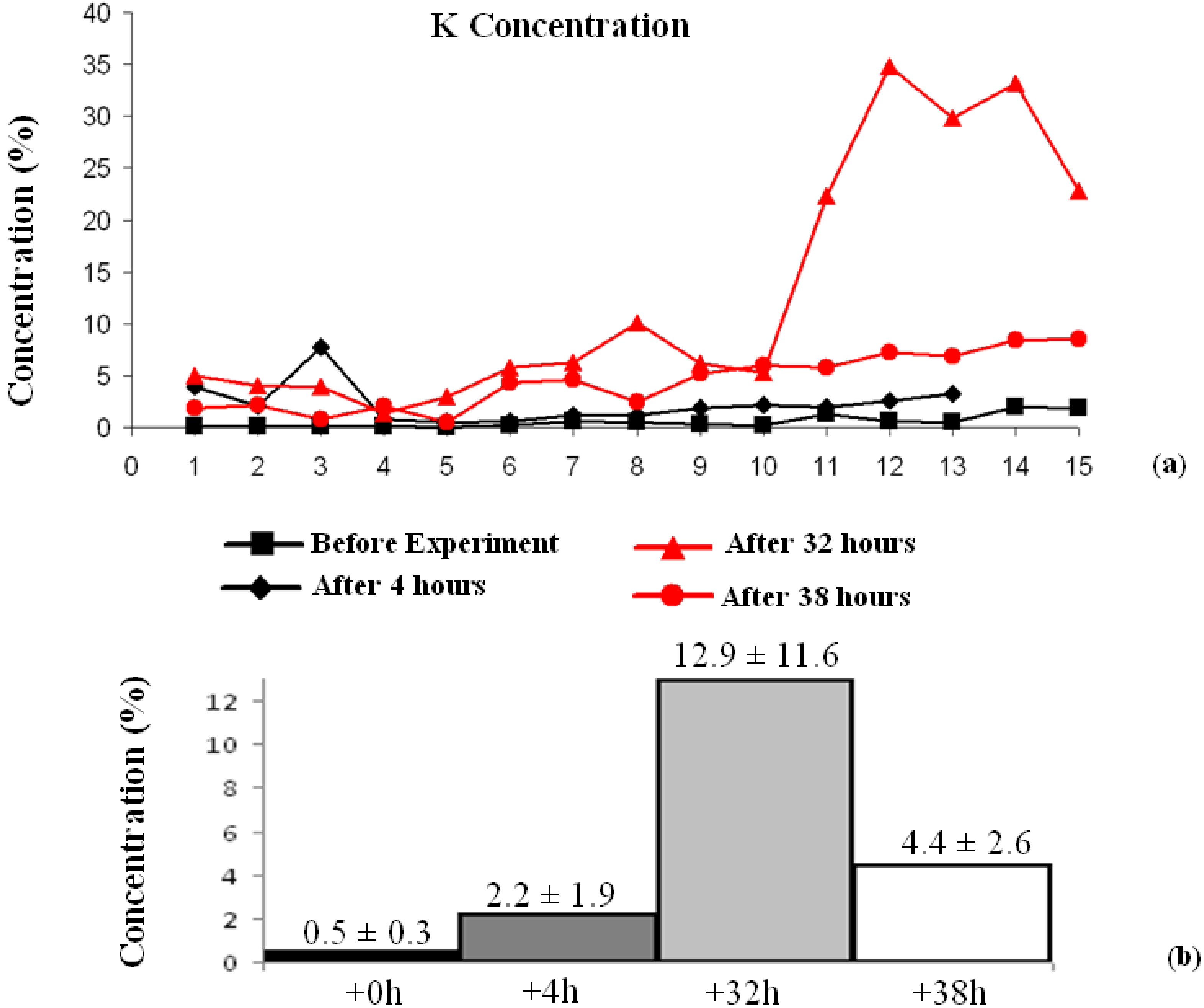

K Concentration
Concentration (%)
40
35
30
25
20
15
10
5
0
0
1
2
3
4
5
6
7
8
9
10
11
12
13
14
15
(a)
Before Experiment
After 4 hours
After 32 hours
After 38 hours
Concentration (%)
12.9 ± 11.6
4.4 ± 2.6
2.2 ± 1.9
0.5 ± 0.3
12
10
8
6
4
2
0
+0h
+4h
+32h
+38h
(b)